Université d'Ottawa · University of Ottawa

PERMISSION DE REPRODUIRE ET DE DISTRIBUER LA THÈSE

PERMISSION TO REPRODUCE AND DISTRIBUTE THE THESIS

NOM DE L'AUTEUR / NAME OF AUTHOR: ENRIGHT, Dave S.

ADRESSE POSTALE / MAILING ADDRESS:
513 BOUL DES HAUTES PLAINES
HULL QC J8Z2H8

GRADE / DEGREE: M.Sc. (Chemistry)

ANNÉE D'OBTENTION / YEAR GRANTED 2003

TITRE DE LA THÈSE / TITLE OF THESIS: The Search for New Catalysts for Ziegler-Natta Olefin Polymerization: Exploratory Studies in Unusual Direction

L'auteur permet, par la présente, la consultation et le prêt de cette thèse en conformité avec les règlements établis par le bibliothécaire en chef de l'Université d'Ottawa. L'auteur autorise aussi l'Université d'Ottawa, ses successeurs et cessionnaires, à reproduire cet exemplaire par photograhie ou photocopie pour fins de prêt ou de vente au prix coûtant aux bibliothèques ou aux chercheurs qui en feront la demande.

Les droits de publication par tout autre moyen et pour vente au public demeureront la propriété de l'auteur de la thèse sous réserve des règlements de l'Université d'Ottawa en matière de publication de thèses.

N.B. LE MASCULIN COMPREND ÉGALEMENT LE FÉMININ

The author hereby permits the consultation and the lending of this thesis pursuant to the regulations established by the Chief Librarian of the University of Ottawa. The author also authorizes the University of Ottawa, its successors and assignees, to make reproductions of this copy by photographic means or by photocopying and to lend or sell such reproductions at cost to libraries and to scholars requesting them.

The right to publish the thesis by other means and to sell it to the public is reserved to the author, subject to the regulations of the University of Ottawa governing the publication of theses.

7/03/2003
DATE

D Enright
(AUTEUR) SIGNATURE (AUTHOR)

Université d'Ottawa · University of Ottawa

Université d'Ottawa · University of Ottawa

FACULTÉ DES ÉTUDES SUPÉRIEURES
ET POSTDOCTORALES

FACULTY OF GRADUATE AND
POSTDOCTORAL STUDIES

ENRIGHT, Dave S.
AUTEUR DE LA THÈSE - AUTHOR OF THESIS

M.Sc. (Chemistry)
GRADE - DEGREE

Chemistry
FACULTÉ, ÉCOLE, DÉPARTEMENT - FACULTY, SCHOOL, DEPARTMENT

TITRE DE LA THÈSE - TITLE OF THE THESIS

The Search for New Catalysts for Ziegler-Natta Olefin Polymerization:
Exploratory Studies in Unusual Direction

Sandro Gambarotta
DIRECTEUR DE LA THÈSE - THESIS SUPERVISOR

EXAMINATEURS DE LA THÈSE - THESIS EXAMINERS

A. St-Amant

S. Sundararajan

J.-M. De Koninck, Ph.D.
LE DOYEN DE LA FACULTÉ DES ÉTUDES
SUPÉRIEURES ET POSTDOCTORALES

SIGNATURE

DEAN OF THE FACULTY OF GRADUATE
AND POSTDOCTORAL STUDIES

THE SEARCH FOR NEW CATALYSTS FOR ZIEGLER-NATTA OLEFIN POLYMERIZATION : EXPLORATORY STUDIES IN UNUSUAL DIRECTION

Dave S. Enright B.Sc.

Thesis submitted to the
Faculty of Graduate and Postdoctoral Studies
University of Ottawa
in partial fulfillment of the requirements for the
M.Sc. degree in the

Ottawa-Carleton Chemistry Institute

Thèse soumise à la
Faculté des études supérieures et postdoctorales
Université d'Ottawa
en vue de l'obtention de la maîtrise en sciences à

l'Institut de chimie d'Ottawa-Carleton

Candidate

Dave S. Enright

Supervisor

Dr. Sandro Gambarotta

National Library
of Canada

Acquisitions and
Bibliographic Services

395 Wellington Street
Ottawa ON K1A 0N4
Canada

Bibliothèque nationale
du Canada

Acquisitions et
services bibliographiques

395, rue Wellington
Ottawa ON K1A 0N4
Canada

Your file Votre référence

Our file Notre référence

0-612-76522-9

"If we knew what it was we were doing, it would not be called research, would it?"

Albert Einstein (1879-1955)

To my two girls.

Your love carried me through when all seemed lost
and lifted me to heights I could not have imagined.

Abstract

The preparation of two tetravalent d^2 chromium alkyls is revisited. Their ability to work both as starting materials for further functionalization and as Ziegler-Natta catalysts is investigated. The clarification of the reaction pathway through which a trivalent chromium salt may form a homoleptic tetravalent derivative is also considered. Finally, the elucidation of the nature of the Cr-Cr interaction in a unique $[R_2Cr]_4$ tetranuclear cluster and evaluation of its stability is undertaken.

This is followed by a reassessment of the stability of tetravalent vanadium alkyls. Wilkinson first reported, in the seventies, the preparation of homoleptic R_4V species [$R = C_6H_5$, $CH_2Si(CH_3)_3$]. The full characterisation of a homoleptic R_4V, by crystal structure, and testing the catalytic activity is reported.

The α,α-diiminopyridine ligand $\{\alpha,\alpha'\text{-}[2,6\text{-}(i\text{-}Pr)_2PhN{=}C(Me)]_2(C_5H_3N)\}$ has recently attracted considerable attention because of its ability to form highly active polymerization catalysts. Recent work from this research group and others has shown that this α,α'-diiminopyridine ligand can be involved in the organometallic transformations of the metal center. The ability of the ligand to accept or to donate negative charge to the metal is central to the fine tuning of the redox potential of the metal, and of its Lewis acidity that in turn determines the catalytic behaviour.

A clarification for the ability of this remarkable ligand system to accept negative charge is offered. Reductions of $\{\alpha,\alpha'\text{-}[2,6\text{-}(i\text{-}Pr)_2PhN{=}C(Me)]_2(C_5H_3N)\}$ with strong reductants such as Li and Li(naftalenide) and *in the absence* of transition metals were carried out to yield rare case trilithium organyls.

Acknowledgements

There have been many contributions to this work over the past two years. I would like to thank members of the Gambarotta group, past and present, with whom I have been fortunate to work with and learn from: Dr. Ghazar Aharonian, Dr. Jingwen Guan, Dr. Carola Schulzke, Dr. Ilia Korobkov, Dr. Damien Reardon, Dr. David Harding, Dr. Hiroyasu Sugiyama, Christian Bérubé, Chris McManus, Jenny Scott and Pat Crewdson. Each of you has played a part in making my work enjoyable and interesting.

I would also like to thank Dr. H.M. Budzelaar and Mr. G. Leblanc for the theoretical calculations performed on various compounds as well as Dr. G. Yap for his expertise in solving X-Ray crystal structures and Dr. L. Thompson for the variable temperature magnetic moment results.

Special thanks to Dr. Sandro Gambarotta for his leadership, guidance and always open door policy. Your patience in answering the multitude of questions was very much appreciated. The expertise, wealth of knowledge, excitement concerning your work and life in general that you show perpetually encourage all around you.

I would also like to thank my parents. You have always supported me wherever my choices have brought me and you have taught me to strive for excellence… all the while making sure I took enough time to enjoy myself along way. Merci Maman et Papa!

Thank you Rachel for always knowing when a hug is needed. And all the kisses that I keep safely in my heart… I can bring them out again when things aren't so bright.

Finally, thank you to my wife Cheryl. You have shown me that I can make my dreams come true. You have given me strength to keep going when no matter what colour it was supposed to be it turned *nasty brown*. The last two years has led me to find what I want to and what I want to be in my life… it gives me even greater pleasure to share it with you.

List of Publications

Enright D., Gambarotta S., Schultz C., Yap G.P.A., "Highly Active Tetravalent Homoleptic Vanadium Alkyl", **2003**, Manuscript in writing.

Enright D., Gambarotta S., Yap G.P.A., Budzelaar H.M., "The Ability of the α,α'-Diiminopyridine Ligand System to Accept Negative Charge : Isolation of Paramagnetic and Diamagnetic Trianions", **2002**, *Angew. Chem. Int. Ed.*, **41**, *20*, 3873-3876.

Schulzke C., **Enright D.**, Sugiyama H., Leblanc G., Gambarotta S., Yap G.P.A., Thompson L.K., Wilson D.R., Duchateau R., "The Unusual Stability of Homoleptic Di- and Tetravalent Chromium Alkyls", **2002**, *Organometallics*, **21**, *18*; 3810-3816.

Table of Contents

CHAPTER II – THE UNUSUAL STABILITY OF HOMOLEPTIC DI- AND TETRAVALENT CHROMIUM ALKYLS

Results

CHAPTER III – THE HIGH ACTIVITY OF A HOMOLEPTIC TETRAVALENT VANADIUM ALKYL

CHAPTER IV – THE ABILITY OF THE α,α'-DIIMINE PYRIDINE LIGAND SYSTEM TO ACCEPT NEGATIVE CHARGE : ISOLATION OF THE PARAMAGETIC AND DIAMAGNETIC TRIANIONS

Results

Experimental Procedures

APPENDIX I - CRYSTALLOGRAPHIC DATA : HOMOLEPTIC CHROMIUM ALKYLS

APPENDIX II - CRYSTALLOGRAPHIC DATA : HOMOLEPTIC VANADIUM ALKYL

APPENDIX III - CRYSTALLOGRAPHIC DATA : $\{2,6\text{-bis}[2,6\text{-}(i\text{-}Pr)2PhN{=}C(Me)]_2(C_5H_3N)\}Li_3$

LIST OF TABLES AND FIGURES

CHAPTER I

INTRODUCTION TO ZIEGLER-NATTA CATALYSTS

Introduction to Ziegler-Natta Catalysts

With the increased emphasis on recyclable materials, there has been and will continue to be, an increase in the consumption of specialized plastics. Within this class of materials, olefin based polymers are predicted to encompass the majority of the polymers produced in the near future[1] (Table 1.1). The availability of starting components from the oil cracking process and the relative absence of harmful by-products (CO_2 and H_2O) make these specialized plastics indispensable in a world growing towards *sustainable development.*[2]

	Polyethylene LDPE	Polyethylene LLDPE/HDPE	Polypropylene PP	Fraction of plastics produced (%)
1983	11.3	7.9	6.4	-
1990	14.0	16.1	12.6	43
1995	14.4	22.1	17.1	47
2005	**15.8**	**36.1**	**27.7**	**55**

Table 1.1 - The annual worldwide production of various olefin based polymers ($x10^6$ tons).

The implications of this increased demand involves research into the improvement and design of optimized processes for the production of polyolefins.

Heterogeneous Catalysts

A large number of these industrial scale polymerization processes today are based on Ziegler-Natta catalyst systems. Original experiments done by Ziegler[3] and Natta[4] combined $TiCl_3$ with $Al(CH_2CH_3)_2Cl$ or $Al(CH_2CH_3)_3$ on a $MgCl_2$ support to produce semi-crystalline polyethylene. Even now, this original type of group IV heterogeneous system is still most often used.[5] In the case of propene polymerization, Lewis bases such as ethylbenzoate or silanes are added. These *control agents* improve the stereocontrol of the polymerization thereby affecting the physical properties of the final product. However, these heterogeneous catalysts are complex systems and a multitude of acitve sites can be present on the surface of the support. Therefore, the influence of the additives to the polymer structure is limited.

The Philips Catalyst

Since the discovery of the Aufbau reaction by Zeigler[6], a variety of alternatives using other metals have demonstrated a range of olefin polymerization activity.[7] The Cr based Phillips catalyst is used in roughly one third of all polyethylene being produced. The preparation of this material involves the impregnation of silica with an inorganic chromium compound such as CrO_3. This intermediate is then calcined in the presence of oxygen.[8] The calcination produces a hexavalent chromium species **1** represented in scheme **1.1**.

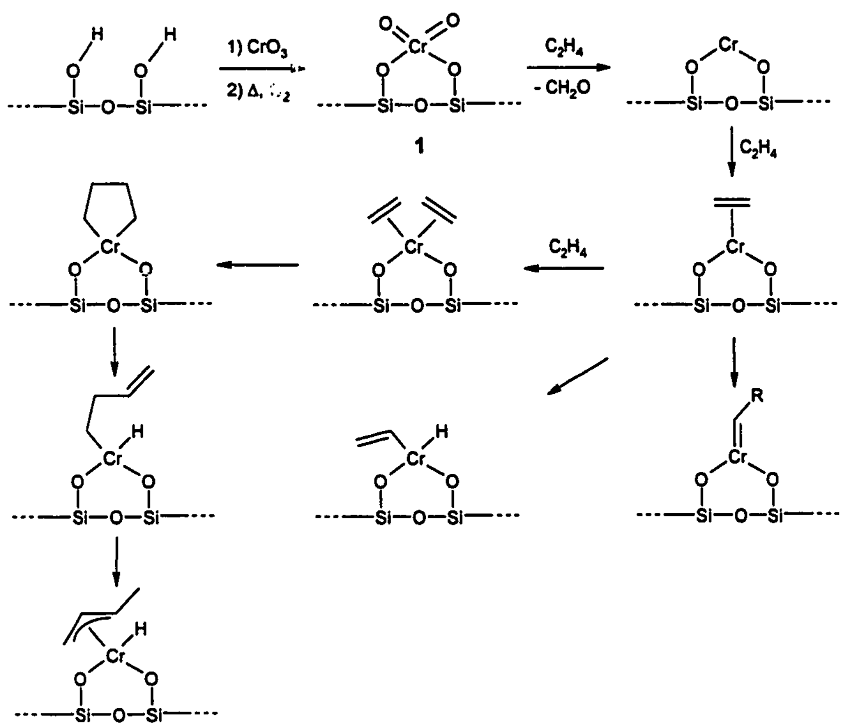

Scheme 1.1 - Proposed initiation mechanism for the Philips catalyst.[9]

When the catalyst is exposed to ethylene, the metal is reduced. This ultimately forms the catalytically active species. However, the chemical structure, valence state and mechanism of formation of the active site are still the subject of a longstanding controversy. This is demonstrated by the three possible pathways illustrated in scheme 1.1.

Much of the debate has centered on the valence (i.e. the formal oxydation state) of the catalytically active chromium. Speculation has included almost every stable oxydation state of Cr as being the initiator of catalysis at one time or another. The use of an alternative reducing agent such as CO can push the reduction of the surface-bound Cr to its divalent state (Cr^{II}). This species will polymerize ethylene,[10] however, the nature of the initiation step has yet to be clarified. It should be noted that well-characterized Cr^{II}

complexes, prepared with the aim of searching for a homogeneous model of the Philips system (see below), have never shown any significant polymerization activity.[11]

The Union-Carbide Catalyst

Another Cr catalyst was discovered by Karapinka[12] and developed by Karol et al.[13] at Union-Carbide in the early 1960's. Again this catalyst is prepared by impregnation of SiO_2. The difference with the Philips catalyst is in the use of chromocene (CpCr) as the "active" agent. While not in use industrially at present, the Union-Carbide catalyst shares some of the advantages of the Philips catalyst. Both are very active and they do not require the addition of Al based cocatalyst. As opposed to the Philips system however, the chromocene based catalyst demonstrates high selectivity between ethylene and other α-olefins (propylene, 1-hexene). Thus no copolymerization occurs upon the use of multiple types of monomers. On the other hand, the Union-Carbide catalyst responds well to hydrogen (H_2) for MW control of the final product.

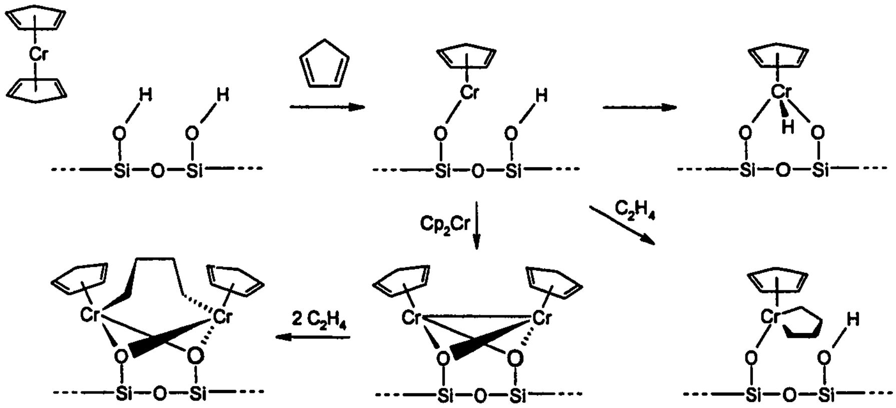

Scheme 1.2 - Proposed initiation mechanisms of the Union-Carbide catalyst.

It has been generally accepted that the organometallic molecule reacts with the remaining hydroxyl groups on the silica surface thereby losing one of its cyclopentadienyl ligands. This forms a surface bound CpCr fragment as shown in scheme **1.2**. However, it is also clear that the polymer chain growth is not initiated by the unchanged Cp group. The later stays coordinated to the Cr throughout the process of catalysis. This poses the same questions as to the chemical structure, valence sate, and mechanism of formation of the active site in the Union-Carbide catalyst.

Difficulties in Studying Heterogeneous Catalysts

The proposed initiation mechanisms depicted in schemes **1.1** and **1.2** are the result of meticulous spectroscopic investigations on heterogeneous catalysts in combination with studies on known organometallic structures carved out in an effort to elucidate reasonable structures of the intermediates. There remain questions however, as to the relevance of this great multitude of proposals. Most of the analytical work utilizes IR spectroscopy,[14] with some EXAFS[15] and solid state NMR results[16] added relatively recently. These techniques are not considered to be definitive in the case of most substances. That is to say, a detailed molecular structure such as that presented in the above reaction schemes should not be based exclusively on these results. Careful consideration should also be given to the number of catalytically active sites on the support. Studies in this area have demonstrated that less than 1% of the surface bound Cr would actually represent a potentially active species.[14b] We can therefore imagine that the spectroscopic information that is available would involve inactive Cr species.

The strong paramagnetism of most model Cr compounds, limiting the use of NMR spectroscopy as a tool,[17] is at the base of the difficulty encountered by researchers to clarify the mechanism. Cr alkyls in intermediate oxydation states of interest (II-IV) typically behave as *metallaradicals*. This would mean that these species have unpaired electrons and react similarly to organic radicals. This confines the study of heterogeneous catalysts to model studies carved out with homogeneous species where *conventional* analytical methods may be more informative and contribute to a deeper understanding of heterogeneous counterparts. This may also lead to the development of a new generation of catalysts. Therefore functional models, i.e. well-defined compounds that catalyze the polymerization of olefins, must be created. In describing his model for the Union-Carbide catalyst (discussed below), Theopold described the task at hand.

"The preparation and catalytic activity of molecules incorporating the structural elements required for an active catalyst will be the best arbiter of their relevance. If a structurally characterized Cr^{II} species, for example, does not polymerize ethylene in solution then it is unlikely to do so on a silica surface."[9]

Homogeneous Catalysts

In comparison, homogeneous systems have made great strides and a large variety of systems with different metals and ligand combinations have been synthesized and developed although their activity remains substantially lower (at least for Cr species) than the heterogeneous counterparts. More importantly, the study of homogeneous systems has provided important insights into the puzzle of heterogeneous catalysis.

Chromocenes as Models for the Union-Carbide Catalyst

While trying to model the heterogeneous Union-Carbide catalyst, Theopold and his group have used a variety of homogeneous cyclopentodienyl derivatives of Cr. It was concluded that *coordinatively unsaturated* Cp*Cr^{III} complexes, provide credible structural as well as a functional modeling of the active site of the Union-Carbide catalyst.

The reactivity observed for these Cr^{III} model compounds shows many similarities with the reactivity of the heterogeneous catalyst. Careful consideration of this family of compounds indicates that the final structure representing a coordinatively unsaturated Cr^{III} alkyl in figure 1.1 below is a good approximation of the Cr site in the act of chain propagation. The presence of the alkyl group in the latter has not, as yet, been explained.

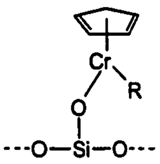

Figure 1.1 – The Cr^{III} active site proposed by Theopold.

It should be noted however that both the Union-Carbide catalyst and its model systems based on the cyclopentadienyl Cr^{III} complexes have an observed induction period. Although the exact nature of this induction period has not been identified, it is reasonable to speculate that a higher oxydation state may in fact be responsible for the initiation of polymer chain growth. This possibility is challenged by the inactivity of isolated Cr^{IV} metallacycles[18] towards polymerization. However, the systems characterized to date all show the metal center to be coodinatively saturated (**Figure 1.2**) and so would not meet the requirements discussed in more detail in a following section for the generation of an active polymerization site.

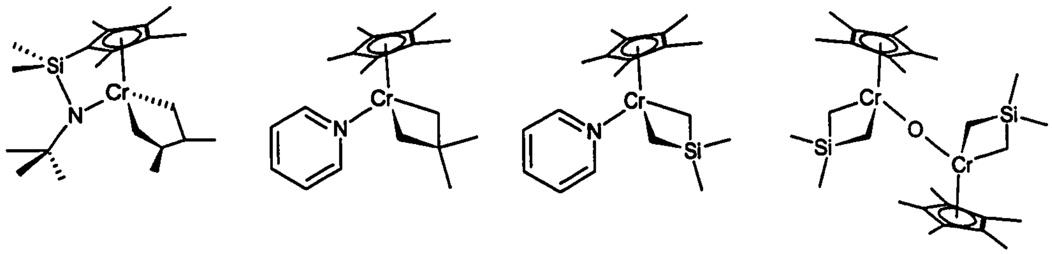

Figure 1.2 - Examples of characterized Cr-metallacycle species showing coordinative saturation.

Modeling the Philips Catalyst

There have been several attempts to model the activation of the Phillips catalyst in homogeneous solution. The success of these models has been very limited and the detailed nature of the active site is still largely undetermined. One example of such a model used cyclohexane solutions of bis(triphenylsilyl)chromate. Without the addition of cocatalyst, polymerization of ethylene occurred at high temperatures (T > 130°C) and pressures (P = 350 – 1500 atm).[19] In contrast with the parent Philips catalyst, polymerization of ethylene at room temperature and atmospheric pressure took place only after the addition of an aluminum alkyl and the reduction of the chromium center.

Looking at a similar case, Feher et al.[20] suggested a chromate ester of a silasesquioxane as an alternative model. This is probably the best available structurally characterized model of the oxidized Phillips catalyst. Benzene solutions of this compound, when activated with $AlMe_3$ to produced dark orange mixtures which polymerized ethylene at room temperature and atmospheric pressure. The proposed model does not however, clarify the oxidation state nor the chemical nature of the catalytic active site.

From the information available so far, it can be deduced that the active site of the Phillips catalyst involves a chromium species in a reduced state. Conclusive determination of the exact oxidation state of the metal still has not been accomplished and arguments persist. Since these homogeneous systems have all been shown to be less active then the heterogeneous counterparts, we must take another look at the basic structure of the catalytic active site in an effort to make improvements.

The Homogeneous Acitve Site

The *generic* catalytically active species in olefin polymerization is commonly accepted as a coordinatively unsaturated cationic alkyl complex $[L_nMR]^+$. This complex is stabilized by chelating ligands L. Three different strategies (A,B and C) can be employed to generate such species. These are illustrated in scheme 1.3.

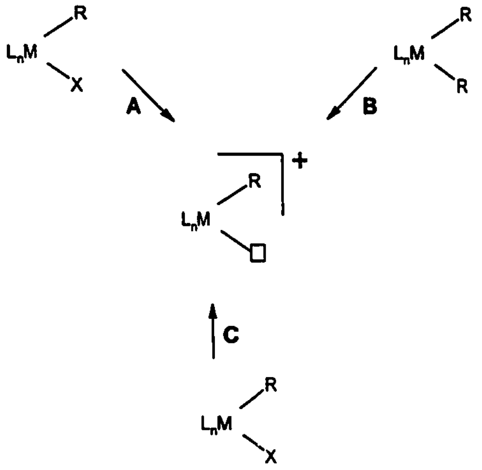

Scheme 1.3 – Three methods for the generation of the catalytically active species $[L_nMR]^+$.   represents the site of coordinative unsaturation.

Route A involves the abstraction of an anionic ligand such as a halide. This is then substituted with a *noncoordinating* (usually bulky) anion by precipitation under the form of insoluble salts. Common reagents are $Na\{B[3,5\text{-}(CF_3)_2C_6H_2]_4\}$[21] or silver salts such as $AgBF_4$ or $AgOSO_2CF_3$ (AgOTf) for the later transition metals.

In method B, an alkyl ligand (anion) is abstracted from the parent dialkyl compound. Reagents used in these abstraction are most commonly the perfluorinated arylboranes (BARF) compounds: $[Ph_3C][B(C_6F_5)_4]$, $[PhNHMe_2][B(C_6F_5)_4]$, $[H\{OEt_2)_2][B\{3,5\text{-}(CF_3)_2C_6H_3\}_4]$[21] or $B(C_6F_5)_3$. It is noteworthy that the use of $B(C_6F_5)_3$ only partially abstracts the alkyl ligand. This leads to a *cation-like* catalytic species.[22]

Lastly, route C combines the alkylation and abstraction process. This is achieved by treating a dihalide parent compound with an alkylating species, followed by reaction with a ligand abstracting compound such as those previously mentioned. For example treatment with a trialkylaluminum compound could be followed by $B(C_6F_5)_3$. The advent of methylaluminoxane (MAO)[23] whose structure is schematically represented in figure 1.3 has combined both requisites by reducing this operation to one step, the cocatalyst acting as both alkylating and ligand abstracting agent.

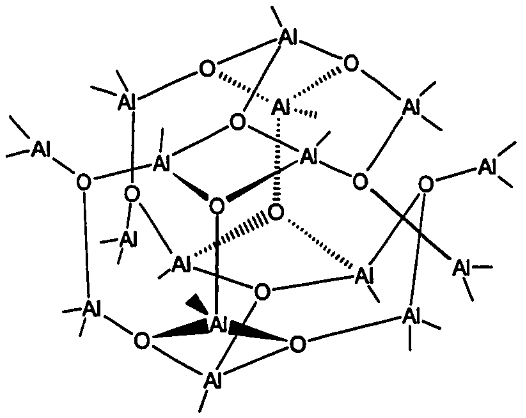

Figure 1.3 - Proposed structure of methyaluminoxane.[24]

What is evident is that strong Lewis acidity of the metal center is crucial to the activation process. This promotes the coordination of ethylene to the reactive site. Another key aspect is the presence of M-C bonds where the coordinated olefin can be inserted and the alkyl group included in the growing polymer backbone.

The Mechanics of Polymerization

According to a mechanism proposed by Cossee,[25] once the catalytically active species is generated, although several pathways can be followed, only one of these leads to polymerization of the olefin monomer. The insertion of olefin as shown in scheme 1.4 is obviously the most crucial step in the polymerization mechanism. From the olefin coordinated transition state, propagation occurs via the subsequent insertion of the olefin into the M-C bond adjacent to the coordination site. Therefore, the relative energy required for this coordination should be low when compared to the β-hydrogen elimination termination process (scheme 1.4). The latter would lead from the active precursor to the corresponding hydrido olefin complex.

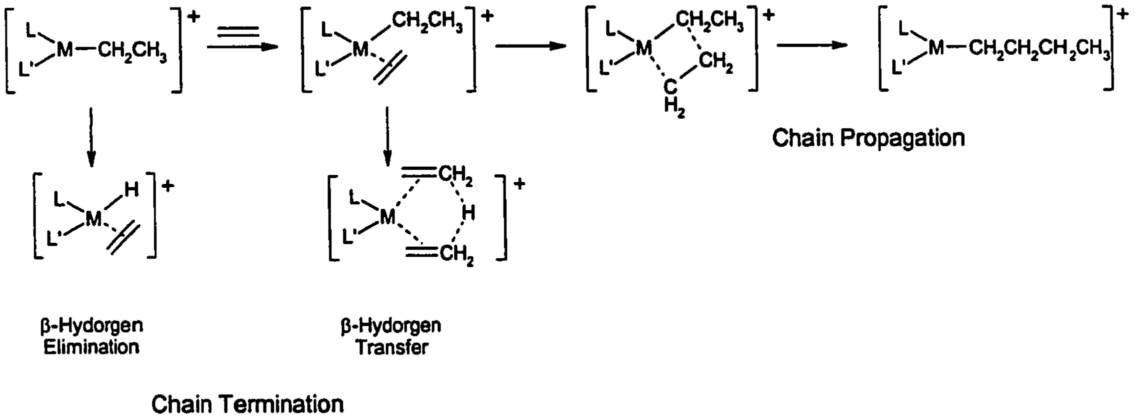

Scheme 1.4 - Elementary steps of chain propagation and chain termination.

Furthermore, the evolution of the olefin coordinated transition state towards propagation must be more prevalent, i.e. more energetically favorable, than the possible termination of the propagation cycle by β-hydrogen transfer. In the later, a H from the alkyl function already bound to the metal center is transferred to the coordinating olefin. This results in the exchange of the olefinic function to the polymer chain. Here the catalyst active site can be seen as remaining *intact*, however no further chain growth occurs. In a practical setting, substantial difference in activation energy between propagation and termination steps translates into the generation of high MW polymers as opposed to oligomerization.

The optimization of the active site represented in scheme **1.3** must represent the underlying goal of any research undertaken. Of the two approaches to be taken in this endeavor, chapters II & III of this work concentrate on the selection of a specific metal centers (Cr, V) to increase the reactivity of the catalytic active site towards ethylene insertion.

Reactive Metal Centers (Cr)

As stated by Theopold in the development of his model the Union-Carbide catalyst: "*a minimum requirement for the active site is an alkyl group (or hydride) bonded to the chromium.*"[9] Furthermore, Ziegler et al. investigated model systems of first row transition metals having electronic configurations ranging between d^1 to d^4 in an effort to identify the role of the metal oxydation state in determining catalytic activity.[26] A study of the energy requirements for the propagation processes highlighted in scheme **1.4** as opposed to the energy requirements for the chain termination processes has shown that a

d^2 electronic configuration in first row transition metals such as V^{III}, Cr^{IV}, Mn^{V} would generate highly active olefin polymerization catalysts.

Given this proposal, the simplest strategy for the creation of an *optimal* active site would involve homoleptic alkyl species. The use of single species where all of the alkyl groups are equivalent could reduce the possibility of "ligand effect" thereby generating an active site where the sole remarkable promoter is the oxydation state of the metal center. This may help to clarify the role of the electronic configuration of the metal in the active site.

In the case of tetravalent chromium compounds, the stability of homoleptic alkyls was first demonstrated by Wilkinson in the 1970's. The trimethylsilylmethyl Cr species[27] was claimed to have an astonishing inertness towards protic reagents. The obvious advantage associated with this apparent inertness is that the β-hydrogen termination reactions (scheme **1.4**), considered to be the obstacles to chain propagation, would be eliminated.

The proposed synthetic strategy for Cr^{IV} alkyls per say, raises an interesting question. The reaction uses a trivalent salt ($CrCl_3THF_3$) to produce the Cr^{IV} alkyl, yet the pathway by which the Cr species is oxydized to the tetravalent product, in the presence of reducing RLi reagents, remains unexplored. The elucidation of these steps by which a trivalent Cr salt generates a tetravalent homoleptic alkyl may provide valuable information. Chapter II is a revisitation of the chemistry of two tetravalent homoleptic Cr alkyls proposed by Wilkinson, investigating their reactivity both towards ethylene and other reagents.

During efforts to clarify the mechanism, a rare case tetrameric Cr^{II} homoleptic alkyl species was also isolated and characterized. This compound was first reported by Smith in the 1990's.[28] A crystallographic study and interpretation of its magnetic properties is presented in conjunction with the tetravalent counterparts. The stability of the tetranuclear cluster is investigated and suggests the existence of strong Cr-Cr bonding interaction.

Reactive Metal Centers (V)

In parallel, a study was undertaken to probe the behavior of vanadium derivatives. A similar synthetic route afforded a d^1 tetravalent vanadium compound that is isostructural with the Cr derivative. The synthesis of this homoleptic V alkyl species has been claimed in literature [27a,29] although no crystallographic data or information as to activity towards polymerization has been recorded.

Having the availability of this isostructural compound was attractive since it allowed to tentatively correlate the modification of the electronic configuration (from d^2 to d^1) to activity and polymer quality. Vanadium compounds are usually more reactive than their Cr counterparts and so the remarkable stability, which proved problematic during the functionalization of the latter materials, may not be so limiting in the case of V. An increased activity was observed in this case through the relative thermal instability of the tetravalent V compound as compared to the Cr equivalent. The tetrakis-trimethylsilylmethyl-vanadium species described in Chapter III provides the first crystallographic characterization of a VR_4 species and was a very potent olefin polymerization catalyst.

Stabilizing Ligand

A look back at the general active site shown in scheme **1.3** can suggest an alternate method of improving the reactivity of metal center. The focus can be drawn away from the metal center in search of a particular ligand system to be employed.

The chelating ligands in active polymerization catalyst have a fourfold function:

1) control over the metal coordination number
2) control over the metal coordination geometry
3) control over the formal oxidation state of the metal
4) steric protection of the active site and influence over (stereo)selectivity

To illustrate these points, a series of compounds is represented in figure **1.4**. The nature of chelating dianionic diamide ligand controls the geometry such that the metal halide moiety of the catalysts can be stabilized in a pseudo-tetrahedral environment or in distorted trigonal-bypyramidal environments as in the complexes **2-4** illustrated below.

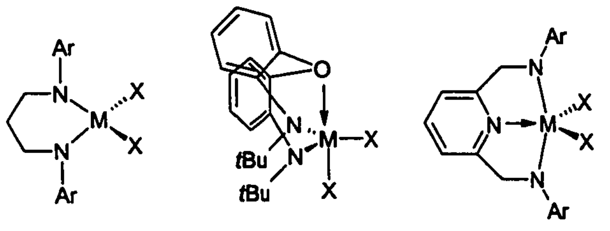

2 **3** **4**

Figure 1.4 - Effect of the ligand on the metal environment.

In the three examples depicted above, the presence of an etheral or pyridyl bridge influences the relative dispositions of the metal-attached atoms. The N,O,N atoms of the ligand are arranged in a trigonal disposition in the case of **3** with the oxygen in the axial position of the trigonal bipyramid. In comparison, the N,N,N tridentate chelating ligand of **4** enforces a planar arrangement, relating the chloro ligands to the equatorial sites of the trigonal bypiramid.

Work by Brookhart et al. has demonstrated that Ni^{II} and Pd^{II} complexes can be transformed from olefin oligomerization catalysts into extremely active polymerization catalyst when the steric bulk on the ligands is increased.[30] This effect has been the target of theoretical calculations that suggested a larger destabilization of the chain termination transition state relative to the chain propagation transition state.[31] (Scheme **1.4**).

The particular α,α'-diiminopyridine ligand used in these cases (see **4** in figure **1.4**) has made quite a stir in recent literature. Indeed the isolation, through the utilization of this ligand, of active catalyst systems employing metals previously not considered for polymerization processes (Ni, Pd, Fe, Co)[30,32] has opened the door to a multitude of possible active centers. However, the growing number of isolated derivatives show a significant transformation of the ligand itself upon reaction with various activating Al species. Alkylating agents have been shown to attack the imino function[33] and all of the pyridine ring atoms including the N.[34] In addition, dimerization may be achieved via imine reductive coupling or via cycloaddition of two pyridine rings to form a tri-cyclic system.[34b] During this unusual variety of transformations, the metal center coordinated to the ligand may engage in redox reactions thereby lowering or even increasing its oxidation state.[34a,35] The α,α'-diiminopyridine moiety thus plays more than an ancillary stabilizing role in the initiation process.

The ability of the ligand to engage in internal exchange processes with the metal directly affects the Lewis acidity of the active center and its behavior as a potential catalyst. Chapter IV of this work takes a closer look at the popular α,α'diiminopyridine ligand to examine its rather unique characteristics in reactivity. Two rare case trilithium organyls are characterized from the reaction of the free ligand with strong reducing agents (Li metal and Li-naphtalenide).

References

---

1. Kaminsky W., *J. Chem. Soc., Dalton Trans.*, **1998**, 1413-1418.
2. Le Devoir - Édition spéciale, le samedi 31 août et le dimanche 1^{er} septembre 2002, *Le Sommet de Johanisburg*, Montréal, www.ledevoir.com/dossiers/244/.
3. Ziegler K., *Nobel Lectures in Chemistry, 1963-1970*; Elsevier: Amsterdam, 1972; p.6.
4. Natta G., *Nobel Lectures in Chemistry, 1963-1970*; Elsevier: Amsterdam, 1972; p.27.
5. Soga K., Shiono T., *Prog. Polym. Sci.*, **1997**, 22, 1503.
6. a) Zeigler K., *Belgian Patent 533,362*, **1954**. b) Zeigler K., Holzkamp E., Martin H., Breil H., *Angew. Chem.*, **1956**, 68, 393.
7. Britovsek G.J.P., Gibson V.C., Wass D.F., **1999**, 38, 428-447
8. McDaniel M.P., *Adv. Catalysis*, **1985**, 33, 47.
9. Theopold K.H., *Eur. J. Inorg. Chem.*, **1998**, 15-24 *and references therein.*
10. a) Krauss H.L., Stach H., *Inorg. Nucl. Chem. Lett.*, **1968**, 4, 393. b) Krauss H.L., Stach H., *Z. Anorg. Allg. Chem.*, **1969**, 366, 280.
11. a) Hermes A.R., Morris R.J., Girolami G.S., *Organometallics*, **1988**, 7, 2372. b) Frysuk M.D., Leznoff D.B., Rettig S.J., *Organometallics*, **1995**, 14, 5193.
12. Karapinka G.L., *U.S. Patent 3,709,853*, **1973**.
13. Karol F.J., Karapinka G.L., Wu C., Dow A.W., Johnson R.N., Carrick W.L., *J. Polym. Sci., Part A-1*, **1972**, 10, 2621.
14. a) Fu S.L., Lunsford J.H., *Langmuir*, **1990**, 6, 1774. b) Fu S.L., Rosyneck M.P., Lunsford J.H., *Langmuir*, **1991**, 7, 1179. c) Zecchina A., Spoto G., Ghiotti G.,

---

Garrone E., *J. Mol. Catal.*, **1994**, 86, 423. d) Scarano D., Spoto G., Bordiga S., Carnelli L., Ricchiardi G., Zecchina A., *Langmuir*, **1994**, 10, 3094. e) Zecchina A., Spoto G., Bordiga S., *Faraday Discuss. Chem. Soc.*, **1989**, 87, 149. f) Conway S.J., Falconer J.W., Rochester C.H., *J. Chem. Soc. Faraday Trans.*, **1989**, 85, 79. g) Rebenstorf B., *J. Catal.*, **1989**, 117, 71. h) Zielinski P., Dalla Lana I.G., *J. Catal.*, **1992**, 137, 368.

15. a) Zhang G., Auburn P.R., Beach D.L., *Jpn. J. Appl. Phys.*, **1993**, 32, 511. b) Ellis P.J., Joyner R.W., Maschmeyer T., Masters A.F., Niles D.A., Smith A.K., *J. Mol. Cat. A*, **1996**, 111, 297.

16. Schnellbach M., Köhler F.H., Blümel J., *J. Organomet. Chem.*, **1996**, 520, 227.

17. a) Grohmann A., Köhler F.H., Müller G., Zeh H., *Chem. Ber.*, **1989**, 122, 897. b) Hebendanz N., Köhler F.H., Scherbaum F., Schlesinger B., *Magn. Reson. Chem.*, **1989**, 27, 798. c) Blümel J., Hofmann P., Köhler F.H., *Magn. Reson. Chem.*, **1993**, 31,2. d) Köhler F.H., Metz B., Strauss W., *Inorg. Chem.*, **1995**, 34, 4402. e) Blümel J., Herker M., Hiller W., Köhler F.H., *Organometallics*, **1996**, 15, 3474. f) Heintz R.A., Neiss T.G., Theopold K.H., *Angew. Chem. Int. Ed. Engl.*, **1994**, 33, 2326. g) Bhandari G., Kim Y., McFarland J.M., Rheingold A.L., Theopold K.H., *Organometallics*, **1995**, 14, 738.

18. a) Liang Y., M. Sc. thesis, University of Delaware, **1996**. b) Papp R.. M. Sc. thesis, University of Delaware, **1989**.

19. Baker L.M., Carrick W.L., *J. Org. Chem.*, **1970**, 35, 774.

20. Feher F.J., Blanski R.L., *J. Chem. Soc. Chem. Commun.*, **1990**, 1614.

21. Brookhart M., Grant B., Volpe A.F., *Organometallics*, **1992**, 11, 3920.

---

22. a) Yang X., Stern C.L., Marks T.J., *J. Am. Chem. Soc.*, **1991**, 113, 3623. b) Yang X., Stern C.L., Marks T.J., *J. Am. Chem. Soc.*, **1994**, 116, 10015.

23. a) Kaminsky W., *Macomol. Chem. Phys.*, **1996**, 197, 3907. b) Pasynkiewicz S., *Polyhedron*, **1990**, 9, 429. c) Pasynkiewicz S., *Macromol. Symp.*, **1995**, 97, 1-13. d) Barron A.R., *Macromol. Symp.*, **1995**, 97, 15-25.

24. Sinn H., *Macromol. Symp.*, **1995**, 97, 27.

25. Cossee P., *J. Catal.*, **1964**, 3, 80.

26. Schmid R., Ziegler T., *Organometallics*, **2000**, 19, 2756.

27. a) Mowat W., Shortland A., Yagujpsky G., Hill N.J., Yagupsky M., Wilkinson G., *J. Chem. Soc. Dalton Trans.*, **1972**, 533. b) Mowat W., Shortland A., Hill N.J., Wilkinson G., *J. Chem. Soc. Dalton Trans.*, **1973**, 770.

28. a) Smith P.D., Hsieh E.T., U.S. Patent 4,587,227, 1986. b) Smith P.D., McDaniel M.P., *J. Polym. Sci. A, Polym. Chem.*, **1990**, 28, 3587.

29. Razuvaev G.A., Latyaeva V.N., Vyshinskaya L.I., Drobotenko V.V., *J. Organomet. Chem.*, **1981**, 208, 169

30. a) Johnson L.K., Killian C.M., Brookhart M.J., *J. Am. Chem. Soc.*, **1995**, 117, 6414. b) Johnson L.K., Mecking S., Brookhart M.J., *J. Am. Chem. Soc.*, **1996**, 118, 267. c) Killian C.M., Tempel D.J., Johnson L.K., Brookhart M.J., *J. Am. Chem. Soc.*, **1996**, 118, 11664. d) Rix F.C., Brookhart M., White P.S., *J. Am. Chem. Soc.*, **1996**, 118, 4746.

31. a) Deng L., Margl P.M., Ziegler T., *J. Am. Chem. Soc.*, **1997**, 119, 1094. b) Deng L., Woo T.K., Cavallo L., Margl P.M., Ziegler T., *J. Am. Chem. Soc.*, **1997**, 119, 6177. c) Froese R.D.J., Musaev D.G., Morokuma K., *J. Am. Chem. Soc.*, **1998**,

---

120, 1581. d) Musaev D.G., Froese R.D.J., Morokuma K., *Organometallics*, **1998**, 17, 1850.

32. Small B.L., Brookhart M., Bennett A.M.A., *J. Am. Chem. Soc.*, **1998**, 120, 4049. b) Britovsek G.J.P., Gibson V.C., Kimberley B.S., Maddox P.J., McTavish S.J., Solan G.A., White A.J.P., Williams D.J., *J. Chem. Soc. Chem. Commun.*, **1998**, 849.

33. Bruce M., Gibson V.C., Redshaw C., Solan G.A., White A.J.P., Williams D.J., *J. Chem. Soc. Chem. Commun.*, **1998**, 2523.

34. a) Reardon D., Conan F., Gambarotta S., Yap G.P.A., Wang Q., *J. Am. Chem. Soc.*, **1999**, 121, 9318. b) Sugiyama H., Aharonian G., Gambarotta S., Yap G.P.A., Budzelaar P.H.M., *J. Am. Chem. Soc.*, in press. c) Korobkov I., Gambarotta S., Yap G.P.A., Budzelaar P.H.M., *Organometallics*, in press. b) Clentsmith G.K.B., Gibson V.C., Hitchcock P.B., Kimberly B.S., Rees C.W., *J. Chem. Soc. Chem. Commun.*, **2002**, 1498.

35. a) Reardon D., Aharonian G., Gambarotta S., Yap G.P.A., *Organometallics*, **2002**, 21, 786. b) Kooistra M., Knijnenburg Q., Smits J.M.M., Horton A.D., Budlezaar P.H.M., Gal A.W., *Angew. Chem.*, **2001**, 40, 4719. b) Gibson V.C., Humphries M., Tellmann K., Wass D., White A.J.P., Williams D.J., *Chem. Comm.*, **2001**, 2252.

CHAPTER II

THE UNUSUAL STABILITY OF HOMOLEPTIC DI- AND TETRAVELENT CHROMIUM ALKYLS

The Unusual Stability of Homoleptic Di- and Tetravalent Chromium Alkyls

Introduction

The +4 oxidation state of chromium is not easily accessible despite the great potential that may be envisioned for tetravalent chromium complexes as polymerization catalysts. Homoleptic, tetravalent chromium alkyls, first isolated and characterized by Wilkinson in the seventies, can be prepared by reaction of $CrCl_3(THF)_3$ with an equivalent amount of the Grignard reagents.[1] The isolation of species having stable M-C bonds with Cr, requires the use of ligands which do not have H (or other atoms easily transferred to the metal) on the β-position adjacent to the metal center thereby preventing alkene elimination.

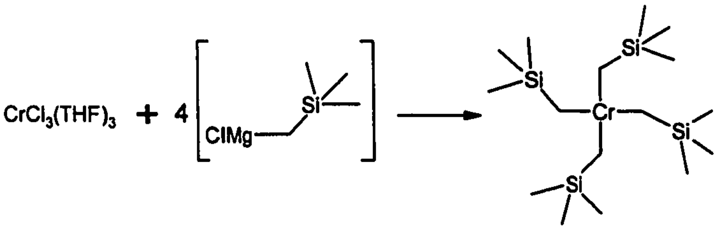

Scheme 2.1 – Synthesis of stable homoleptic tetravalent Cr-alkyl by Wilkinson.[1]

Several ligand systems have been successfully used to produce metal alkyls and as such, have dispelled the myth that such metal to carbon bonds are very weak.[2] In fact, these rare species seem to possess surprising chemical inertness including resistance to the attack of acidic aqueous solutions.[2] Given the uncommon stability of isolated Cr alkyl species, some limitations may be anticipated in using them as starting materials.

Besides the tetravalent derivatives, a few air-sensitive divalent chromium alkyls, both monomeric[3] and dimeric[4], are known. The diamagnetism or residual paramagnetism in the dinuclear complexes was taken as an indication for the existence of a debated Cr-Cr multiple bonding interaction.[5] A unique case of a tetranuclear divalent chromium cluster was reported by Smith.[6] Trivalent chromium tris-alkyl compounds remain almost unknown[7] apart from the cyclopentadienyl derivatives.[8]

What renders chromium organometallic complexes particularly appealing is the established ability of the Cr-C bond to perform ethylene polymerization[9] or selective trimerization,[10] which is being exploited for the commercial production of polymers or oligomers important to a wide range of industrial applications. Thus, it is at least strange that all the chromium organometallic complexes reported to date, including species grafted on solid state supports,[11] display only moderate catalytic activity. While information about catalytic activity of tetravalent chromium species is non-existent, theoretical calculations have predicted that the d^2 electronic configuration may be particularly promising for a performing catalyst.[12]

Following interest in homoleptic Cr alkyls,[4g-i] the preparation of two tetravalent d^2 chromium alkyls[1] was revisited. Of particular interest, was their ability to work both as starting materials for further functionalization and as Ziegler-Natta catalysts. The clarification of the reaction pathway through which a trivalent chromium salt may form a homoleptic tetravalent derivative[1,2] was also considered to be beneficial. Finally we were interested in elucidating the nature of the Cr-Cr interaction in the unique $[R_2Cr]_4$ tetranuclear cluster[6] and evaluating its stability.

For this work the Me_3SiCH_2 and neopentyl ligands were selected because of their well-known ability to stabilize the M-C functionality for a variety of metals. These ligands are also known to be involved in the formation of carbenes and stabilized olefin polymerization catalyst precursors.[8n,9]

Results

Synthesis of $Cr[CH_2C(CH_3)_3]_4$ (**5a**) *and $Cr[CH_2Si(CH_3)_3]_4$* (**5b**).

The preparation of the two homoleptic derivatives R_4-Cr [R = Me_3CCH_2 (**5a**), Me_3SiCH_2 (**5b**)] was carried out according to the original preparation described by Wilkinson.[1] Reaction in ether of freshly prepared solutions of RMgCl with a suspension of $CrCl_3(THF)_3$ afforded dark brown and dark violet crystals, respectively, of the corresponding complexes **5a** and **5b** (Scheme **2.2**). Both products were isolated in moderate yield upon crystallization from hexane followed by sublimation. Correct combustion analysis results were obtained for the expected formulation. The room temperature magnetic moments for these two compounds are in good agreement with the values reported by Wilkinson (**5a** $\mu_{eff} = 2.91\ \mu_B$, **5b** $\mu_{eff} = 2.89\ \mu_B$) and are as expected for the high-spin d^2 electronic configuration of tetravalent chromium centers. The two complexes are thermally robust and did not show signs of decomposition upon refluxing in toluene for 24 hours.

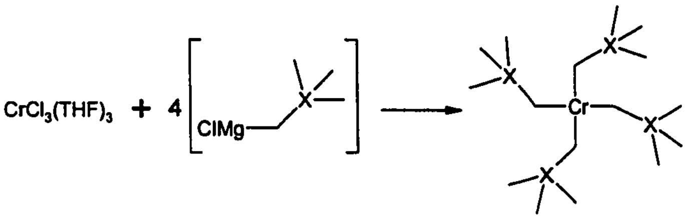

5a X = C
5b X = Si

Scheme 2.2 – Reaction of $CrCl_3(THF)_3$ with Grignard reagents.

Since crystallographic data are not available for these two complexes, an X-ray diffraction study was undertaken. Crystals of both **5a** and **5b** diffracted rather poorly. Nevertheless, it was possible after several attempts to obtain single crystals that produced data files of sufficient quality to solve the structure of each compound and to confirm the connectivity.(1,2) The two complexes possess the expected tetrahedral structure (Figures **2.1** and **2.2**) with C-Cr-C-angles varying in the range 106.1°-115.5° for **5a** and 107.3°-108.9° for **5b**. The Cr-C distances also compare rather well ranging from 1.961 Å to 2.031 Å for **5a** and from 1.954 Å to 1.983 Å for **5b**. The geometrical parameters compare well with those of the neophyl derivative of very similar structure.[2d]

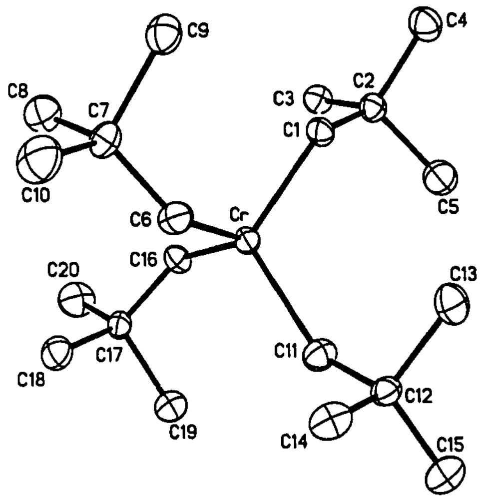

Figure 2.1 - Thermal ellipsoid representation of (**5a**) $C_{20}H_{44}Cr$

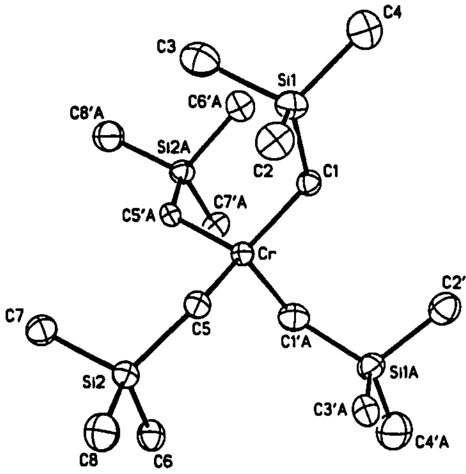

Figure 2.2 - Thermal ellipsoid representation of (**5b**) $C_{16}H_{44}CrSi_4$

Both structures displayed conformational disorder arising from the flipping over two positions of the CH_2 groups directly attached to chromium, and some rotational disorder of the t-Bu and Me_3Si groups along the CH_2-C and CH_2-Si bonds. This behavior was reflected in the convergence factors which remain unpleasantly high.

---

[1] For full details of the structures obtained see Appendix I – Crystallographic Data: Homoleptic Chromium Alkyls.

[2] A list of significant bond lengths and angles are given in table 2.1 at the end of this chapter.

Reactions of **(5a)** *and* **(5b)**.

Both **5a** and **5b** are pyrophoric and immediately ignite upon exposure to air (**Warning!**). Nevertheless, these species display, in agreement with Wilkinson's observation, a remarkable inertness towards protic reagents. No reaction was observed upon refluxing in toluene, while reaction with either phenols or carboxylic acid took place *only after refluxing in toluene for 15 h*, affording decomposition.

In sharp contrast to this surprising inertness towards protic agents, a smooth reaction took place at room temperature with tetraphenyldisiloxane-1,3-diol, producing the trimeric $[Ph_2SiO]_3$ in good yield (Scheme **2.3**). Regrettably, the fate of the chromium moiety remained unclear despite repeated attempts to isolate a tractable product.

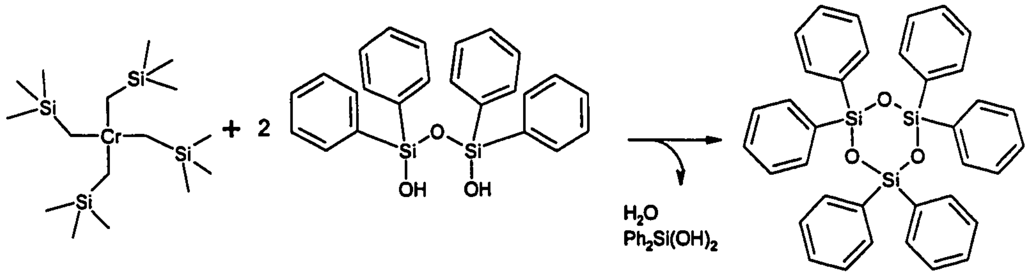

3

Scheme 2.3 - Reaction of $Cr[CH_2Si(CH_3)_3]_4$ (**5b**) with tetraphenyldisiloxane-1,3-diol.

The formation of $[Ph_2SiO]_3$ implies a formal abstraction of one molecule of water from the disilanolate. Thus, different perspectives might be envisioned about the grafting of CrR_4 on silica surfaces,[10] where a similar dehydration might actually occur as an alternative to the grafting process.

Polymerization Testing

Solutions of **5** do not react appreciably with ethylene or other α-olefins at room temperature and atmospheric pressure. However, in the presence of 2 equiv. of $AlCl_3$ a vigorous reaction forming polyethylene took place. The catalytic activity of **5b** of 1.1 kg of PE/mol/h/atm is moderate and in the range of the other homogeneous chromium catalysts reported so far in the literature.[19,20] The polyethylene displayed a fairly high MW of 699 500 g/mol and rather broad polydispersity (5.0).

Synthesis of $Cr_4[CH_2Si(CH_3)_3]_8$ (**6b**).

Compound **6b** was conveniently prepared by reacting $CrCl_2(THF)_2$ with 2 equiv. of the lithium reagent. Attempts to prepare a neopentyl derivative, which we presumed would proceed in a similar manner, afforded only intractable materials. The formation of **6b** in high yield via reduction of a trivalent species is not particularly surprising given the well-known ability of organolithium reagents to act as reductants. We have analyzed the mother liquor solutions for the possible presence of **5b** as a partner product of a disproportionation process. However, not even traces of **5b** could be detected upon sublimation of the dried residues, thus ruling out that its formation might be due to a disproportionative pathway.

Since the atomic coordinates and the geometrical parameters of **6b** were not available from the patent literature, another crystal structure determination was undertaken. This confirmed the tetrameric structure of **6b** as composed of four square planar divalent chromium centers bridged by the eight methylene groups of the trimethylsilyl groups (Figure 2.3). Each chromium is connected to two neighbor chromium centers by two bridging trimethylsilylmethyl groups, while the four chromium atoms define a nearly regular square plane [deviation from the plane 0.0173 Å, Cr-Cr-Cr-angles ranging between 89.65° and 90.30°].

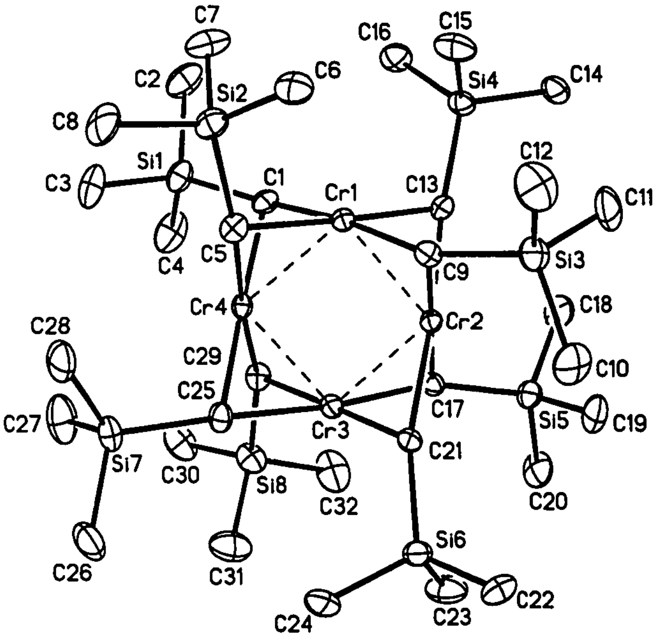

Figure 2.3 - Thermal ellipsoid representation of **(6b)** $C_{32}H_{88}Si_8Cr_4$

The overall structure can be described in terms of a nearly regular cube with the eight methylene groups of the CH_2SiMe_3 groups occupying each corner and the chromium atoms located in the center of the four side faces while the top and bottom faces remain unoccupied. The coordination geometry around each of the chromium centers is regular square planar and rather similar to that of $Cr_2(CH_2SiMe_3)_4(PMe_3)_2$ and $[Cr_2(CH_2SiMe_3)_6]^{2-}$.[4d,j] The Cr-C-Cr-angles range between 62.98° and 65.22° and are as expected for CH_2-trimethylsilyl bridging groups.

Magnetic Properties

The Cr · · · Cr distances in **6b** (ranging from 2.331 Å to 2.402 Å) fall in a range consistent with metal-metal multiple bonding,[5] yet the complex is paramagnetic at room temperature with a low magnetic moment of about 1.61 μ_B (mol) at 300 K, dropping to 0.3 μ_B at 2 K. This is represented below in figure **2.4**.

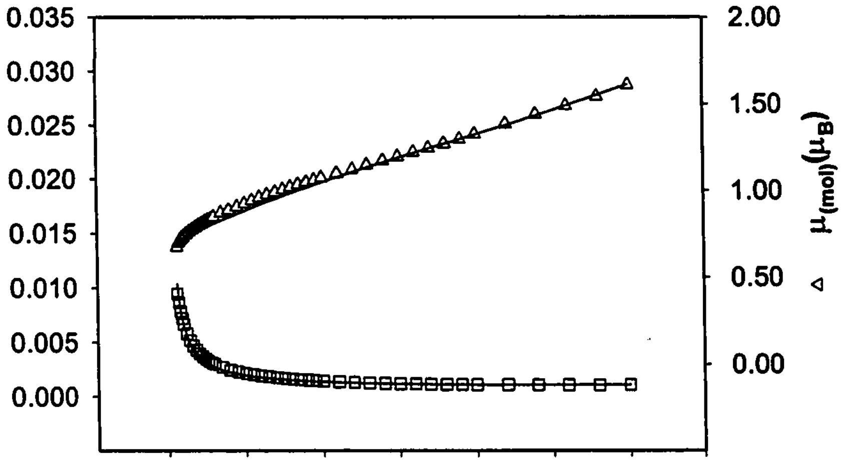

Figure 2.4 - Plot of the 1/χ and of the μ_{eff} against T for **6b**. Best fitting was obtained with g = 2.188, J = -510, TIP = 0.00079, ρ = 0.004 θ = -0.05

High spin mononuclear Cr^{II} systems in a weak square-planar field are expected to show much higher moments at room temperature (4.7-4.9 μ_B), with minor depression of the moment as temperature is lowered. For a low spin system, significant spin-orbit coupling effects can lead to significant depression of the moment from room temperature values around 3-3.3 μ_B to 0 μ_B, but only at temperatures approaching 0 K. The mononuclear Cr^{IV} complexes **5a** and **5b** have moments at room temperature consistent with the presence of two unpaired electrons (**5a** μ_{eff} = 2.91 μ_B, **5b** μ_{eff} = 2.89 μ_B), as would be expected. The Cr centers in **6b** are nominally square-planar, and so might be expected to exist in a high spin configuration (d^4). However the very low overall moments exhibited by **6b**, and the significant drop on lowering temperature, are more reasonably associated with intramolecular spin coupling, through a superexchange mechanism, which would be antiferromagnetic in nature. The data for **6b** were fitted to an isotropic exchange model for four $\mathrm{Cr^{II}}$ centers arranged in a square with a single exchange integral, according to the appropriate Hamiltonian expression (eqn. 1).

$$\mathrm{H = -J\{S_1.S_2 + S_2.S_3 + S_3.S_4 + S_1.S_4\}} \text{------------------------} (1)$$

$$\chi_M f = \frac{N\beta^2 g^2 \rho \sum S(S'+1)(2s'+1)exp[-E(S')/kT]}{3k(T-\theta)\sum S'(2S'+1)\exp[-E(S')/kT]} \text{------------------------} (2)$$

$$\chi_M = \chi_{M'}(1-\rho) + \frac{2N\beta^2 g^2 \rho}{3kT} + TIP \text{----------------------------------} (3)$$

Using the vector coupling scheme, the appropriate energy levels and spin states were derived and substituted into the Van Vleck equation (eqn. 2), and corrections made for TIP (temperature independent paramagnetism), Weiss like temperature effects (θ) and paramagnetic impurity fraction (ρ) (eqn. 3).[22] A satisfactory fitting of the magnetic data was obtained by using the integrated software package MAGMUN 4.0.[23] The data for **6b** were fitted to eqn. 3 for both low spin (d^2) and high spin (d^4) cases. Reasonable fits were obtained in both cases with $g = 2.188$, $J = -510\ \mathrm{cm^{-1}}$, TIP = $0.00079\ \mathrm{cm^3.mol^{-1}}$, $\rho = 0.004$, $\theta = -0.05$, ($10^2\mathrm{R} = 6.1$; $\mathrm{R} = [\,(\chi_{obs.} - \chi_{calc.})^2/\chi_{obs}^{\,2}]^{1/2}$) for the d^4 case and $g = 2.193$, $J = -475\ \mathrm{cm^{-1}}$, TIP = $0.000765\ \mathrm{cm^3.mol^{-1}}$, $\theta = 0.012$, $\theta = 0$ ($10^2\mathrm{R} = 6.4$) for the d^2 case. The solid line in figure **2.4** is calculated with the best fit data for the high spin case. The data below 6 K show quite a sharp drop in moment, perhaps indicative of zero-field splitting effects. These data have not been included in the data fit.

However since zero-field splitting is likely to be very much smaller than $|J|$ the exchange coupling clearly dominates.

Theoretical Calculations

Given the magnetic behavior, Density Functional Theory (DFT) calculations were carried out on the singlet state. In good agreement with this working hypothesis, the LUMO (-3.972 eV), HOMO (-4.069 eV) and HOMO-1 (-4.087 eV) are nearly degenerate with a HOMO-LUMO gap of only 0.097 eV (Figure **2.5**) thus explaining the appearance of magnetism by incrementing the temperature. The reason for the incomplete degeneracy is likely to be ascribed to the unequal Cr-Cr bond distances ranging from 2.34 to 2.40 Å.

Among the frontier orbitals, the HOMO, HOMO-1, HOMO-3, HOMO-4, HOMO-6 and HOMO-8 all are between 97 and 100% Cr-centered (Figure **2.5**) indicating a surprising non-participation of the ligand bridging carbon atoms and the presence of a substantial Cr-Cr bond interaction. The LUMO and the HOMO-1 are pure Cr-Cr δ-bonds with identical shapes but different orientation in the sense that the two vertical nodal planes are perpendicular to each other, while the horizontal nodal plane coincides for both orbitals with the molecular plane. Both MO's are generated by the overlap of the *d* orbitals orthogonal to the molecular plane (Figure **2.5**), forming four lobes in the center of the tetrametallic unit. The HOMO can be described as a combination of two Cr-Cr π-bonds each between one couple of chromium atoms generated by in plane combination of *d* orbitals forming four out of phase lobes lying on the molecular plane. A second MO with a strong π-character is provided by HOMO-2 (-4.783 eV) formed by the in-phase hybrid combination of *d* orbitals perpendicular to the molecular plane and oriented towards the center of the molecule. The main feature consists of two large lobes located on the

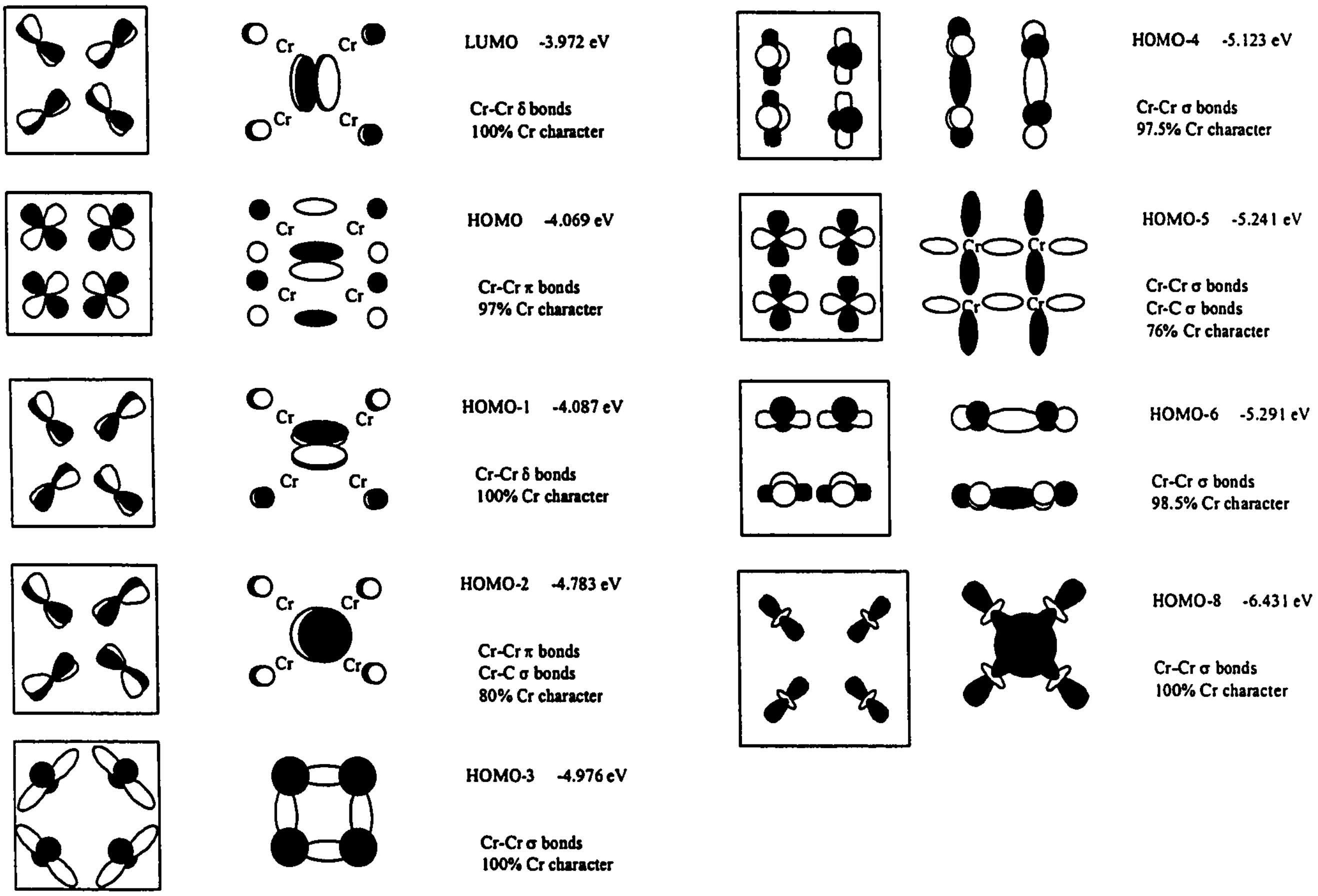

Figure 2.5 - Schematic representation of the frontier molecular orbitals of **6b**.

two sides of the molecular plane. There is, however, a small but non-negligible participation of the bridging carbon atoms *p* orbitals (20 %). On the same line, HOMO-7 (-6.340 eV) also is a Cr-Cr π-bond again forming two large lobes in the center of the molecules above and below the plane defined by the tetrametallic unit. In this MO however, the participation of the bridging carbon atoms appears to be more significant, the Cr-Cr bond character being only 60%. The Cr-Cr σ-bonding interaction is realized through a series of five MO's (from HOMO-3 to HOMO-6) arising from overlap of the lobes of *d* orbitals located either coplanar or perpendicular to the tetrametallic unit. Particularly appealing is HOMO-8 (-6.431 eV), consisting of a large lobe located in the center of the molecule. The orbital appears to be formed by hybrid combination of *d* atomic orbitals strongly reminiscent in shape of the d_{z^2} lying on the molecular plane and directed towards the center of the molecule. Though not considered in great detail in this report, frontier orbitals HOMO-9 through HOMO-14 all exhibit some Cr-Cr bonding character but with a major participation of the ligand bridging carbon atoms.

Reactions of $Cr_4[CH_2Si(CH_3)_3]_8$ (**6b**).

Similar to the case of **5a** and **5b**, complex **6b** displays a remarkable chemical inertness towards protic agents, and to our surprise no reactivity could be observed even with carboxylic acid, phenols, pyroles, etc. In contrast to the case of $Me_8Cr_2Li_4(THF)_4$ whose short Cr-Cr quadruple bond could be reversibly cleaved via coordination of Lewis base,[4h] the tetranuclear structure of **6b** seems to be surprisingly robust since no cleaving was observed upon treatment with TMEDA and unreacted **6b** was always recovered in good yield. Nevertheless, a smooth reaction with ethylene took place at room temperature in toluene solution, producing substantial amounts of polyethylene (MW = 510,000, PD = 2.4). Although the catalytic activity was very modest (0.5 kg of PE/mol/hr/atm), as expected for a divalent chromium species, we found remarkable that the reaction does not require the presence of a cocatalyst.

Discussion

The formation of tetravalent **5** starting from a trivalent salt and by using reducing Grignard reagents can in principle be ascribed to a disproportionation reaction of an unstable and *in situ* generated R_3Cr intermediate. However, the fact that the yields are above 50% in the case of **5a** might dismiss this possibility. Attempts to identify divalent chromium species as possible byproducts of the reaction were inconclusive possibly due to the presence of magnesium salts as byproducts which would be likely to be engaged with chromium in the formation of polymeric structures. However, when the reaction of $CrCl_3(THF)_3$ was carried out with the corresponding lithium reagent Me_3SiCH_2Li, a new *divalent* and tetrameric species $[(Me_3SiCH_2)_2Cr]_4$ (**6b**) previously reported by Smith[6] was isolated in 83% yield.

The low observed magnetic moment for **6b** seems to substantiate the ability of polynuclear Cr species to form metal-metal bonds. Since both isotropic exchange models used for the magnetic susceptibility can account reasonably for the data with large $|J|$ values, it is clear that the magnetic properties of **6b** can be interpreted in terms of very strong intramolecular antiferromagnetic coupling. This could be manifested through superexchange via the bridging methylene groups, although the close proximity of the Cr^{II} centers within the square, and the possibility of direct metal-metal interactions, might also be a significant contributing factor in the overall exchange process. On the other hand, complex **6b** displays an unusual chemical inertness that in principle could be ascribed to the existence of a robust Cr-Cr direct bonding interaction.

In conclusion, the ability of the Cr-C bond in these complexes to perform ethylene insertion reactions along with the surprising inertness toward H-transfer reactions might be the key to understand the tremendous efficiency of the Cr catalyst commercially used for ethylene homopolymerization. A strong tendency to perform ethylene insertion, counterbalanced by poor, if any, tendency of the Cr-C bond to undergo hydrogen transfer, may well account for the formation of high molecular weight polymers with virtually no branching. Thus, understanding the factors determining this behavior will be critical for the design of more efficient catalysts and provides motivation for the development of new Cr-based catalysts.

Experimental Procedures

General

All operations were performed under inert atmosphere by using standard Schlenk type techniques. $CrCl_3(THF)_3$,[12] $CrCl_2(THF)_2$,[13] $(CH_3)_3SiCH_2Li$,[14] $(CH_3)_3CCH_2MgCl$,[15] $(CH_3)_3SiCH_2MgCl$,[16] and tetraphenyldisiloxane-1,3-diol[24] were prepared according to published procedures. Infrared spectra were recorded on a Mattson 9000 and Nicolet 750-Magna FTIR instruments from Nujol mulls prepared in a dry-box. Samples for magnetic susceptibility measurements were weighed inside a dry-box equipped with an analytical balance and sealed into calibrated tubes. Magnetic measurements were carried out with a Gouy balance (Johnson Matthey) at room temperature for **5a** and **5b** and at variable temperature for **6b** using a Quantum Design MPMS5S SQUID magnetometer at 1.0 *T*, in the temperature range 2-300 K. The sample was sealed in a 5 mm quartz tube in a dry-box prior to transfer to the SQUID. Sample mass was determined by difference by breaking the tube after data collection. Background data on the cleaned, empty tube were obtained under identical experimental conditions. Corrections for the quartz tube and for underlying diamagnetism were applied to the data. Elemental analyses were carried out with a Perkin Elmer 2400 CHN analyzer for **5**. Data for the X-ray crystal structure determinations were collected on a Bruker AX SMART 1k CCD diffractometer equipped with a Smart CCD area detector.

Preparation of $Cr(CH_2C(CH_3)_3)_4$ (5a)

A filtered solution of freshly prepared $(CH_3)_3CCH_2MgCl$ (200 mL, 25.0 mmol, 0.125 M) in ether was added to a suspension of $CrCl_3(THF)_3$ (2.3 g, 6.1 mmol) in the same solvent (50 mL). The color of the solution initially changed to light orange-brown. After 30 min., a further color change to intense dark blue was observed. Upon stirring overnight at RT the color finally became maroon. The solvent was removed *in vacuo* and the residue was suspended in hexane (150 mL). The mixture was stirred for 1 h at RT and filtered. The residue was washed with three portions of hexane (10 mL each). The combined hexane extracts were dried *in vacuo* and the residue was sublimed *in vacuo* at 60°C. X-ray quality dark brown pyrophoric (**WARNING**) crystals of **5a** were thus obtained (Yield: 1.26 g, 3.7 mmol, 61 %). Anal. Calc.(found) for $C_{20}H_{44}Cr$ (FW: 336.57 g/mol) [%]: C 71.37 (72.04), H 13.18 (13.85). IR (Nujol mull, cm^{-1}) ν: 1245 (vs), 1015 (w), 898 (vs), 730 (m), 693 (s), 681 (s), 612 (w), 536 (w), 515 (w). $\mu_{eff} = 2.91$ B.M.

Preparation of $Cr(CH_2Si(CH_3)_3)_4$ **(5b)**

The addition of a solution of freshly prepared $(CH_3)_3SiCH_2MgCl$ (200 mL, 30.0 mmol) in ether to a suspension of $CrCl_3(THF)_3$ (3.2 g, 8.5 mmol) in the same solvent turned the color dark purple. The mixture was stirred at RT for 1 h, then concentrated to dryness. The residue was suspended in hexane (150 mL) and the mixture was further stirred for 1 h at RT and filtered. The residue was washed with three portions of hexane (10 mL each). The combined hexane extracts were dried *in vacuo* and the residue was sublimed *in vacuo* at 60°C. X-ray quality dark violet pyrophoric (**WARNING**) crystals of **5b** were obtained (Yield: 1.0 g, 2.5 mmol, 29 %). Anal. Calc.(found) for $C_{16}H_{44}Si_4Cr$ (FW: 400.87 g/mol) [%]: C 47.94 (47.88) H 11.06 (10.91). I.R. (Nujol mull, cm^{-1}) ν: 1259 (vs), 1079 (vs), 1021 (s), 884 (s), 808 (vs), 744 (w), 694 (s), 612 (w), 536 (w), 516 (w). $\mu_{eff} = 2.89$ B.M.

Preparation of $Cr_4(CH_2Si(CH_3)_3)_8$ **(6b)**

Method A: A solution of $(CH_3)_3SiCH_2Li$ (1.7 g, 18.1 mmol) in hexane (100 mL) was added to a stirred suspension of $CrCl_3(THF)_3$ (1.8 g, 4.8 mmol) also in hexane (50 mL). The color of the slurry immediately changed to dark purple. The mixture was stirred at RT for 3 h, then filtered and the residue was washed with three portions of hexane (10 mL each). The solution was concentrated to 50 mL and allowed to stand at -34°C for 12 hours. The color of the solution slowly turned dark brown upon standing at that temperature. X-ray quality dark brown crystals of **6b** were formed, which were isolated by cold filtration, washed twice with pre-cooled hexane (5 mL) and dried *in vacuo*. (Yield: 0.9 g, 0.99 mmol, 83 %).

Method B: A solution of $(CH_3)_3SiCH_2Li$ (1.0 g, 10.3 mmol) in hexane (100 mL) was added to a stirred suspension of $CrCl_2(THF)_2$ (1.4 g, 5.2 mmol) in the same solvent (50 mL) cooled to -50°C. The color of the slurry immediately changed to dark brown. The mixture was allowed to warm to room temperature over a period of 2.5 hours, then filtered and the residue was extracted three times with hexane (10 mL each). The combined extracts were concentrated to 30 mL and allowed to stand at -34°C. The resulting crystals were filtered while cold, washed twice with cold hexane (5 mL) and dried in vacuo. (Yield: 0.7 g, 0.77 mmol, 60 %). Anal. Calc.(found) for $C_{32}H_{88}Si_8Cr_4$ (FW: 905.73 g/mol) [%]: C 42.44 (42.38) H 9.79 (9.69). IR (Nujol mull [cm^{-1}]) ν: 1461 (vs), 1378 (s), 1325 (w), 1256 (m), 1244 (s), 971 (m), 945 (s), 842 (vs), 739 (s), 716 (vs), 677 (m), 570 (w), 449 (w). ^1H-NMR (500MHz, 25°C, benzene d^6) δ: 0.53 (s, CH_3, 72 H) 1.40 (m, CH_2, 16 H).

Reaction of **5b** *with tetraphenyldisiloxane-1,3-diol*

A solution of **5b** (0.35 g; 1.0 mmol) in toluene (20 mL) was added to a solution of tetraphenyldisiloxane-1,3-diol (0.4 g; 1.0 mmol) in the same solvent (80 mL). The mixture was stirred at room temperature for 62 hours upon which the color of the solution changed from maroon to brown. The solution was concentrated *in vacuo* to 30 mL. Standing at –34 °C for 2 days yielded colorless crystals of $Ph_6Si_3O_3$ of apparent X-ray quality. (Yield: 0.26 mg, 65 %). Anal. Calc.(found) for $C_{36}H_{30}O_3Si_3$ (FW: 594,90 g/mol) [%]: C 72.68 (72.04), H 5.08 (4.97). IR (Nujol mull, cm^{-1}) ν: 1591m, 1568 w, 1428 s, 1366 w, 1189 w, 1158 w, 1128 s, 1118 s, 1037 vs, 1016 vs, 995vs, 766 w, 744 m, 737 m, 726 s, 698 s, 678 m, 620 w, 528 vs, 487 m, 481 m.

X-ray Crystallography

Suitable crystals were selected, mounted on thin, glass fibers using paraffin oil and cooled to the data collection temperature. Data were collected using 0.3° ω-scans at 0, 90, and 180° in ϕ. Unit cell parameters were determined from 60 data frames collected at different sections of the Ewald sphere. Semi-empirical absorption corrections based on equivalent reflections were applied.[17] Systematic absences in the diffraction data and unit-cell parameters were consistent with *C*2/*c* and *Cc* for **5b** and, uniquely, $P2_1/n$ for **6b**, and *Pbca* for **5a**. Refinement in the centrosymmetric space group option for **5b** yielded computationally stable and chemically reasonable results of refinement. The structures were solved by direct methods, completed with difference Fourier syntheses and refined with full-matrix least-squares procedures based on F^2. The compound molecule of **5b** is located at a two-fold rotation axis. All carbon and hydrogen atoms for **5b** and for **5a** excepting the tertiary carbon atoms were located disordered in two positions with a 50/50 site occupancy distribution. All non-hydrogen atoms were refined with anisotropic displacement parameters. All hydrogen atoms were treated as idealized contributions. All scattering factors and anomalous dispersion factors are contained in the SHELXTL 5.10 program library.[18]

Density Functional Theory calculations

All theoretical results were obtained using the Becke-Perdew exchange correlation functional, within the Amsterdam density functional (ADF) program. The standard double-ζ basis sets were used for H, C, and Si atoms, while the standard triple-ζ basis sets were employed for the Cr atoms. The 1s electrons of C as well as the 1s-2p electrons of Si and Cr were treated as a frozen core. Graphical representations of orbitals and other functions computed by ADF have been prepared using the MOLEKEL program.

Table 2.1 - Selected Bond Distances (Å) and Angles (deg) of compounds **5** - **6b**.

5a		**5b**		**6b**	
Cr-C(11')	1.961(13)	Cr-C(1)	1.954(14)	Cr(1)-C(5)	2.184(4)
Cr-C(6')	1.976(13)	Cr-C(1)#1	1.954(14)	Cr(1)-C(13)	2.188(4)
Cr-C(16)	1.986(12)	Cr-C(1')	1.958(16)	Cr(1)-Cr(2)	2.3310(10)
Cr-C(6)	1.996(13)	Cr-C(1')#1	1.958(16)	Cr(1)-Cr(4)	2.4026(10)
Cr-C(11)	2.002(13)	Cr-C(5)#1	1.972(14)	Cr(2)-C(9)	2.183(4)
Cr-C(1)	2.016(12)	Cr-C(5)	1.972(14)	Cr(2)-C(17)	2.205(4)
Cr-C(16')	2.025(12)	Cr-C(5')	1.983(14)	Cr(2)-Cr(3)	2.4004(10)
Cr-C(1')	2.031(12)	Cr-C(5')#1	1.983(14)	Cr(3)-C(29)	2.192(5)
				Cr(3)-C(21)	2.191(4)
				Cr(3)-Cr(4)	2.3396(10)
				Cr(4)-C(25)	2.200(5)
				Cr(4)-C(1)	2.207(5)
C(11')-Cr-C(6')	106.3(6)	C(1)-Cr-C(1)#1	72.7(8)		
C(11')-Cr-C(16)	143.7(5)	C(1)-Cr-C(1')	50.6(6)		
C(6')-Cr-C(16)	100.7(6)	C(1)#1-Cr-C(1')	108.1(7)		
C(11')-Cr-C(6)	74.4(6)	C(1)-Cr-C(1')#1	108.1(7)		
C(6')-Cr-C(6)	40.0(5)	C(1)#1-Cr-C(1')#	150.6(6)	C(5)-Cr(1)-C(13)	177.91(17)
C(16)-Cr-C(6)	115.5(5)	C(1')-Cr-C(1')#1	156.7(11)	C(5)-Cr(1)-Cr(2)	121.74(13)
C(11')-Cr-C(11)	39.7(5)	C(1)-Cr-C(5)#1	90.8(6)	C(13)-Cr(1)-Cr(2)	60.09(12)
C(6')-Cr-C(11)	144.3(5)	C(1)#1-Cr-C(5)#1	108.9(6)	C(5)-Cr(1)-Cr(4)	59.51(13)
C(16)-Cr-C(11)	107.0(5)	C(1')-Cr-C(5)#1	111.6(6)	C(13)-Cr(1)-Cr(4)	122.08(13)
C(6)-Cr-C(11)	106.1(5)	C(1')#1-Cr-C(5)#1	73.5(6)	Cr(2)-Cr(1)-Cr(4)	90.30(3)
C(11')-Cr-C(1)	101.2(5)	C(1)-Cr-C(5)	108.9(6)	C(9)-Cr(2)-C(17)	179.08(18)
C(6')-Cr-C(1)	77.3(5)	C(1)#1-Cr-C(5)	90.8(6)	C(9)-Cr(2)-Cr(1)	60.59(12)
C(16)-Cr-C(1)	108.1(5)	C(1')-Cr-C(5)	73.5(6)	C(17)-Cr(2)-Cr(1)	119.19(13)
C(6)-Cr-C(1)	106.6(5)	C(1')#1-Cr-C(5)	111.6(6)	C(9)-Cr(2)-Cr(3)	120.26(12)
C(11)-Cr-C(1)	113.6(5)	C(5)#1-Cr-C(5)	155.9(9)	C(17)-Cr(2)-Cr(3)	58.82(12)
C(11')-Cr-C(16')	108.6(5)	C(1)-Cr-C(5')	156.5(6)	Cr(1)-Cr(2)-Cr(3)	89.90(3)
C(6')-Cr-C(16')	113.4(5)	C(1)#1-Cr-C(5')	113.7(6)	C(29)-Cr(3)-C(21)	179.34(18)
C(16)-Cr-C(16')	36.7(5)	C(1')-Cr-C(5')	107.4(7)	C(29)-Cr(3)-Cr(4)	59.87(12)
C(6)-Cr-C(16')	102.2(5)	C(1')#1-Cr-C(5')	91.8(7)	C(21)-Cr(3)-Cr(4)	120.41(13)
C(11)-Cr-C(16')	79.1(5)	C(5)#1-Cr-C(5')	107.3(6)	C(29)-Cr(3)-Cr(2)	121.78(13)

C(1)-Cr-C(16')	143.0(5)
C(11')-Cr-C(1')	114.9(5)
C(6')-Cr-C(1')	106.4(5)
C(16)-Cr-C(1')	79.0(5)
C(6)-Cr-C(1')	143.2(5)
C(11)-Cr-C(1')	100.6(5)
C(1)-Cr-C(1')	38.1(5)
C(16')-Cr-C(1')	107.4(5)
C(5)-Cr-C(5')	50.3(6)
C(1)-Cr-C(5')#1	113.7(6)
C(1)#1-Cr-C(5')#1	156.5(6)
C(1')-Cr-C(5')#1	91.8(7)
C(1')#1-Cr-C(5')#1	107.4(7)
C(5)#1-Cr-C(5')#1	50.3(6)
C(5)-Cr-C(5')#1	107.3(6)
C(5')-Cr-C(5')#1	70.2(8)
Si(1)-C(1)-Cr	127.0(8)
Si(2)-C(5)-Cr	127.1(7)
Si(1)-C(1')-Cr	128.1(9)
Si(2)-C(5')-Cr	127.3(7)

Symmetry transformations used
to generate equivalent atoms:
#1 -x,y,-z+1/2

C(21)-Cr(3)-Cr(2)	58.88(11)
Cr(4)-Cr(3)-Cr(2)	90.15(3)
C(25)-Cr(4)-C(1)	178.40(17)
C(25)-Cr(4)-Cr(3)	59.99(12)
C(1)-Cr(4)-Cr(3)	118.86(12)
C(25)-Cr(4)-Cr(1)	119.70(12)
C(1)-Cr(4)-Cr(1)	58.86(12)
Cr(3)-Cr(4)-Cr(1)	89.65(3)
Si(1)-C(1)-Cr(4)	107.2(2)
Si(2)-C(5)-Cr(1)	108.3(2)
Si(3)-C(9)-Cr(2)	109.1(2)
Si(4)-C(13)-Cr(1)	105.4(2)
Si(5)-C(17)-Cr(2)	105.8(2)
Si(6)-C(21)-Cr(3)	108.4(2)
Si(7)-C(25)-Cr(4)	109.8(2)
Si(8)-C(29)-Cr(3)	107.7(2)

References

1. a) Mowat W., Shortland A. J., Yagupsky G., Hill N.J., Yagupsky M., Wilkinson G., *J. Chem. Soc., Dalton Trans.*, **1972,** 533. b) Mowat W., Shortland A.J., Hill N.J., Wilkinson G., *J. Chem. Soc., Dalton Trans.*, **1973,** 770.
2. a) Bower B.K., Tennent H.G., *J. Am. Chem. Soc.*, **1972**, 94, 2512. b) Stavropoulos P., Savage P.D., Tooze R.P. Wilkinson G., Hussain B., Motevalli M., Hursthouse M.B., *J. Chem. Soc. Dalton Trans.*, **1987**, 557. c) Bochman M., Wilkinson G., Young G.B., *J. Chem. Soc. Dalton Trans.*, **1980,** 1879. d) Gramlich V., Pfefferkorn K., *J. Organomet. Chem.*, **1973**, 61, 247
3. a) Girolami G.S., Salt J.E., Wilkinson G., Thornton-Pett M., Hursthouse M.B., *J. Am. Chem. Soc.*, **1983,** *105*, 5954. b) Girolami G.S., Wilkinson G., Galas A.M.R., Thornton-Pett M., Hursthouse M.B., *J. Chem. Soc., Dalton Trans.*, **1985,** 1339. c) Hermes A.R., Morris R.J., Girolami G.S., *Organometallics*, **1988,** *7*, 2372. d) Edema J.J.H., Gambarotta S., VanBolhuis F., Smeets W.J.J., Spel A.L., Chiang M.Y., *J. Organomet. Chem.*, **1990,** *389*, 47. e) Betz P., Jolly P.W., Krüger C., Zakrewski U., *Organometallics*, **1991,** *10*, 3520. f) Hubbard J.V., McVicar W.K., *Inorg. Chem.*, **1992,** *31*, 910 and references cited therein g) Fryzuk M.D., Leznoff D.B., Rettig S.J., *Organometallics*, **1995,** *14*, 5193. h) Kuzelka J., Legzdins P., Rettig S.J., Smith K. M., *Organometallics*, **1997,** *16*, 3569.
4. a) Aoki T., Furusaki A., Tomiie Y., Ono K., Tanaka K., *Bull. Chem. Soc. Jpn.*, **1969,** *42*, 545. b) Krausse J., Schodl J., *J. Organomet. Chem.*, **1971,** *27*, 59. c) Hursthouse M.B., Abdul Malik K.M., Sales K.D., *J. Chem. Soc., Dalton Trans.*,

1978, 1314. d) Andersen R.A., Jones R.A., Wilkinson G., *J. Chem. Soc., Dalton Trans.*, **1978,** 446. e) Cotton F.A., Hanson B.E., Ilsley W.H., Rice G.W., *Inorg. Chem.*, **1979,** *18*, 2713. f) Koschneider S.U., McGilligar B.S., McDermott G., Arnold J., Wilkinson G., Hursthouse M.B., *J. Chem. Soc., Dalton Trans.*, **1990,** 3427. g) Edema J.J.H., Gambarotta S., *Organometallics*, **1992,** *11*, 2452. h) Hao S., Gambarotta S., Bensimon C., *J. Am. Chem. Soc.*, **1992,** *114*, 3556. i) Hao S., Song J.-I., Berno P., Gambarotta S., *Organometallics*, **1994,** *13*, 1326 j) Morse P.M., Spencer M.D., Wilson S.R., Girolami G.S., *Organometallics*, **1994,** *13*, 1646. k) Steinborn D., Neumann O., Bruhn C., Ruffer T., Boese R., Heinemann F.W., *Chemistry – A European Journal*, **1998,** *4*, 2204 l) Becke F., Wiegeleben P., Ruffer T., Wagner C., Boese R., Blaser D., Steinborn D., *Organometallics*, **1998,** *17*, 475.

5. Edema J.J.H., Gambarotta S., *Comm. Inorg. Chem.* **1991,** *4*, 195 and ref. cited therein.
6. a) Smith P.D., Hsieh E.T., U.S. Patent 4,587,227, 1986. b) Smith P.D., McDaniel M.P., *J. Polym. Sci. A, Polym. Chem.*, **1990,** 28, 3587.
7. a) Barker G.K., Lappert M.F., Howard J.A.K., *J. Chem. Soc., Dalton Trans.*, **1978,** 734. b) Manzer L. E., *J. Am. Chem. Soc.*, **1978,** *100*, 8068. c) Gardner T.G., Girolami G.S., *J. Chem. Soc., Chem. Comm.*, **1987,** 1758.
8. a) Tajima Y., Tani K., Yuguchi S., *J. Polym. Sci. B; Polym.Lett.*, **1965,** *3*, 529. b) Krausse J., Marx G., Schodl G., *J. Organomet. Chem.*, **1970,** *21*, 159. c) Karoly F.J., Karapinka G.L., Wu C., Dow A.W., Johnson R.N., Carrick W.L., *J. Polym. Sci.A-1B*, **1972,** *10*, 2621, d) Krausse J., Marx G., *J. Organomet. Chem.*, **1974,**

65, 215. e) Noh S.K., Sendlinger S.C., Janiak C., Theopold K.H., *J. Am. Chem. Soc.*, **1989,** *114*, 9127. f) Noh S.K., Heintz R.A., Janiak C., Sendlinger S.C., Theopold K.H., *Angew. Chem., Int. Ed. Engl.*, **1990,** *29*, 775 e) Thomas B.J., Noh S. K., Schulte G.K., Sendlinger S.C., Theopold K.H., *J. Am. Chem. Soc.*, **1991,** *113*, 893. g) Bhandari G., Kim Y., McFarland M., Rheingold A.L., Theopold K.H., *Organometallics*, **1995,** *14*, 738 h) Krohn R.D., Kociak-Krohn G., Haufe M., *J. Organomet. Chem.*, **1995,** *501*, 303 i) Wilke G., Bogdanovic B., Hardt P., Heimbach P., Keim W., Kröner M., Oberkirch W., Tanaka K., Steinbrücke E., Walter D., Zimmermann H., *Angew. Chem., Int. Rd. Engl.*, **1996,** *5*, 151 j) Heinemann O., Jolly P.W., Krüger C., Verhovnik G.P.J., *Organometallics*, **1996,** *15*, 5462. k) Emrich R., Heinemann O., Jolly P.W., Krüger C., Verhovnik G.P.J., *Organometallics*, **1997,** *16*, 1511. l) Heintz R.A., Leelasubcharon S., Liable-Sands L.M., Rheingold A.C., Theopold K.H., *Organometallics*, **1998,** *17*, 5477. m) Bade O.M., Blom R., Ystenes M., *J. Mol. Cat. A: Chemical*, **1998,** *135*, 163 n) Theopold K.H., *Eur. J. Inorg. Chem.*, **1998,** 15.

9) a) Preishuber-Pflügl P., Buchacher P., Eder E., Schitter R.M., Stelzer F., *J. Mol. Cat. A: Chemical*, **1998,** *133*, 151 b) Herndon G.W., *Coord. Chem. Rev.*, **1999,** *181*, 177 and references cited therein c) Hlatky C.G., *Coord. Chem. Rev.*, **2000,** *199*, 235 and references cited therein d) Barluenga J., Fañanás F.J., *Tetrahedron*, **2000,** *56*, 4597 e) Yasuda H., *Prog. Polym. Sci.*, **2000,** *25*, 573 f) Beckhaus R., Santamaria C., *J. Organomet. Chem.*, **2001,** *617-618:1*, 81 g) Herndon G.W., *Coord. Chem. Rev.*, **2001,** *214*, 215 and references cited therein.

10) Kohn R.D., Haufe M., Kaciok-Kohn G., Grimm S., Wassescheid P., Keim W., *Angew. Chem. Int. Ed. Engl.* **2000**, 39, *4337.*

11) Nait Ajjou J.A., Scott S.L., Paquet V., *J. Am. Chem. Soc.*, **1998**, *120*, 415.

12) Schmid R., Ziegler T., *Organometallics*, **2000**, *19*, 2756.

13) Herwig W., Zeiss H.H., *J. Org. Chem.*, **1958**, *23*, 1404.

14) Kohler F.H., Prossdorf W., *Z. Naturforsch.*, **1977**, *32B*, 1026.

15) Tessier-Youngs C., Beachley O.T. Jr., *Inorg. Synth.*, **1986**, *24*, 95.

16) Zimmer H., Hechenbleikne I., Homberg O.A., Danzik M., *J. Org. Chem.*, **1963**, *29*, 2632.

17) Thomson S. K., Young G. B., *Polyhedron*, **1988**, 7, 1953.

18) Blessing R., *Acta Cryst.*, **1995**, A51, 33.

19) Sheldrick G.M., Bruker AXS, Madison, WI, **1997**.

20) a) Liang Y., Yap G.P.A., Rheingold A.L., Theopold K.H., *Organometallics,* **1996**, *15*, 5284; b) White P.A., Calabrese J., Theopold K.H., *Organometallics* **1996**, *15*, 5473.

21) Kim W.K., Fevola M.J., Liable-Sands L.M., Rheingold A.L., Theopold K.H., *Organometallics* **1998**, *17*, 4541.

22) Kambe R.K., *J. Phys. Soc. Japan*, **1950**, 5, 38.

23) Xu Z., Thompson L.K., He K., Waldmann O., MAGMUN4.0 Available free of charge from http://www.chem.mun.ca/resinst/ (no source codes available).

24) Harris G.I., *J. Chem. Soc.*, **1963**, 5978

CHAPTER III

THE HIGH ACTIVITY OF A HOMOLEPTIC TETRAVALENT VANADIUM ALKYL

The High Activity of a Homoleptic Tetravalent Vanadium Alkyl

Introduction

The discovery that the presence of a positive charge on a transition metal in combination with alkyl function may substantially boost the activity of olefin polymerization catalysts, has marked a milestone in the design and understanding Ziegler-Natta catalysts. Today, cationic alkyls are regarded as the latest generation of Ziegler-Natta catalysts.[1] For this reason, there is no surprise that considerable efforts have been devoted to the design of new activators, i.e. potent Lewis acids capable of cationizing organometallic compounds.[2] Nevertheless, these activators are typically not straightforward to be prepared nor to handle and always expensive. Thus, a most recent research direction in this field is for the design of catalysts that do not require activation.

In the chemistry of metal promoted olefin polymerization and co-polymerization, vanadium has always played a minor role since all the vanadium catalysts reported to date are systematically affected by chronic low-activity.[3] Nevertheless, there is something unique amongst V catalysts that still make them irreplaceable. That is the ability to perform super-random copolymerizations.[4] This is a critical feature in the manufacture of synthetic rubber and understanding the factors at the basis of this behaviour is even today target of research and debate. Obviously, given the unique characteristic of vanadium as a catalyst, efforts have been made to improve the activity or at least to understand the factors responsible for catalyst deactivation. The poor stability of medium and high-valent vanadium alkyl and the ability of vanadium to span across several oxidation states is commonly regarded as the main feature responsible for catalyst deactivation.[5] Therefore, the search for vanadium catalysts provided of high activity and at the same time preserving the desirable performances of commercially employed catalysts starts from the understanding of the factors that determine the stability of V-C bond in relation to ligand system and oxidation state.

For this purpose, we have recently embarked on a project for the synthesis of trivalent vanadium complexes where the nature of the ligand donor atom was systematically varied. The results of this work can be summarized as follows. The nitrogen donor atom has the ability to stabilize tetravalent vanadium alkyls and to sustain a reasonable level of catalytic activity.[6] Oxygen donor atoms such in alkoxides certainly produce the highest activity but also the most rapid deactivation due to inefficient stabilization of the organometallic functions.[7] As a common trend in the variety of transformations reported, vanadium shows tendency to disproportionate towards the di- and tetravalent state. While the divalent state has been shown mostly inactive, tetravalent complexes always displayed the highest activity. The obvious consequence is that in the chemistry of tetravalent complexes may be the answer to cure the chronic illness of vanadium catalysts.

The starting point of this study was a reassessment of the stability of tetravalent vanadium alkyls. Wilkinson first reported, in the seventies, the preparation of homoleptic R_4V species [$R = C_6H_5$, $CH_2Si(CH_3)_3$]. This complex was claimed exclusively on the basis of analytical and magnetic data.[8] After 30 years no additional information about thermal stability and catalytic has been made available. Keeping in mind the unusual stability of homoleptic tetravalent Cr alkyls presented in the previous chapter and their ability to be activated by simple $AlCl_3$, we became interested in fully characterising a homoleptic R_4V, hopefully by crystal structure, and testing the catalytic activity.

Results

Synthesis of V[CH$_2$Si(CH$_3$)$_3$]$_4$ (7)

The fact that there is no homoleptic tetravalent vanadium alkyl ever structurally characterised in the literature gave to us the impression that these species might be highly unstable. For this reason, we have selected the Me$_3$SiCH$_2$ alkyl that notoriously provides good stability and even allows for the formation of alkylidene derivatives upon C-H σ-bond metathesis. The preparation was carried out in a straightforward manner and according to the Wilkinson's recipe[8] by reacting a solution of VCl$_4$ in heptane with the alkyl lithium derivative in the appropriate stoichiometric ratio at low- T and under Ar atmosphere. The complex was isolated in moderate yield as thermally unstable dark-green crystals.

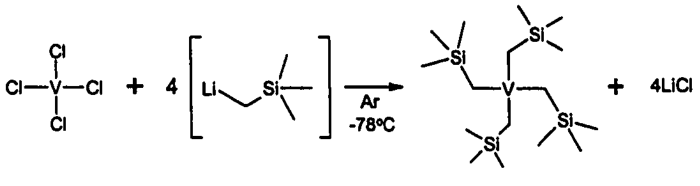

7

Scheme 3.1 - Synthesis of V[CH$_2$Si(CH$_3$)$_3$]$_4$ (7).

The complex possesses the expected regular tetrahedral structure (Figure **3.1**) with C-V-C angles varying in the range 107.3°-108.9°. The V-C distances also compare rather well ranging from 1.961 Å to 2.031 Å. Conformational disorder arising from the flipping over two positions of the CH$_2$ groups directly attached to vanadium and some rotational disorder of the Me$_3$Si groups reflected in the convergence factors which remain unpleasantly high. Nevertheless, the structure was sufficient to prove the connectivity and confirm the tetravalent state. Regarding this last point, we also observed an unusually low magnetic moment (1.81 BM). This is substantially lower than expected for a spin only d^1 electronic configuration and was also observed by Wilkinson.[8] Given the monomeric nature of the complex, intermolecular antiferromagnetic exchange is most likely responsible for this anomaly.

The V^{IV} tetra-alkyl complex **7** (Figure **3.1**) shows the same tetrahedral coordination of the metal center previously obtained with the Cr analog.(1,2) The C-V bond lengths (1.9-2.0Å) and angles (104.9-116.6°)are also very comparable. The final structure shows the same disorder in the occupancy of the CH_2 groups connected to the metal center thereby increasing the convergence factors. The isostructural nature of compound 7 with its Cr counterpart allows comparison of the d_1 vs d_2 electronic configuration towards polymerization of α-olefins and the relative thermal stability of the associated compounds.

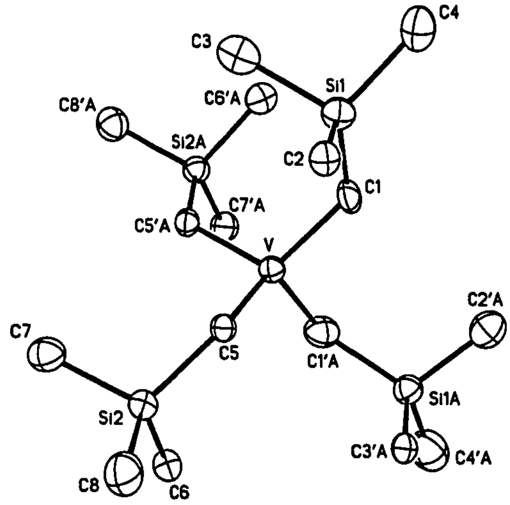

Figure 3.1 –Thermal ellipsoid representation of 7. $C_{16}H_{44}Si_4V$

---

[1] See Chapter II – Unusual Stability of Homoleptic Di- and Tetravalent Chromium Alkyls

Polymerization Testing

Complex 7 is thermally unstable and it slowly decomposes in solution and at room temperature to afford intractable materials. While attempts to use it as starting material for the preparation of a series of tetravalent organometallic derivatives via protonolysis reaction systematically led to decomposition, 7 reacted smoothly at room temperature and in toluene with $AlCl_3$ to afford a new species that proved to be a potent catalysts for ethylene polymerization. The activity (314 kg of PE/mol/h/atm) was the highest ever observed for a vanadium catalyst and is superior to the commercially available[5] $(acac)_3V$ and the recently reported[6a] $\{\alpha,\alpha'\text{-}[2,6\text{-}(i\text{-}Pr)_2PhN{=}C(Me)]_2(C_5H_3N)\}VCl_3$. The quality of the PE produced was also interesting showing very high molecular weight (480,000 g/mol). The polydispersity was slightly broad (3.7) but still in the acceptable range. Curiously enough, other α–olefins display tendency to deactivate the catalyst and greatly reduce the activity. Treatment with styrene completely quenched the catalyst activity.

Discussion

The fact that the reaction mixture of VR_4 with $AlCl_3$ produces a thermally stable species (polymerization may be started after 12 hours from time of mixing) indicates that the catalyst is sufficiently thermally stable. This is a substantial departure from all the other vanadium catalysts, typically remaining active only in the first few minutes of polymerization, and indicates that the tetravalent state is stable even in the absence of supporting ligands. The absence of supporting ligand in this particular system is likely to

---

[2] A full list of significant bond distances and angles is provided in Appendix II – Crystallographic Data : Homoleptic Vanadium Alkyl.

be the cause for the broad polymer polydispersity due to the multiplicity of processes that can be envisioned for a vanadium atom surrounded exclusively by alkyl and chlorine functions.

In summary, we have proved the existence and the monomeric nature of a tetravalent vanadium alkyl species. Its existence could be otherwise argued on the basis of literature data about stability of these species and complete absence of structural characterization. Complex **7** possesses an inferior thermal stability with respect to the isostructural Cr derivative but displays a remarkably higher catalytic activity (1.1 kg of PE/mol/h/atm for Cr vs. 314 kg of PE/mol/h/atm for V). This of course raises expectations and optimism for further work in the direction of preparing highly active and stable V^{IV} alkyl compounds that can be transformed into potent olefin polymerization catalyst by activation with simple and inexpensive $AlCl_3$.

Experimental Procedures

Preparation of $V[CH_2Si(CH_3)_3]_4$ (7)

A solution of $LiCH_2Si(CH_3)_3$ in hexane (9.42g, 200mL) was cooled to -78°C in an acetone dry ice bath. VCl_4 (2.6mL) was dissolved in hexane (80mL) and added dropwise to the cooled reaction mixture. The reaction was stirred for an additional hour while cold and then allowed to warm to room temperature slowly. The resultant mixture was filtered and solvent was removed *in vacuo*. The residue was redissolved in hexanes, (100mL) filtered once more and the solution was concentrated to 15mL. Dark green crystals of 7 (1.65g, 55.56%) were obtained after 48 hours at -78°C.

Anal. Calc. (Found) [%] for VC16H44Si4: C 48.07 (47.51), H 11.09 (11.28)

IR(Nujol [cm^{-1}]): 1256 s, 1245 vs, 1118 w, 1040 w, 1020 w, 880 vs, 840 vs, 741 vs, 720 s, 686 vs, 612 m, 504 s, 430 m.

μ_{eff} = 1.38 BM

Polymerization Experiments

$AlCl_3$ (220mg, 1.6mmol) was added to a solution of **7** (320mg, 0.8mmol) in hexanes (100mL). This mixture was stirred at room temperature overnight to yield a dark brown solution. A 5mL aliquot of the centrifuged solution was collected for testing the polymerization activity with ethylene while a 10mL aliquot was collected to test the copolymerization of 1-hexene with ethylene.

Ethylene: 5mL of an $8x10^{-3}$ M solution of **7**/$AlCl_3$ were diluted with 200mL of toluene. C_2H_4 was added under vigorous stirring for 15min. The remaining solution was canulated and the polymer dried *in vacuo*. Polymer Yield: 3.14g Activity: 314 kg of PE/mol V/h/atm.

Copolymerization: 10mL of an $8x10^{-3}$ M solution of **7**/$AlCl_3$ was diluted with 200mL of toluene. 1-hexene (1.5mL) and C_2H_4 were added under vigorous stirring for 45min. The polymerization was stopped by adding a solution of 15% HCl in ethanol. The remaining solution was canulated and the polymer dried *in vacuo*. Polymer Yield: 0.68g Activity: 11.33 kg·of PE/mol V/h/atm.

References

1. a) Temme B., Erker G., Karl J., Luftmann H., Fröhlich R., Kotila S., *Angew. Chem. Int. Ed Engl.*, **1995**, 34, 1755. a) Temme B., Karl J., Erker G., *Chem. Eur. J.*, **1996**, 2, 919. c) Karl J., Erker G., *Chem. Ber.*, **1997**, 130, 1261. d) Piers W.E., *Chem. Eur. J.*, **1998**, 4, 13. e) Devore D.D., Timmers F.J., Hasha D.L., Rosen R.K., Marks T.J., Deck P.A., Stern C.L., *J. Am. Chem. Soc.*, **1995**, 14, 3132. f) Sun Y., Piers W.E., Rettig S.J., *Chem. Commun.*, **1998**, 127. g) Duncan A.P., Mullins S.M., Arnold J., Bergman R.G., *Organometallics*, **2001**, 20(9), 1808. h) Svejda S.A., Brookhart M., *Organometallics*, **1999**, 18(1), 65. i) Warren T.H., Schrock R.R., Davis W.M., *Organometallics*, **1998**, 17(3), 308. j) Li J., Yang X., Stern C.L., Marks T.J., *Organometallics*, **1997**, 16(5), 842. k) Horton A.D., De With J., van der Linden A.J., van de Weg H., *Organometallics*, **1996**, 15(12), 2672. l) Dias E.L., Brookhart M., White P.S., *Organometallics*, **2000**, 19(24), 4995.
2. a) Brookhart M., Grant B., Volpe A.F., *Organometallics*, **1992**, 11, 3920. b) Yang X., Stern C.L., Marks T.J., *J. Am. Chem. Soc.*, **1991**, 113, 3623. c) Yang X., Stern C.L., Marks T.J., *J. Am. Chem. Soc.*, **1994**, 116, 10015. d) Piers W.E., Chivers T., *Chem. Soc. Rev.*, **1997**, 26, 345.
3. a) Witte P.T., Meetsma A., Hessen B.J., *J. Am. Chem. Soc.*, **1997**, 119, 10561. b) Murphy V.J., Turner H., *Organometallics*, **1997**, 6, 2495. c) Schuere S., Fischer J., Kress J., *Organometallics*, **1995**, 14, 2627. d) Zambelli A., Proto A., Longo P., *Ziegler-Natta Catalysis*, Fink G., Mulhaupt R., Brintzinger H.H., Eds : Springer-

Verlag, Berlin, **1995**. e) Kim W.K., Fevola M.J., Liable-Sands L.M., Rheingold A.L., Theopold K.H., *Organometallics*, **1998**, 17, 4541. f) Feher K.J., Walzer J.F., Blanski R.L., *J. Am. Chem. Soc.*, **1991**, 113, 3618. g) Czaja K., Bialek M., *Macromol. Rapid Commun.*, **1998**, 19, 163. h) Buhl M., *Angew. Chem. Int. Ed.*, **1998**, 37, 142.i) Chan M.C.W., Cole J.M., Gibson V.C., Howard J.A.K., *J. Chem. Soc. Chem. Commun.*, **1997**, 2345 and references therein. j) Gibson V.C., Redshaw C., Elsigood M.R.J., *J. Chem. Soc. Dalton Trans.*, **2001**, 767. k) Henderson R.A., Hughes D.L., Janas Z., Richards R.L., Sobota P., Szafert S., *J. Organomet. Chem.*, **1998**, 554, 195. l) Choukroun R., Moumboko P., Chevalier S., Etienne M., Donnadieu B., *Angew. Chem. Int. Ed.*, **1998**, 3, 3169. m) Lorber C., Donnadieu B., Choukroun R., *Organometallics*, **2000**, 19, 1963. n) Hagen H., Bezemer C., Boersma J., Kooijman H., Lutz M., Spek A.L., van Koten G., *Inorg. Chem.*, **2000**, 39, 3970.

4. a) Elston C.T., *U. S. Patent 3,645,992*, **1972**. b) Hogan J.P., Hsieh E.T., Randall J.C., *U. S. Patent 4,522,987*, **1985**.
5. Ma Y., Reardon D., Gambarotta S., Yap G.E., Zahalka H., Lemay C., *Organometallics*, **1999**, 18, 2773.
6. a) Reardon D., Conan F., Gambarotta S., Yap G.E., Wang Q., *J. Am. Chem. Soc.*, **1999**, 121, 9318. b) Desmangles N., Gambarotta S., Bensimon C., Davis S., Zahalka H., *J. Organomet. Chem.*, **1997**, 562, 53.
7. a) Theopold K.H., *Organometallics*, **1998**, 17, 4541. b) Ma Y., Reardon D., Gambarotta S., Yap G., *Unpublished Results*.

8. Mowat W., Shortland G., Yagupsky N.J.H., Yagupsky M., Wilkinson G. *J. Chem. Soc. Dalton Trans.* **1972,** 533.

CHAPTER IV

THE ABILITY OF THE α,α'-DIIMINE PYRIDINE LIGAND TO ACCEPT NEGATIVE CHARGE : THE ISOLATION OF PARAMEGNETIC AND DIAMAGNETIC TRIANIONS

The ability of the α,α-diimine pyridine ligand system to accept negative charge: isolation of paramagnetic and diamagnetic trianions.

Introduction

The α,α-diiminopyridine ligand $\{\alpha,\alpha'\text{-}[2,6\text{-}(\mathrm{i\text{-}Pr})_2\mathrm{PhN{=}C(Me)}]_2(\mathrm{C_5H_3N})\}$ has recently attracted considerable attention because of its ability to form highly active polymerization catalysts. For example, in combination with iron halides and other late transition metals (Co, Ni, Pd) it has produced a catalyst system that, when activated with methylaluminoxane (MAO), has displayed the highest activity ever reported for a homogeneous system.[1] The $\{\alpha,\alpha'\text{-}[2,6\text{-}(\mathrm{i\text{-}Pr})_2\mathrm{PhN{=}C(Me)}]_2(\mathrm{C_5H_3N})\}\mathrm{FeCl_2}$ complex is the only catalytic system based on Fe capable of substantial olefin polymerization activity. Its Co analogue also polymerises ethylene although to a lesser extent (450-1740 kg of PE/mol/h/atm). Our interest has been mainly focused on the mechanistic aspects. In other words, we were interested in unveiling the factors making this compound capable of sustaining such remarkable catalytic activity. It was hoped that by understanding the performance of this family of catalysts a new series, perhaps even more active, could be designed.

Recent work from this research group and others has shown that this α,α'-diiminopyridine ligand can be involved in the organometallic transformations of the metal center.[2-7] Mild alkylating agents may attack the imino function of one of the carbon atoms on the ligand backbone as shown in scheme **4.1**. Further treatment of compound **8** with the now common $\mathrm{B(C_6F_5)_3}$ or BARF activators leads to a cationic Al compound which shows very moderate activity.[2]

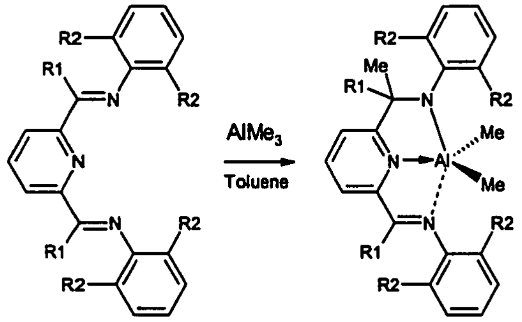

8

Scheme 4.1 – Alkylation of the imino function of the α,α'-diiminopyridine ligand.

The pyridine ring carbon atoms including the N atom can also be alkylated. In the case of the $\{\alpha,\alpha'\text{-}[2,6\text{-}(i\text{-}Pr)_2PhN{=}C(Me)]_2(C_5H_3N)\}VCl_3$ complex, a first methylation with methylaluminoxane (MAO) occurs at the ortho position of the pyridine ring.[3] This is illustrated in scheme 4.2. The resulting V complex displays a very high activity albeit slightly lower then the Fe congeners, yet producing polymers of comparable quality.

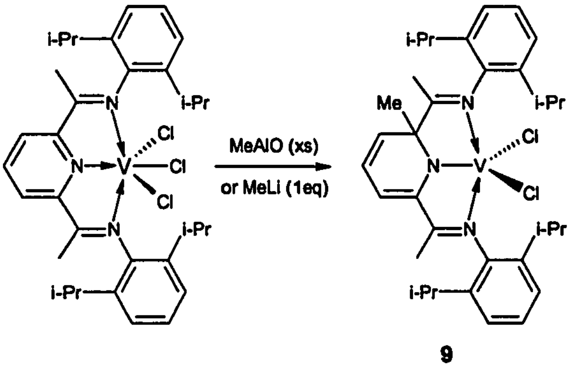

9

Scheme 4.2 – First alkylation of the ortho-position of the pyridine ring.

Further treatment of the methylated equivalent of 9 (Scheme 4.3), with a stronger alkylating agent (MeLi) results in the removal of the initial methyl group (10) or additional methylation at the meta position of the pyridine ring (**11**), always accompanied by a reduction of the metal center.

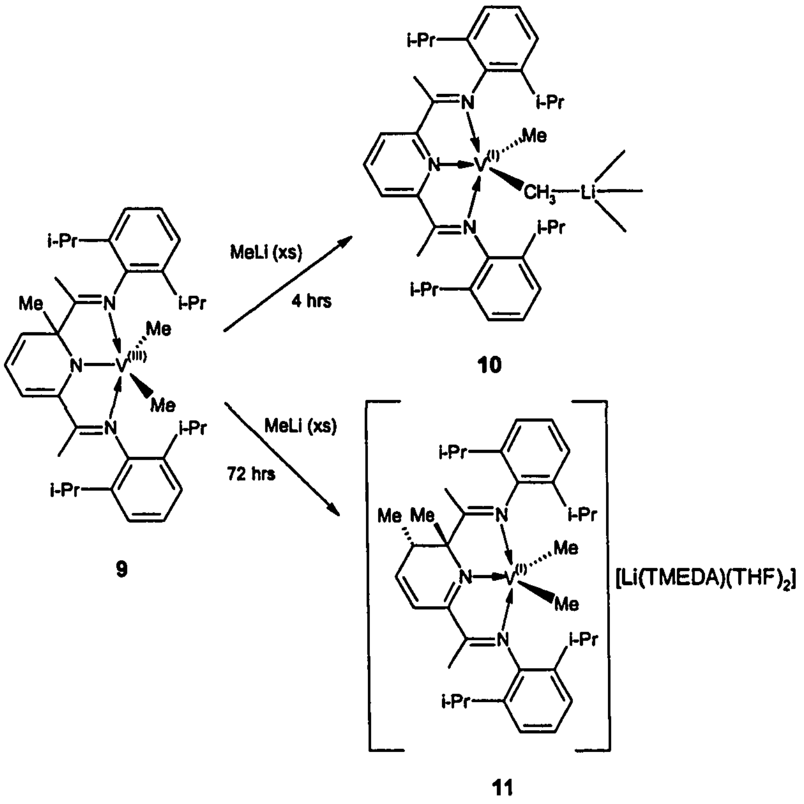

Scheme 4.3 – Secondary alkylation of para position vs. reduction of the methylated product.

This unusual result relating catalyst deactivation to extensive alkylation highlights the limitation coming from this ligand system. Reduction of the metal center was observed in the case of Cr as well, resulting in complete inactivity. The chromium chloride complex is alkylated (scheme 4.4) at the para position of the pyridine ring by a strong alkylating agent ($PhCH_2MgCl$) and the ligand is further transformed via C-C coupling.[4]

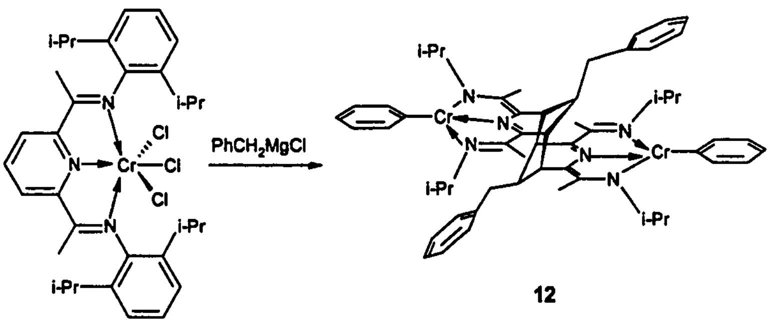

12

Scheme 4.4 - Alkylation at the para-position with C-C coupling.

Conditions closer to those employed in polymerization experiments afforded a μ-Cl bridged mixed Cr-Al species upon treatment with a milder alkylating agent ($AlMe_3$), also containing divalent Cr. The final product in scheme 4.5 illustrates that the metal center is reduced without involving the α,α'-diiminopyridine ligand. However this reduction results in a Cr^{II} metal center which is inactive towards ethylene polymerization. This facile reduction of the metal center explains the lack of activity from the parent tri-chloride compound tested with a variety of cocatalysts.[4]

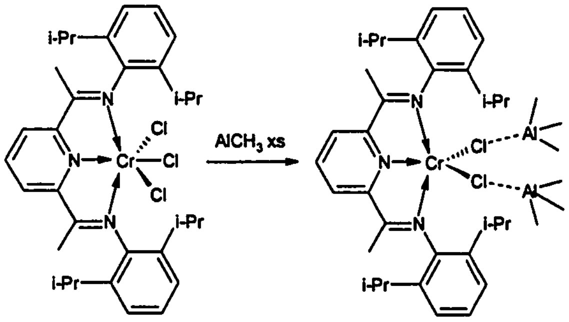

13

Scheme 4.5 - Reduction of the Cr metal center without involvement of the ligand.

Completing the series, the $\{\alpha,\alpha'\text{-}[2,6\text{-}(i\text{-}Pr)_2PhN{=}C(Me)]_2(C_5H_3N)\}MnCl_2$ adduct leads to yet another possible ligand transformation making the compound inactive towards olefin polymerization. In this case, dimerization occurs via imine reductive coupling,[4] as is represented in scheme **4.6**.

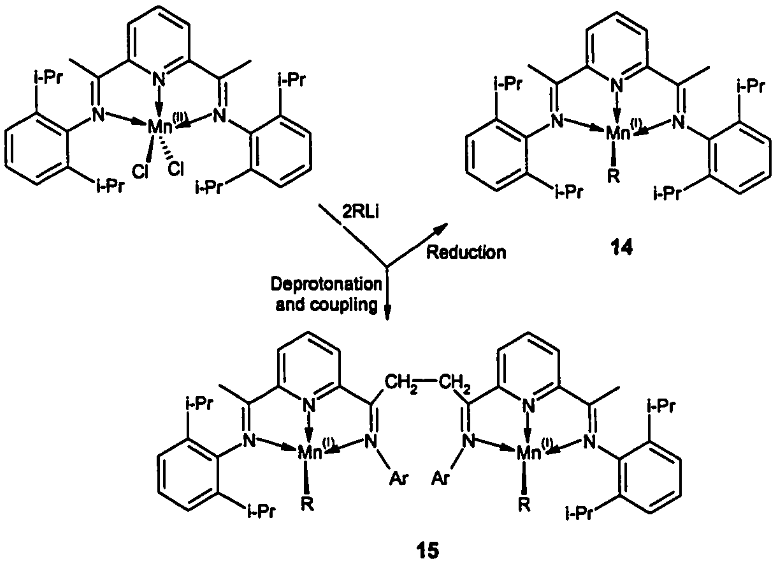

Scheme 4.6 - Dimerization of the ligand through partial dehydrogenation vs. simple metal center reduction.

In parallel to all these transformations either one of the two CH_3 groups attached to the imine functions may be partly dehydrogenated *in the absence of a transition metal.*[4,5] This is represented in scheme **4.7** where reaction of the α,α'-diiminopyridine ligand with MeLi produced a reversible alkylation at the N position of the pyridine ring (**16**) and subsequent heating of the alkylated product results in dehydrogenation (**17**).

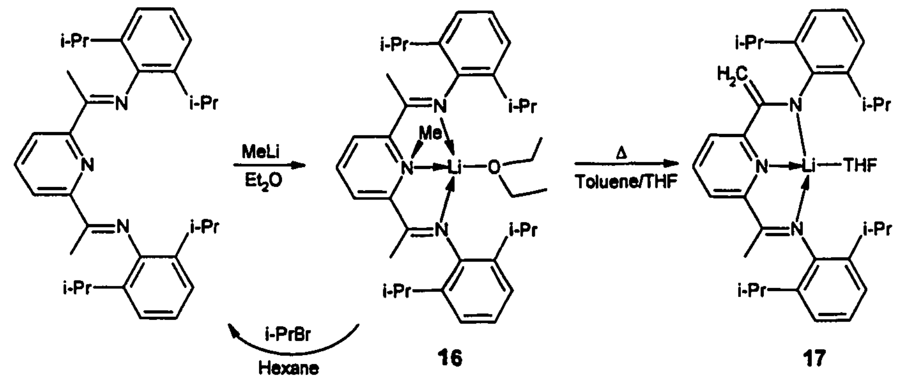

Scheme 4.7 – Alkylation of the pyridine N and subsequent dehydrogenation.

This behaviour speaks for a unique ability of this ligand system to:

a) accept negative charge with preferential spin density localisation on the imine groups and the pyridine N and C_{para} atoms.

b) engage in internal redox processes with the coordinated metal.

The ability of the ligand to accept or to donate negative charge to the metal is central to the fine tuning of the redox potential of the metal, and of its Lewis acidity that in turn determines the catalytic behaviour.

Given the above scenario, we became interested to clarify the ability of this remarkable ligand system to accept negative charge. For this purpose, reductions of {α,α'-[2,6-(i-Pr)$_2$PhN=C(Me)]$_2$(C$_5$H$_3$N)} with strong reductants such as Li and Li(naftalenide) and *in the absence* of transition metals were carried out.

Results

General Reaction

Reactions were carried out by reacting a solution of {α,α'-[2,6-(i-Pr)$_2$PhN=C(Me)]$_2$ (C_5H_3N)} in THF with either metallic Li under Ar or Li(naftalenide) under N_2.(1) Regardless of the stoichiometric ratio, the two reductions afforded a mixture of {α,α'-[2,6-(i-Pr)$_2$PhN=C(Me)]$_2$ (C_5H_3N)}[Li(THF)]$_3$} (**18**) and of ({α-[2,6-(i-Pr)$_2$PhN=C(Me)]}{α'-[2,6-(i-Pr)$_2$PhN-C(=CH_2)]} C_5H_3N)[Li(THF)]$_2$[Li(THF)$_2$]) (**19**) through a well-reproducible process. Both species contain a trianionic ligand (Scheme **4.8**).

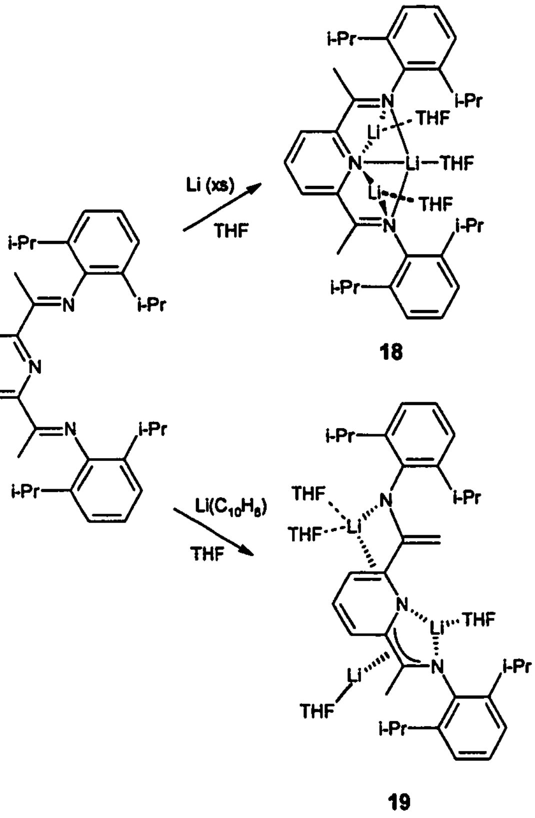

Scheme 4.8 - 3 electron reduction of the α,α'-diiminopyridine ligand.

---

[1] See Experimental Procedures section of this chapter for further details.

Separation of the two extremely air-sensitive species was possible because of their different solubility in hexane. However, we observed that reaction carried out with 3 equivalents of Li(naftalenide) at low temperature afforded **19** as the only tractable compound (67 %) with no tangible evidence for the presence of **18**.

The connectivity of **18** was elucidated by an X-ray crystal structure (Figure **4.1**). The complex shows the intact ligand adopting the usual chelating tridentate conformation around the first Li atom that is in turn coordinated to one molecule of THF with an overall distorted square-planar geometry. Two additional lithium atoms, each solvated by one molecule of THF are symmetrically placed on the two sides of the plane defined by the central lithium atom and the three donor atoms. Each of these lithium atoms is connected to the molecule by coordinating to a $N_{py}CCN_{im}$ fragment in a geometry reminiscent of metal-diene complexes. As a result, the pyridine N atom is pentacoordinated displaying an almost regular trigonal bipyramidal geometry. Counting only the N and O donor atoms, the two out-of-plane Li atoms have a trigonal planar environment.

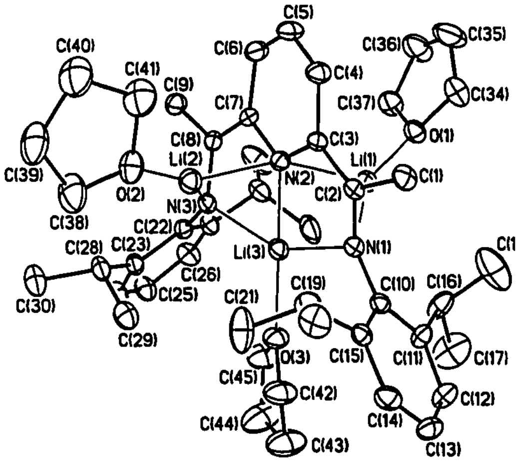

Figure 4.1 - Thermal ellipsoid plot of (**18**). $C_{45}H_{67}N_3Li_3O_3$

Magnetic Properties

Complex **18** is a rare case of a paramagnetic lithium organyl showing a magnetic moment [$\mu_{eff} = 1.30\ \mu_B$] that is lower than expected for one unpaired electron per molecule. The presence of antiferromagnetic (AF) exchange between the radical anions has been confirmed by variable temperature magnetic moment measurements. As discussed in a previous chapter, a significant drop in the magnetic moment at temperatures approaching 0 K (Figure **4.2**) is indicative of spin-orbit coupling that would be antiferromagnetic in nature.

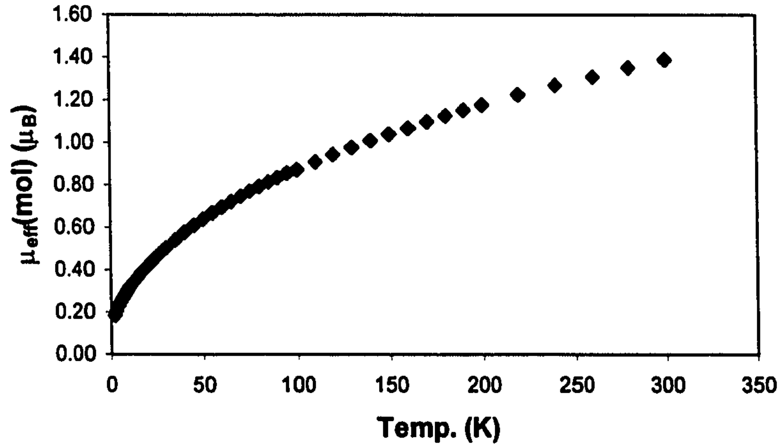

Figure 4.2 – Plot of the μ_{eff} against T for **18**.

The crystal structure of **18**, when expanded to reveal periodicity, shows the closest point of contact between adjacent molecules to be between a terminal carbon of the i-Pr groups on the aryl side chains and the π-ring system of the aryl group on the next molecule. The ESR spectrum shows a single resonance peak at g = 2.002 with a hyperfine pattern appearing as a complex 23 line spectrum.

Theoretical Calculations

Density Functional Theory calculations (B3LYP)[2] on a complex **18a** (with the aryl substituents replaced by hydrogen) indicated the presence of a rather substantial HOMO-LUMO gap (ca 2.3 eV) thus accounting for the low spin electronic configuration. The SOMO and HOMO are essentially identical to the LUMO and LUMO+1 of the free ligand. Both orbitals (Figure 4.3) are antibonding in the pyridine ring and between the imine C and N atoms; the HOMO has substantial density at the pyridine N and C_{para} atoms, whereas the SOMO has a nodal plane through these atoms.

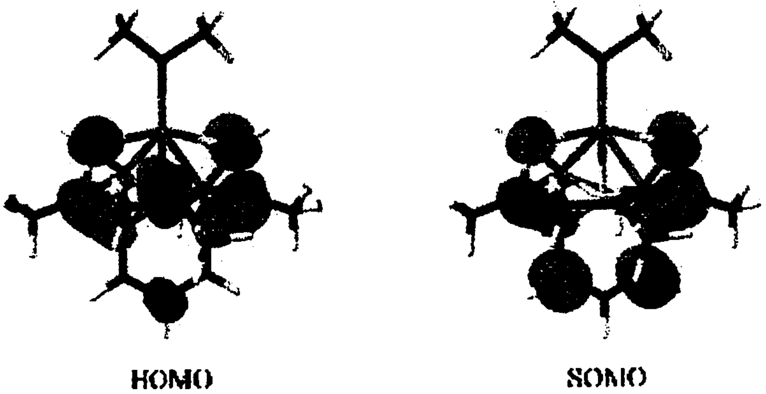

Figure 4.3 - Figure showing the SOMO and HOMO orbitals of **18a**.

This behavior is in nice agreement with the bond distances displayed by the crystal structure(3) showing that the C-C bond formed between the C_{ortho} and C_{meta} atoms of the pyridine ring are essentially single bonds (1.479 Å) whereas the C-C bonds formed by the C_{para} and C_{meta} atoms are substantially shorter (1.410 Å).

---

[2] Geometry optimizations of the minima and transition states were performed with the GAMESS-UK package[8] using the B3LYP hybrid density functional[9] with the split-valence 3-21G basis set.[10] Geometries were optimized without constraints.

Although arising from the same reaction and containing the same ligand skeleton, the structure of **19** is remarkably different. From the *formal* point of view it can also be regarded as a rare case trilithium organyl. It shows the ligand system where one of the two methyl groups has been deprived of one H atom and engaged in the formation of a double bond with the adjacent C atom (Figure **4.4**).

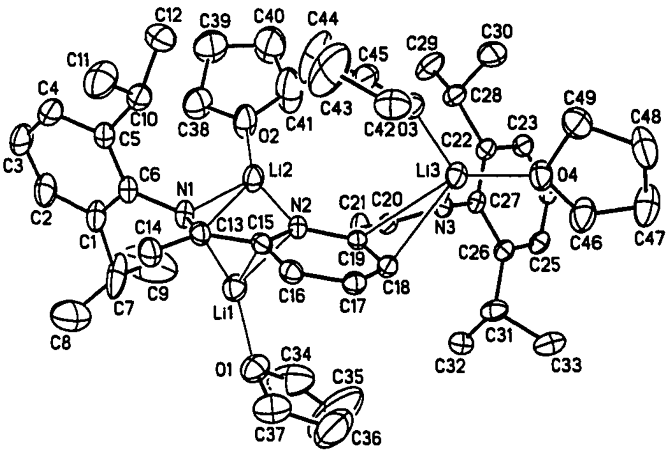

Figure 4.4 - Thermal ellipsoid representation of (**19**) $C_{49}H_{74}N_3O_4Li_3$

The olefinic function is rotated out of the pyridine ring plane (ca 30°). One lithium atom is chelated in a normal way by the tridentate iminopyridine moiety. The second lithium sits above the ring plane and binds to the $N_{py}CCN_{im}$ fragment in much the same way as the out-of-plane lithium atoms of **18**. Both of these lithium atoms are coordinated by one THF molecule. The third lithium atom is σ-bound to the dangling enamide nitrogen and is coordinated by two THF molecules. The pattern of bond lengths indicates substantial localization in the sense of resonance structure depicted previously in scheme **4.8**.

---

[3] See Appendix III – Crystallographic Data: $\{2,6\text{-bis}[2,6\text{-(i-Pr)2PhN=C(Me)}]_2(C_5H_3N)\}Li_3$

Nuclear Magnetic Resonance (NMR)

The loss of one H atom from one of the two methyl groups attached to the imine carbon during the formation of **19** was conclusively demonstrated by NMR. The H^1 and C^{13} spectra show the presence of the two CH_2 protons at 2.04 and 3.01 ppm coupled to each other and to the same carbon atom at 66.39 ppm. The identity of this group as a CH_2 was confirmed by a DEPT experiment. The spectrum also showed a remarkable upfield shift of the three pyridine resonance, two different phenyl rings and two sets of i-Pr groups.

H^1- NMR (500 MHz, d^8-THF, 23°C) δ: $CH_{(i\text{-}Pr)}$: two overlapping septets 4H at 3.40; $Me_{(i\text{-}Pr)}$: six overlapping doublets 24H at 1.19, 1.17, 1.09, 1.08; $Me_{(imino)}$: one singlet 3H at 1.38; CH_2: two broad singlets 1H each at 2.04 and 3.01; $CH_{(pyridine)}$: three broad singlets 1H each at 5.49, 5.34 and 4.68; $CH_{(aromatic)}$: poorly solved multiplets at 6.88 (2H) and 6.63 (1H) and 6.75 (2H) and 6.36 (1H); coordinated THF: m at 3.67 and 1.76 12H each.

C^{13}-NMR (125.72 MHz, d^8-THF, 23°C) δ: ($CH_{(i\text{-}Pr)}$): 28.21, 28.01; ($Me_{(i\text{-}Pr)}$): 23.56, 24.50, 24.93, 24.99; ($Me_{(imino)}$): 14.49; (CH_2): 66.39; ($CH_{(pyridine)}$): 83.09, 114.35, 125.88; ($CH_{(aromatic)}$): 115.38, 119,38, 119.76, 112.66, 122.83, 123.01; (THF): 66.39 and 25.44; (quaternary C_{imine}): 35.55, 32.57; (quaternary C): 108.31, 143.82, 144.24, 154.80, 155.66, 157.98, 165.96, 167.52.

Reaction of 19 with O_2

Reaction of **19** with dry oxygen afforded the previously isolated[5] monolithium salt **17**. From the formal point of view, this requires the loss of Li_2O_2 as a by-product of the oxydation. Experimental details are given below however it is interesting to note that the change in colour from the parent red/brown **19** to the blue/green isolated product **17** only occurs in the absence of coordinating solvents such as THF or Et_2O. This would imply a loosely coordinated di-oxygen complex without a breakdown of the parent coordination structure as proposed in scheme 4.9.

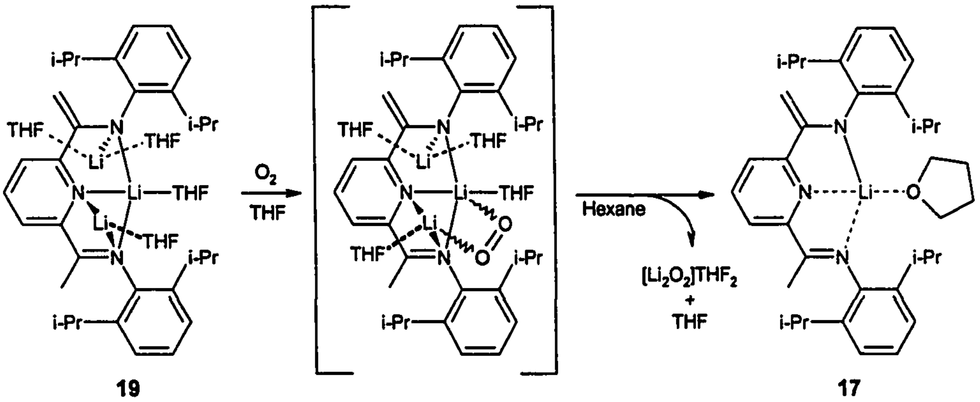

19

17

Scheme 4.9 – Proposed intermediate for the production of the monolithium salt (17) from the reaction of (19) with O_2.

Discussion

In agreement with the observed diamagnetism of **19**, the conversion of **18** to **19** implies a formal loss of one hydrogen atom, which corresponds to a formal one-electron oxidation. This might explain why a stronger reducing agents such as Li is necessary for the formation of **18** while a milder reducing agent [Li(naftalenide)], may favor the formation of **19**. In addition, the basicity of Li(naftalenide) may play a role, leading to competition between reduction and hydrogen abstraction during its reaction with the free ligand. Finally we have observed that **18** is thermally unstable and completely converts to **19** upon heating in toluene.

In conclusion, with this work we have established that $\{\alpha,\alpha'\text{-}[2,6\text{-(i-Pr)}_2\text{PhN=C(Me)}]_2(C_5H_3N)\}$ may accommodate up to three electrons in the antibonding orbitals of the imino function and of the pyridine ring in a low-spin configuration. Assuming that similar metal-to-ligand charge transfer occurs also in its transition metal complexes upon alkylation, the observed variety of transformations may be easily explained.

a) The localization of the spin density on the pyridine C_{meta} atoms explains the cycloaddition observed with Cr.[4]

b) The formation of a double bond explains the reductive coupling observed with Mn.[4,6]

c) The charge localization at the pyridine ring C_{para} position accounts for the lithiation[5a] and for the possibility to transfer alkyl groups directly from the metal center to any position of the pyridine ring.[3-5]

What remains to be unveiled is how this ligand supports high level of catalytic activity with well diversified metals. The ability of the large π-system to accommodate negative charge might suggest ability to increase the Lewis acidity of the metal center with obvious positive impact on catalytic performance. On the other hand, it may also help the stabilization of electron-rich low-valent metals as often observed during alkylations of these derivatives and whose ability to promote polymerization is still controversial.[7]

Experimental Procedures

Preparation of $\{\alpha,\alpha'\text{-}[2,6\text{-}(i\text{-}Pr)_2PhN{=}C(Me)]_2(C_5H_3N)\}[Li(THF)]_3\}$ **(18)**

Freshly cut fragments of lithium foils (0.14g, 21mmol) were washed with hexanes, dried and added to a suspension of 2,6-bis[2,6-(i-Pr)$_2$PhN=C(Me)]$_2$(C$_5$H$_3$N) (1.0g, 2.1mmol) in THF (100mL). The reaction mixture was stirred under an argon atmosphere for 48 hours during which the color of the solution changed from light yellow to dark red/brown. The excess lithium was removed through a glass filter. THF was evaporated *in vacuo* without heating and the dark-brown residue was suspended in pentane (20mL). Compound **19** was isolated as an insoluble microcrystalline powder remaining upon filtration and additional washing with pentane (0.618g, 38%). The filtrate was concentrated to a 15mL solution and cooled to –35°C. Dark red crystals of **18** (0.14g, 10%) suitable for X-ray crystallographic structure determination were isolated from the pentane solution. The extreme air sensitivity, combined with spontaneous loss of solvent and thermal decomposition to **19** limited the available options for analytical characterization.

Preparation of (**19**)

($\{\alpha$-[2,6-(i-Pr)$_2$PhN=C(Me)]$\}\{\alpha'$-[2,6-(i-Pr)$_2$PhN-C(=CH$_2$)]$\}$C$_5$H$_3$N)[Li(THF)]$_2$[Li(THF)$_2$])

A solution of Li(nafthalenide) in THF (10mL) was prepared by stirring a solution of nafthalene (0.8g, 6.2mmol) and freshly cut fragments of lithium foil (0.05g, 6.6mmol). The resulting dark-green solution was diluted with additional THF (50mL) and subsequently treated with 2,6-bis[2,6-(i-Pr)$_2$PhN=C(Me)]$_2$(C$_5$H$_3$N) (1.0g, 2.1mmol). An instant colour change from dark-green to dark-brown occurred. The reaction was stirred for an additional 10 minutes and solvent was removed *in vacuo*. The dry residue was left in dynamic *vacuo* overnight at room temperature to remove the major part of the nafthalene. The residual solid was washed with cold pentane (30mL), filtered and isolated as a brown, diamagnetic, insoluble powder (1.1g, 67%). Crystals of **19** suitable for X-ray diffraction were grown by cooling a saturated solution in hexane to –35°C.

Preparation of (**17**)

({α-[2,6-(i-Pr)$_2$PhN=C(Me)]}{α'-[2,6-(i-Pr)$_2$PhN-C(=CH$_2$)]} C$_5$H$_3$N)[Li(THF)]

A solution of **19** (0.201g) in THF (75mL) was prepared and set to stir at room temperature. Dry O_2 (4mL) was bubbled into the solution using a syringe. A colour change from dark-brown to wine-red occurred. The reaction was sealed and left stirring overnight to react any O_2 in the headspace above the reaction mixture. Solvent was evaporated *in vacuo* to yield a dark red residue. The residue was redissolved in hexanes (15mL) upon which the colour of the solution changed from red to bright blue (dark) with the precipitation of a white powder. The mixture was filtered and the clear blue solution was concentrated to 5mL. Storage at -35°C yielded crystals of **17** of sufficient quality for structure elucidation. $C_{37}H_{51}LiN_3O$ MW: 560.75 (g/mol).

Table 4.1 - Selected Bond Distances (Å) and Angles (deg) of compounds **18** and **19**.

18

C(1)-C(2) = 1.522(4)
C(2)-C(3) = 1,373(4)
C(3)-N(2) = 1.421(4)
C(3)-C(4) = 1,481(4)
C(4)-C(5) = 1.407(5)
C(8)-C(9)= 1.512(4)
Li(3)-N(1) = 2.203(6)
Li(3)-N(2) = 1.993(6)
Li(3)-N(3) = 2.276(6)
Li(1)-N(1) = 1.994(6)
Li(1)-N(2) = 2.077(6)
Li(2)-N(2) = 2.049(6)
Li(2)-N(3) = 1.989(6)

Li(1)-N(2)-LI(2) = 154.6(3)
Li(3)-N(2)-C(3) = 119.1(3)
Li(3)-N(2)-C(7) = 121.2(2).

19

C(20)-C(21) = 1.366(4)
C(20)-N(3) = 1.364(3)
C(20)-C(19) = 1.526(4)
C(19)-C(18) = .374(4)
C(18)-C(17) = 1.442(4)
C(17)-C(16) = 1.352(4)
C(16)-C(15) = 1.446(4)
C(15)-N(2) = 1.451(4)
C(13)-C(15) = 1.394(4)
C(13)-C(14) = 1.514(4)
Li(1)-N(1) = 2.017(6)
Li(1)-C(13) = 2.156(6)
Li(1)-C(15) = 2.171(6)
Li(1)-N(2) = 2.121(6)
Li(2)-N(1) = 1.989(6)
Li(2)-C(13) = 2.779(6)
Li(2)-C(15) =
Li(2)-N(2) = 1.956(6)
Li(3)-N(3) = 1.958(5)
Li(3)-C(18) = 2.528(6)
Li(3)-C(19) = 2.754(6)

C(27)-N(3)-Li(3) = 129.7(2)
C(20)-N(3)-Li(3) = 110.(2)
C(20)-N(3)-C(27) = 118.4(2)
C(19)-C(20)-C(21) = 119.2(3)
N(3)-C(20)-C(21) = 128.1(3)

References

1. a) Britovsek G.J.P., Bruce M., Gibson V.C., Kimberley B.S., Maddox P.J., Mastroianni S., McTavish S.J., Redshaw C., Solan G.A., Strömberg S., White A.J.P., Williams D.J., *J. Am. Chem. Soc.*, **1999**, *121*, 8728; b) Small B.L., Brookhart M., *Polymer Prep. (Am. Chem. Soc., Div. Polym. Chem.)*, **1998**, *39*, 213; c) Bennett A.M.A., (DuPont), WO 98/27124, **1998**, [*Chem Abstr.* **1998**, *129*, 122973x]; b) Bennett A.M.A., *CHEMTECH*, **1999**, *July*, 24-28.

2. Bruce M., Gibson V.C., Redshaw C., Solan G.A., White A.J.P., Williams D.J., *J. Chem. Soc. Chem. Commun.* **1998**, 2523

3. Reardon D., Conan F., Gambarotta S., Yap G.P.A., Wang Q., *J. Am. Chem. Soc.*, **1999**, *121*, 9318.

4. Sugiyama H., Aharonian G., Gambarotta S., Yap G.P.A., Budzelaar P.H.M., *J. Am. Chem. Soc.* in press.

5. a) Korobkov I., Gambarotta S., Yap G.P.A., Budzelaar P., *Organometallics* in press, b) Clentsmith G.K.B, Gibson V.C., Hitchcock P.B., Kimberly B.S., Rees C.W., *J. Chem. Soc. Chem. Commun.* **2002**, 1498.

6. Reardon D., Aharonian G., Gambarotta S., Yap G.P.A., *Organometallics*, **2002**, *21*, 786.

7. a) Kooistra M., Knijnenburg Q., Smits J.M.M., Horton A.D., Budzelaar P.H.M., Gal A.W., *Angew. Chem. Int. Ed. Engl.* **2001**, *40*, 4719;
   b) Gibson V.C., Humphries M., Tellmann K., Wass D., White A.J.P., Williams D.J., *Chem. Comm.*, **2001**, 2252.

8. GAMESS-UK is a package of ab initio programs written by Guest M.F., van Lenthe J.H., Kendrick J., Schoffel K., and Sherwood P., with contributions from Amos R.D., Buenker

R.J., van Dam H.J.J., Dupuis M., Handy N.C., Hillier I.H., Knowles P.J., Bonacic-Koutecky V., von Niessen W., Harrison R.J., Rendell A.P., Saunders V.R., Stone A.J., Tozer D.J., and de Vries A.H. The package is derived from the original GAMESS code due to Dupuis M., Spangler D. and Wendoloski J., NRCC Software Catalog, Vol. 1, Program No. QG01 (GAMESS), **1980**.

9. a) Becke A.D., *J. Chem. Phys.* **1993**, *98*, 5648 b) Lee C., Yang W., Parr R.G., *Phys. Rev. B* **1988**, *37*, 785 c) Miehlich B., Savin A., Stoll H., Preuss H., *Chem. Phys. Lett.* **1989**, *157*, 200.

10. a) Binkley J.S., Pople J.A., Hehre W.J., *J. Am. Chem. Soc.* **1980**, *102*, 939 b) Gordon, M.S., Binkley J.S., Pople J.A., Pietro W.J., Hehre W.J., *J. Am. Chem. Soc.* **1982**, *104*, 2797 c) Frisch M.J., Pople J.A., Binkley J.S., *J. Chem. Phys.* **1984**, *80*, 3265, and references cited therein d) Dobbs K.D., Hehre W.J., *J. Comput. Chem.* **1986**, *7*, 359; *ibid* **1987**, *8*, 861, 880.

11. a) McLean A.D., Chandler G.S., *J. Chem. Phys.* **1980**, *72*, 5639 b) Clark T., Chandrasekhar J., Spitznagel G.W., Schleyer P.V.R., *J. Comp. Chem.* **1983**, *4*, 294 c) Frisch M.J., Pople J.A., Binkley J.S., *J. Chem. Phys.* **1984**, *80*, 3265

12. Gaussian 98, Revision A.9, Frisch M.J., Trucks G.W., Schlegel H.B., Scuseria G.E., Robb M.A., Cheeseman J.R., Zakrzewski V.G., Montgomery Jr. J.A., Stratmann R.E., Burant J.C., Dapprich S., Millam J.M., Daniels A.D., Kudin K.N., Strain M.C., Farkas O., Tomasi J., Barone V., Cossi M., Cammi R., Mennucci B., Pomelli C., Adamo C., Clifford S., Ochterski J., Petersson G.A., Ayala P.Y., Cui Q., Morokuma K., Malick D.K., Rabuck A.D., Raghavachari K., Foresman J.B., Cioslowski J., Ortiz J.V., Baboul A.G., Stefanov B.B., Liu G., Liashenko A., Piskorz P., Komaromi I., Gomperts R., Martin R.L., Fox D.J., Keith T., Al-Laham M.A., Peng C.Y., Nanayakkara A., Challacombe M., Gill P.M.W.,

Johnson B., Chen W., Wong M.W., Andres J.L., Gonzalez C., Head-Gordon M., Replogle E.S., and Pople J.A., Gaussian, Inc., Pittsburgh PA, **1998**.

CHAPTER V

CONCLUSIONS

Conclusions

The goal of this research was the understanding and optimization of the generic homogeneous active site composed of a ligand stabilized, coordinatively unsaturated, transition metal center generated in Ziegler-Natta olefin polymerization catalysis. This increased understanding would potentially lead to models for industrially used catalysts such as the Philips catalyst. Two approaches were used in this endeavor. One of these approaches concentrated on the selection of specific transition metal centers (Cr, V) to increase the reactivity of the catalytic active site towards ethylene insertion. The second focused on the particular ligand system to be employed or more specifically, the α,α'-diiminopyridine ligand whose use has afforded a large variety of highly active polymerization catalysts.

Homoleptic Cr alkyls species were synthesized to gather additional information about these systems. Of the two monomeric tetravalent compounds CrR_4 (R = $CH_2C(CH_3)_3$ for **5a** or R = $CH_2Si(CH_3)_3$ for **5b**) isolated, only the later showed moderate activity towards ethylene polymerization. The key to understanding the remarkable efficiency of the Cr catalyst currently used in industry for the production of polyethylene may relate to the ability of the Cr-C bond in the homoleptic tetravalent alkyl complexes to perform ethylene insertion coupled with their inertness toward H-transfer reactions. A strong tendency to perform ethylene insertion, counterbalanced by poor, if any, tendency of the Cr-C bond to undergo hydrogen transfer, would lead to the formation of high molecular weight polymers with virtually no branching.

A rare tetrameric Cr di-valent alkyl species was also characterized and showed the same inertness towards protic reagents as its monomeric Cr^{IV} counterpart. This Cr^{II} compound surprisingly showed mild activity towards ethylene polymerization even in the absence of Al activators. However, a strong Cr-Cr interaction was confirmed between the metal atoms and it is conceivable that such exchanges would influence the oxidation state of the multiple metal centers from the formal point of view.

Furthermore, the isolation of a monomeric tetravalent vanadium alkyl species puts any arguments as to the possible existence of this material to rest. A structural characterization of this compound will soon be added to the literature. The $V[CH_2Si(CH_3)_3]_4$ complex is less thermally stable than the isostructural Cr derivative. On the other hand, it displays a substantially higher catalytic activity and is activated with simple and inexpensive $AlCl_3$. This rekindles speculation as to the *optimal* electronic configuration of the metal center for the creation of an active olefin polymerization catalyst.

From the ligand perspective, reductions carried out on the popular α,α'-diiminopyridine ligand without the presence of transition metal yielded rare case trilithium organyl species. This has established that the *α,α'*-diiminopyridine ligand may accommodate up to three electrons in the antibonding orbitals of the imino function and of the pyridine ring in a low-spin configuration. This information explains the observed variety of transformations upon attempted activation of the associated transition metal complexes. Similar metal-to-ligand charge transfer can be assumed to occur upon alkylation in the initial steps of the activation process.

a) The localization of the spin density on the pyridine C_{meta} atoms explains the cycloaddition observed with Cr.

b) The formation of a double bond explains the reductive coupling observed with Mn.

c) The charge localization at the pyridine ring C_{para} position accounts for the lithiation and for the possibility to transfer alkyl groups directly from the metal center to any position of the pyridine ring.

What remains to be unveiled is how this ligand supports high level of catalytic activity with well diversified metals.

Future Work

Attempts to further functionalize the di and tetravalent homoleptic Cr alkyls were unsuccessful. This limits the potential use of these compounds as possible starting materials. However, the attempted chemistry, in a sense, involved overpowering the unreactive nature of these compounds towards protic reagents. Further study should be undertaken to find materials with which these compounds would react favorably. The extreme sensitivity to oxygen may give clues as to the avenues to explore.

Further efforts should be directed to capitalize on the increased activity observed for the V^{IV} alkyl species. The extreme thermal instability of this material would be problematic for use on a large scale. However, the potential for improved thermal stability and molecular weight control has not been realized. The random nature of the polymerization may be due to the availability of insertion sites on all sides of the active metal center. It may be possible to limit the *area of attack* by creating a mixed alkyl species making use of bulkier groups in combination with the trimethylsilylmethyl function used here. On the other hand, this would require a multi-step process or alkylating agent capable non-selective alkylations.

The continuing use of the α,α'-diiminopyridine ligand must take into account its facile reduction and consider the lingand's active role in the catalytic initiation process. This is a double-edged sword that has proven to be problematic with early transition metals showing low activity towards ethylene polymerization but highly effective in producing very active catalysts using late transition metals. The order in which the reduction of new complexes is carried out will play a major role in the subsequent activity. While attempted alkylation of transition metal halide complexes has yielded a variety of transformations, the reaction of *pre-activated* ligands such as the trilithium organyls with transition metals may lead to new species of catalysts. Taking it one step further, a reactivation sequence can be envisioned where a deactivated catalyst could be kick-started once again through the transfer of electrons via the ligand.

APPENDIX I

CRYSTALLOGRAPHIC DATA :

HOMOLEPTIC CHROMIUM ALKYLS

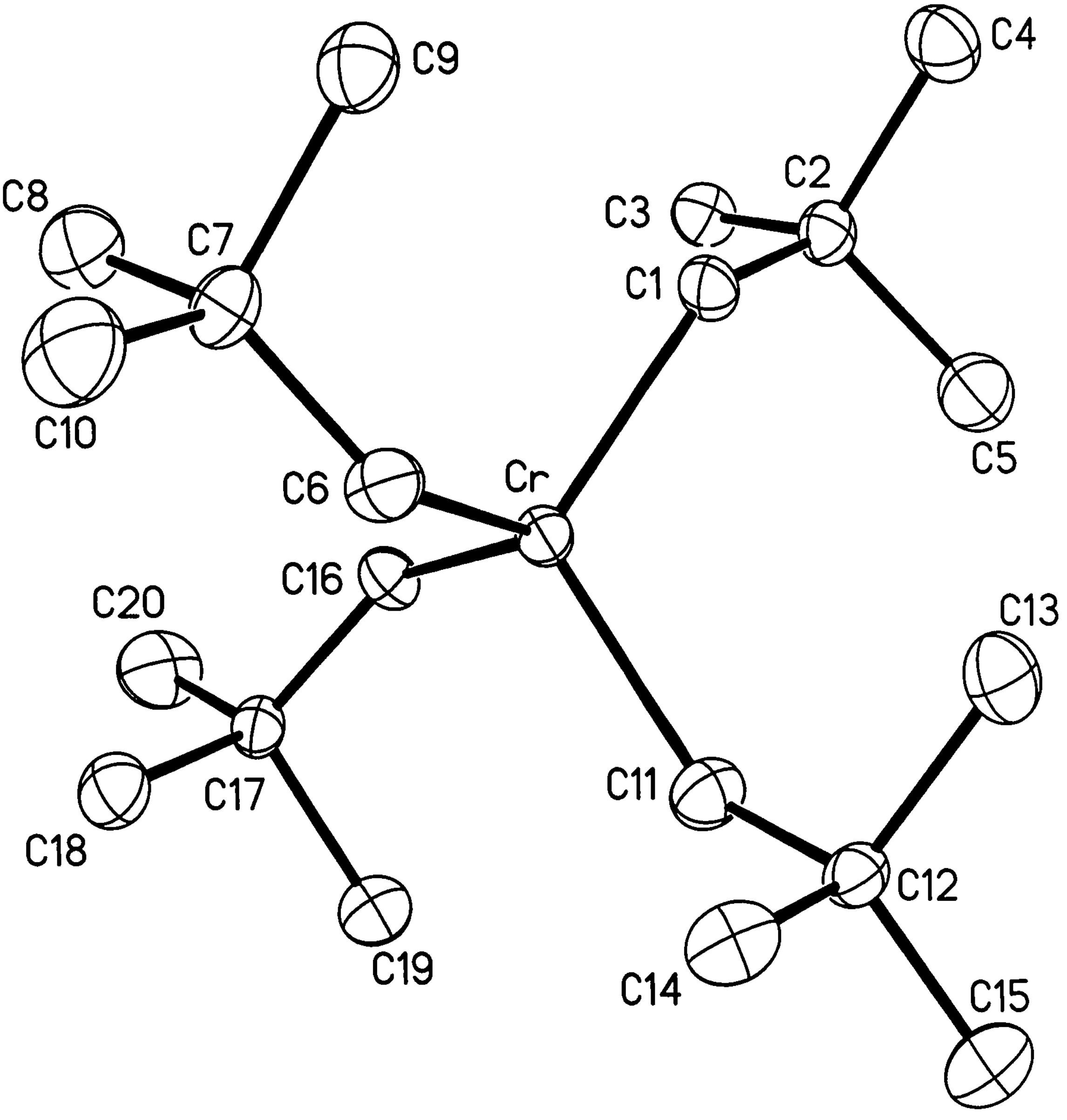
C9
C4
C2
C8
C3
C7
C1
C10
C5
C6
Cr
C16
C20
C13
C17
C11
C18
C12
C14
C19
C15

Table AI.1. Crystal data and structure refinement for sg411.

Identification code	sg411
Empirical formula	C20 H44 Cr
Formula weight	336.55
Temperature	203(2) K
Wavelength	0.71073 A
Crystal system, space group	Orthorhombic, Pbca
Unit cell dimensions	a = 15.7617(18) A alpha = 90 deg. b = 15.8066(18) A beta = 90 deg. c = 17.8368(19) A gamma = 90 deg.
Volume	4443.8(9) A^3
Z, Calculated density	8, 1.006 Mg/m^3
Absorption coefficient	0.511 mm^-1
F(000)	1504
Crystal size	0.1 x 0.1 x 0.1 mm
Theta range for data collection	2.15 to 28.76 deg.
Limiting indices	0<=h<=21, 0<=k<=21, 0<=l<=20
Reflections collected / unique	34844 / 4971 [R(int) = 0.0859]
Completeness to theta = 28.76	86.1 %
Absorption correction	Semi-empirical from equivalents
Max. and min. transmission	0.928078 and 0.781909
Refinement method	Full-matrix least-squares on F^2
Data / restraints / parameters	4971 / 0 / 238
Goodness-of-fit on F^2	1.085
Final R indices [I>2sigma(I)]	R1 = 0.0873, wR2 = 0.2965
R indices (all data)	R1 = 0.1461, wR2 = 0.3154
Largest diff. peak and hole	0.636 and -0.777 e.A^-3

Table AI.2. Atomic coordinates (x 10^4) and equivalent isotropic displacement parameters (A^2 x 10^3) for sg411.
U(eq) is defined as one third of the trace of the orthogonalized Uij tensor.

	x	y	z	U(eq)
Cr	3731(1)	1261(1)	6288(1)	26(1)
C(1)	2738(8)	888(8)	5656(7)	31(2)
C(2)	2587(4)	184(4)	5144(4)	31(1)
C(3)	2606(9)	-669(9)	5588(8)	39(2)
C(4)	1754(9)	271(10)	4704(8)	48(3)
C(5)	3295(10)	152(10)	4532(9)	50(3)
C(1')	3314(8)	281(8)	5649(7)	31(2)
C(2')	2587(4)	184(4)	5144(4)	31(1)
C(3')	1735(8)	206(9)	5605(8)	39(2)
C(4')	2620(10)	-660(10)	4680(9)	48(3)
C(5')	2518(10)	946(10)	4589(9)	50(3)
C(6)	3345(8)	2270(9)	6867(8)	37(2)
C(7)	2635(4)	2412(4)	7404(4)	36(2)
C(8)	2506(10)	1618(11)	7958(9)	51(3)
C(9)	1722(9)	2416(9)	6938(8)	44(2)
C(10)	2691(12)	3196(11)	7851(10)	63(3)
C(6')	2746(9)	1651(8)	6879(8)	37(2)
C(7')	2635(4)	2412(4)	7404(4)	36(2)
C(8')	3512(10)	2550(10)	7850(9)	51(3)
C(9')	2590(9)	3235(9)	6924(8)	44(2)
C(10')	1939(11)	2347(11)	7955(10)	63(3)
C(11)	4733(8)	1642(8)	5686(8)	39(2)
C(12)	4863(4)	2398(4)	5189(4)	31(1)
C(13)	4040(10)	2542(9)	4690(8)	48(3)
C(14)	4907(10)	3197(9)	5682(9)	50(3)
C(15)	5678(9)	2303(9)	4697(9)	48(3)
C(11')	4132(8)	2245(9)	5721(8)	39(2)
C(12')	4863(4)	2398(4)	5189(4)	31(1)
C(13')	4934(10)	1663(9)	4613(8)	48(3)
C(14')	5731(9)	2397(10)	5648(9)	50(3)
C(15')	4766(10)	3235(9)	4759(9)	48(3)
C(16)	4109(8)	280(8)	6898(7)	31(2)
C(17)	4817(4)	142(4)	7436(3)	30(1)
C(18)	4911(9)	936(9)	7949(8)	43(2)
C(19)	5681(8)	113(9)	6976(8)	40(2)
C(20)	4737(10)	-639(10)	7890(10)	56(3)
C(16')	4698(8)	823(8)	6927(7)	31(2)
C(17')	4817(4)	142(4)	7436(3)	30(1)
C(18')	4055(9)	33(10)	7975(8)	43(2)
C(19')	4802(9)	-748(8)	6999(8)	40(2)
C(20')	5608(10)	187(11)	7927(9)	56(3)

Table AI.3. Bond lengths [A] and angles [deg] for sg411.

Cr-C(11')	1.961(13)
Cr-C(6')	1.976(13)
Cr-C(16)	1.986(12)
Cr-C(6)	1.996(13)
Cr-C(11)	2.002(13)
Cr-C(1)	2.016(12)
Cr-C(16')	2.025(12)
Cr-C(1')	2.031(12)
C(1)-C(2)	1.459(13)
C(2)-C(4)	1.536(15)
C(2)-C(5)	1.562(16)
C(2)-C(3)	1.564(15)
C(6)-C(7)	1.489(14)
C(7)-C(10)	1.477(17)
C(7)-C(8)	1.611(17)
C(7)-C(9)	1.661(16)
C(11)-C(12)	1.503(14)
C(12)-C(14)	1.541(16)
C(12)-C(15)	1.563(15)
C(12)-C(13)	1.590(16)
C(16)-C(17)	1.488(13)
C(17)-C(20)	1.482(16)
C(17)-C(18)	1.561(15)
C(17)-C(19)	1.590(14)

C(11')-Cr-C(6')	106.3(6)
C(11')-Cr-C(16)	143.7(5)
C(6')-Cr-C(16)	100.7(6)
C(11')-Cr-C(6)	74.4(6)
C(6')-Cr-C(6)	40.0(5)
C(16)-Cr-C(6)	115.5(5)
C(11')-Cr-C(11)	39.7(5)
C(6')-Cr-C(11)	144.3(5)
C(16)-Cr-C(11)	107.0(5)
C(6)-Cr-C(11)	106.1(5)
C(11')-Cr-C(1)	101.2(5)
C(6')-Cr-C(1)	77.3(5)
C(16)-Cr-C(1)	108.1(5)
C(6)-Cr-C(1)	106.6(5)
C(11)-Cr-C(1)	113.6(5)
C(11')-Cr-C(16')	108.6(5)
C(6')-Cr-C(16')	113.4(5)
C(16)-Cr-C(16')	36.7(5)
C(6)-Cr-C(16')	102.2(5)
C(11)-Cr-C(16')	79.1(5)
C(1)-Cr-C(16')	143.0(5)
C(11')-Cr-C(1')	114.9(5)
C(6')-Cr-C(1')	106.4(5)
C(16)-Cr-C(1')	79.0(5)
C(6)-Cr-C(1')	143.2(5)
C(11)-Cr-C(1')	100.6(5)
C(1)-Cr-C(1')	38.1(5)
C(16')-Cr-C(1')	107.4(5)

C(2)-C(1)-Cr	134.4(8)
C(1)-C(2)-C(4)	113.1(9)
C(1)-C(2)-C(5)	110.2(9)
C(4)-C(2)-C(5)	104.8(9)
C(1)-C(2)-C(3)	109.7(8)
C(4)-C(2)-C(3)	110.7(9)
C(5)-C(2)-C(3)	108.2(9)
C(7)-C(6)-Cr	133.1(9)
C(10)-C(7)-C(6)	115.4(10)
C(10)-C(7)-C(8)	109.3(10)
C(6)-C(7)-C(8)	111.8(9)
C(10)-C(7)-C(9)	108.7(10)
C(6)-C(7)-C(9)	109.2(8)
C(8)-C(7)-C(9)	101.6(9)
C(12)-C(11)-Cr	131.6(8)
C(11)-C(12)-C(14)	108.8(9)
C(11)-C(12)-C(15)	111.5(8)
C(14)-C(12)-C(15)	111.3(9)
C(11)-C(12)-C(13)	109.5(8)
C(14)-C(12)-C(13)	103.9(9)
C(15)-C(12)-C(13)	111.7(9)
C(17)-C(16)-Cr	133.9(8)
C(20)-C(17)-C(16)	114.2(9)
C(20)-C(17)-C(18)	111.0(9)
C(16)-C(17)-C(18)	109.3(8)
C(20)-C(17)-C(19)	109.3(9)
C(16)-C(17)-C(19)	108.3(8)
C(18)-C(17)-C(19)	104.1(8)

Symmetry transformations used to generate equivalent atoms:

Table AI.4. Anisotropic displacement parameters (A^2 x 10^3) for sg411. The anisotropic displacement factor exponent takes the form: -2 pi^2 [h^2 a*^2 U11 + ... + 2 h k a* b* U12]

	U11	U22	U33	U23	U13	U12
Cr	27(1)	27(1)	25(1)	0(1)	-1(1)	0(1)
C(1)	32(4)	31(4)	29(5)	-1(4)	-1(4)	-6(4)
C(2)	34(3)	30(3)	29(3)	4(3)	-1(2)	0(2)
C(3)	36(5)	43(5)	39(5)	-1(4)	-1(4)	-2(4)
C(4)	45(6)	51(6)	47(6)	-7(5)	-7(5)	-3(5)
C(5)	50(6)	50(6)	50(7)	8(5)	-3(5)	-8(5)
C(1')	32(4)	31(4)	29(5)	-1(4)	-1(4)	-6(4)
C(2')	34(3)	30(3)	29(3)	4(3)	-1(2)	0(2)
C(3')	36(5)	43(5)	39(5)	-1(4)	-1(4)	-2(4)
C(4')	45(6)	51(6)	47(6)	-7(5)	-7(5)	-3(5)
C(5')	50(6)	50(6)	50(7)	8(5)	-3(5)	-8(5)
C(6)	34(5)	38(5)	41(5)	-2(4)	2(4)	-4(4)
C(7)	41(4)	34(4)	33(4)	-2(3)	7(3)	4(3)
C(8)	47(6)	57(7)	49(7)	-1(5)	1(5)	5(5)
C(9)	47(6)	43(5)	42(6)	-1(5)	4(5)	8(4)
C(10)	67(8)	58(7)	63(8)	-19(6)	13(7)	-3(6)
C(6')	34(5)	38(5)	41(5)	-2(4)	2(4)	-4(4)
C(7')	41(4)	34(4)	33(4)	-2(3)	7(3)	4(3)
C(8')	47(6)	57(7)	49(7)	-1(5)	1(5)	5(5)
C(9')	47(6)	43(5)	42(6)	-1(5)	4(5)	8(4)
C(10')	67(8)	58(7)	63(8)	-19(6)	13(7)	-3(6)
C(11)	37(5)	37(5)	42(5)	4(4)	3(4)	0(4)
C(12)	28(3)	34(3)	30(3)	2(3)	3(3)	1(2)
C(13)	52(6)	46(6)	45(6)	7(5)	-4(5)	3(5)
C(14)	44(6)	48(6)	58(7)	3(5)	7(5)	-4(5)
C(15)	48(6)	41(5)	56(7)	0(5)	13(5)	2(5)
C(11')	37(5)	37(5)	42(5)	4(4)	3(4)	0(4)
C(12')	28(3)	34(3)	30(3)	2(3)	3(3)	1(2)
C(13')	52(6)	46(6)	45(6)	7(5)	-4(5)	3(5)
C(14')	44(6)	48(6)	58(7)	3(5)	7(5)	-4(5)
C(15')	48(6)	41(5)	56(7)	0(5)	13(5)	2(5)
C(16)	32(4)	32(4)	30(5)	1(4)	-5(4)	-1(3)
C(17)	31(3)	33(3)	24(3)	2(2)	1(2)	4(3)
C(18)	42(5)	48(5)	41(6)	-5(5)	4(4)	5(4)
C(19)	40(5)	35(5)	46(6)	1(4)	2(4)	6(4)
C(20)	50(6)	55(7)	63(8)	14(6)	-5(6)	3(5)
C(16')	32(4)	32(4)	30(5)	1(4)	-5(4)	-1(3)
C(17')	31(3)	33(3)	24(3)	2(2)	1(2)	4(3)
C(18')	42(5)	48(5)	41(6)	-5(5)	4(4)	5(4)
C(19')	40(5)	35(5)	46(6)	1(4)	2(4)	6(4)
C(20')	50(6)	55(7)	63(8)	14(6)	-5(6)	3(5)

Table AI.5. Hydrogen coordinates (x 10^4) and isotropic displacement parameters (A^2 x 10^3) for sg411.

	x	y	z	U(eq)
H(1A)	2272	844	6017	37
H(1B)	2609	1388	5351	37
H(3A)	2167	-664	5969	59
H(3B)	3156	-737	5825	59
H(3C)	2508	-1136	5246	59
H(4A)	1280	284	5051	72
H(4B)	1691	-207	4368	72
H(4C)	1764	791	4415	72
H(5A)	3298	679	4254	75
H(5B)	3184	-314	4191	75
H(5C)	3842	69	4770	75
H(1'A)	3804	134	5337	37
H(1'B)	3253	-187	6006	37
H(3'A)	1737	-248	5971	59
H(3'B)	1259	133	5267	59
H(3'C)	1686	745	5861	59
H(4'A)	2642	-1138	5020	72
H(4'B)	3122	-661	4365	72
H(4'C)	2118	-702	4368	72
H(5'A)	3025	971	4282	75
H(5'B)	2461	1467	4871	75
H(5'C)	2025	871	4270	75
H(6A)	3850	2445	7146	45
H(6B)	3260	2706	6483	45
H(8A)	3010	1546	8264	77
H(8B)	2411	1110	7665	77
H(8C)	2020	1719	8279	77
H(9A)	1732	2862	6564	66
H(9B)	1259	2515	7285	66
H(9C)	1644	1874	6692	66
H(10A)	2770	3676	7519	94
H(10B)	3169	3158	8193	94
H(10C)	2172	3270	8136	94
H(6'A)	2289	1711	6510	45
H(6'B)	2590	1161	7187	45
H(8'A)	3618	2066	8172	77
H(8'B)	3473	3058	8154	77
H(8'C)	3974	2609	7494	77
H(9'A)	2088	3219	6609	66
H(9'B)	3092	3276	6611	66
H(9'C)	2561	3723	7252	66
H(10D)	1407	2257	7694	94
H(10E)	1907	2866	8244	94
H(10F)	2047	1875	8289	94
H(11A)	5196	1675	6051	46
H(11B)	4867	1157	5365	46
H(13A)	3962	2062	4358	71
H(13B)	4109	3052	4394	71

H(13C)	3548	2600	5012	71
H(14A)	5381	3150	6027	75
H(14B)	4384	3254	5964	75
H(14C)	4985	3691	5366	75
H(15A)	5631	1798	4391	72
H(15B)	6171	2258	5019	72
H(15C)	5736	2794	4375	72
H(11C)	3633	2420	5432	46
H(11D)	4206	2682	6105	46
H(13D)	4418	1633	4318	71
H(13E)	5017	1133	4877	71
H(13F)	5413	1764	4283	71
H(14D)	5713	2835	6029	75
H(14E)	6200	2504	5309	75
H(14F)	5808	1850	5886	75
H(15D)	4231	3233	4489	72
H(15E)	5230	3295	4406	72
H(15F)	4774	3703	5110	72
H(16A)	3602	126	7186	37
H(16B)	4182	-173	6529	37
H(18A)	4400	1007	8245	65
H(18B)	4999	1434	7641	65
H(18C)	5394	861	8280	65
H(19A)	5675	-368	6639	61
H(19B)	6154	60	7321	61
H(19C)	5742	630	6688	61
H(20A)	4681	-1123	7559	84
H(20B)	4239	-599	8207	84
H(20C)	5238	-707	8200	84
H(16C)	5158	744	6564	37
H(16D)	4862	1319	7222	37
H(18D)	3994	537	8280	65
H(18E)	4152	-452	8297	65
H(18F)	3541	-55	7686	65
H(19D)	5257	-761	6633	61
H(19E)	4261	-814	6746	61
H(19F)	4878	-1205	7355	61
H(20D)	5616	722	8194	84
H(20E)	6110	142	7615	84
H(20F)	5601	-275	8285	84

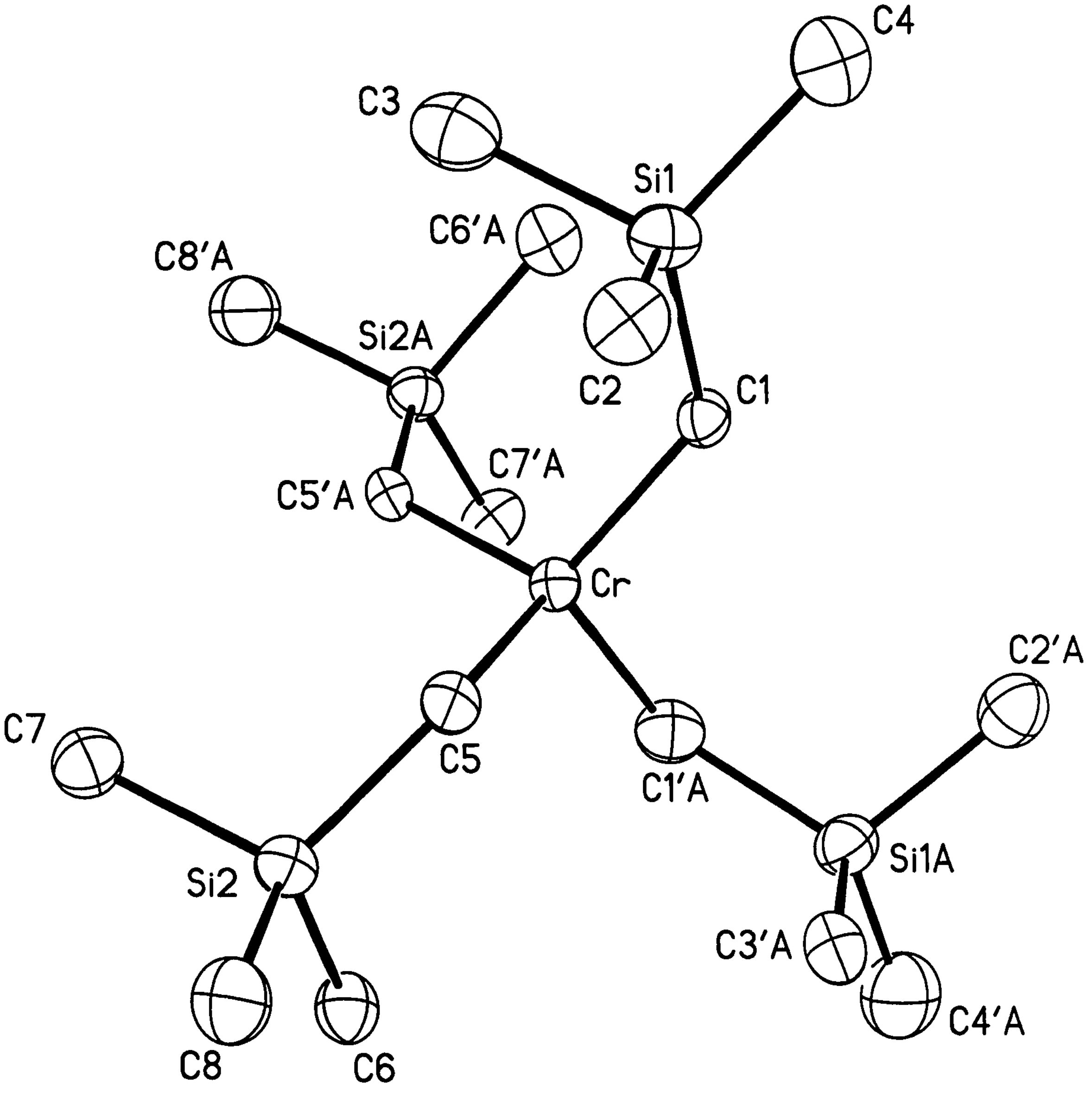
C4
C3
Si1
C6'A
C8'A
Si2A
C2
C1
C7'A
C5'A
Cr
C2'A
C7
C5
C1'A
Si2
Si1A
C3'A
C4'A
C8
C6

Table AI.6. Crystal data and structure refinement for sg412.

Identification code	sg412
Empirical formula	C16 H44 Cr Si4
Formula weight	400.87
Temperature	203(2) K
Wavelength	0.71073 A
Crystal system, space group	Monoclinic, C2/c
Unit cell dimensions	a = 18.7133(18) A alpha = 90 deg. b = 8.3575(8) A beta = 116.2890(10) deg. c = 18.7599(18) A gamma = 90 deg.
Volume	2630.5(4) A^3
Z, Calculated density	4, 1.012 Mg/m^3
Absorption coefficient	0.613 mm^-1
F(000)	880
Crystal size	0.18 x 0.15 x 0.03 mm
Theta range for data collection	2.42 to 25.00 deg.
Limiting indices	-22<=h<=19, 0<=k<=9, 0<=l<=22
Reflections collected / unique	7547 / 2313 [R(int) = 0.0921]
Completeness to theta = 25.00	100.0 %
Absorption correction	Semi-empirical from equivalents
Max. and min. transmission	0.928076 and 0.649701
Refinement method	Full-matrix least-squares on F^2
Data / restraints / parameters	2313 / 0 / 168
Goodness-of-fit on F^2	1.053
Final R indices [I>2sigma(I)]	R1 = 0.0904, wR2 = 0.2388
R indices (all data)	R1 = 0.0972, wR2 = 0.2420
Largest diff. peak and hole	0.388 and -0.412 e.A^-3

Table AI.7. Atomic coordinates (x 10^4) and equivalent isotropic displacement parameters (A^2 x 10^3) for sg412.
U(eq) is defined as one third of the trace of the orthogonalized Uij tensor.

	x	y	z	U(eq)
Cr	0	9857(2)	2500	33(1)
Si(1)	-565(1)	7675(3)	804(1)	52(1)
Si(2)	1697(1)	12076(3)	3041(1)	43(1)
C(1)	-439(9)	7974(17)	1830(8)	36(3)
C(2)	452(11)	7490(20)	809(11)	62(5)
C(3)	-1047(12)	9600(30)	197(11)	72(6)
C(4)	-1164(12)	5900(30)	248(13)	74(6)
C(5)	1050(8)	10350(17)	2545(8)	38(3)
C(6)	1749(10)	12370(20)	4053(10)	52(4)
C(7)	1255(10)	13980(20)	2488(10)	54(4)
C(8)	2695(12)	11940(20)	3137(13)	74(6)
C(1')	-82(10)	9380(20)	1444(10)	54(4)
C(2')	8(11)	5820(20)	1218(11)	65(5)
C(3')	-1563(10)	7360(20)	847(11)	54(4)
C(4')	-728(15)	7720(30)	-271(15)	98(8)
C(5')	670(8)	11798(16)	2897(8)	37(3)
C(6')	2351(10)	10400(20)	3619(11)	57(4)
C(7')	1755(11)	12040(20)	2056(11)	63(5)
C(8')	2153(12)	13950(30)	3589(12)	71(5)

Table AI.8. Bond lengths [A] and angles [deg] for sg412.

Cr-C(1)	1.954(14)
Cr-C(1)#1	1.954(14)
Cr-C(1')	1.958(16)
Cr-C(1')#1	1.958(16)
Cr-C(5)#1	1.972(14)
Cr-C(5)	1.972(14)
Cr-C(5')	1.983(14)
Cr-C(5')#1	1.983(14)
Si(1)-C(1')	1.827(18)
Si(1)-C(2')	1.85(2)
Si(1)-C(1)	1.851(13)
Si(1)-C(4)	1.88(2)
Si(1)-C(4')	1.90(3)
Si(1)-C(2)	1.905(17)
Si(1)-C(3')	1.924(17)
Si(1)-C(3)	1.95(2)
Si(2)-C(8)	1.80(2)
Si(2)-C(5')	1.834(14)
Si(2)-C(5)	1.848(14)

Si(2)-C(6')	1.860(18)
Si(2)-C(8')	1.86(2)
Si(2)-C(6)	1.874(16)
Si(2)-C(7)	1.881(17)
Si(2)-C(7')	1.898(18)
C(1)-Cr-C(1)#1	72.7(8)
C(1)-Cr-C(1')	50.6(6)
C(1)#1-Cr-C(1')	108.1(7)
C(1)-Cr-C(1')#1	108.1(7)
C(1)#1-Cr-C(1')#1	50.6(6)
C(1')-Cr-C(1')#1	156.7(11)
C(1)-Cr-C(5)#1	90.8(6)
C(1)#1-Cr-C(5)#1	108.9(6)
C(1')-Cr-C(5)#1	111.6(6)
C(1')#1-Cr-C(5)#1	73.5(6)
C(1)-Cr-C(5)	108.9(6)
C(1)#1-Cr-C(5)	90.8(6)
C(1')-Cr-C(5)	73.5(6)
C(1')#1-Cr-C(5)	111.6(6)
C(5)#1-Cr-C(5)	155.9(9)
C(1)-Cr-C(5')	156.5(6)
C(1)#1-Cr-C(5')	113.7(6)
C(1')-Cr-C(5')	107.4(7)
C(1')#1-Cr-C(5')	91.8(7)
C(5)#1-Cr-C(5')	107.3(6)
C(5)-Cr-C(5')	50.3(6)
C(1)-Cr-C(5')#1	113.7(6)
C(1)#1-Cr-C(5')#1	156.5(6)
C(1')-Cr-C(5')#1	91.8(7)
C(1')#1-Cr-C(5')#1	107.4(7)
C(5)#1-Cr-C(5')#1	50.3(6)
C(5)-Cr-C(5')#1	107.3(6)
C(5')-Cr-C(5')#1	70.2(8)
C(1')-Si(1)-C(2')	110.7(8)
C(1')-Si(1)-C(1)	54.0(7)
C(2')-Si(1)-C(1)	83.8(7)
C(1')-Si(1)-C(4)	169.9(8)
C(2')-Si(1)-C(4)	70.3(9)
C(1)-Si(1)-C(4)	117.0(8)
C(1')-Si(1)-C(4')	118.9(9)
C(2')-Si(1)-C(4')	104.7(10)
C(1)-Si(1)-C(4')	171.0(9)
C(4)-Si(1)-C(4')	69.5(10)
C(1')-Si(1)-C(2)	81.8(8)
C(2')-Si(1)-C(2)	62.5(8)
C(1)-Si(1)-C(2)	109.8(7)
C(4)-Si(1)-C(2)	106.8(9)
C(4')-Si(1)-C(2)	72.5(10)
C(1')-Si(1)-C(3')	106.7(7)
C(2')-Si(1)-C(3')	105.0(8)
C(1)-Si(1)-C(3')	69.7(7)
C(4)-Si(1)-C(3')	63.9(8)
C(4')-Si(1)-C(3')	110.1(9)
C(2)-Si(1)-C(3')	167.2(8)
C(1')-Si(1)-C(3)	72.8(8)
C(2')-Si(1)-C(3)	166.3(8)

C(1)-Si(1)-C(3)	108.0(7)
C(4)-Si(1)-C(3)	108.8(9)
C(4')-Si(1)-C(3)	63.2(10)
C(2)-Si(1)-C(3)	105.9(8)
C(3')-Si(1)-C(3)	86.1(8)
C(8)-Si(2)-C(5')	168.9(8)
C(8)-Si(2)-C(5)	114.9(8)
C(5')-Si(2)-C(5)	54.3(6)
C(8)-Si(2)-C(6')	60.6(8)
C(5')-Si(2)-C(6')	111.5(7)
C(5)-Si(2)-C(6')	79.7(7)
C(8)-Si(2)-C(8')	78.2(9)
C(5')-Si(2)-C(8')	112.5(8)
C(5)-Si(2)-C(8')	166.7(8)
C(6')-Si(2)-C(8')	106.9(9)
C(8)-Si(2)-C(6)	108.8(9)
C(5')-Si(2)-C(6)	75.3(7)
C(5)-Si(2)-C(6)	109.8(7)
C(6')-Si(2)-C(6)	77.4(8)
C(8')-Si(2)-C(6)	61.7(8)
C(8)-Si(2)-C(7)	106.9(9)
C(5')-Si(2)-C(7)	81.4(7)
C(5)-Si(2)-C(7)	110.7(7)
C(6')-Si(2)-C(7)	167.0(7)
C(8')-Si(2)-C(7)	64.7(8)
C(6)-Si(2)-C(7)	105.1(8)
C(8)-Si(2)-C(7')	65.9(9)
C(5')-Si(2)-C(7')	111.3(7)
C(5)-Si(2)-C(7')	78.8(7)
C(6')-Si(2)-C(7')	104.4(8)
C(8')-Si(2)-C(7')	109.9(9)
C(6)-Si(2)-C(7')	171.4(8)
C(7)-Si(2)-C(7')	71.2(8)
Si(1)-C(1)-Cr	127.0(8)
Si(2)-C(5)-Cr	127.1(7)
Si(1)-C(1')-Cr	128.1(9)
Si(2)-C(5')-Cr	127.3(7)

Symmetry transformations used to generate equivalent atoms:
#1 -x,y,-z+1/2

Table AI.9. Anisotropic displacement parameters (A^2 x 10^3) for sg412.
The anisotropic displacement factor exponent takes the form:
-2 pi^2 [h^2 a*^2 U11 + ... + 2 h k a* b* U12]

	U11	U22	U33	U23	U13	U12
Cr	33(1)	33(1)	33(1)	0	15(1)	0
Si(1)	51(1)	57(2)	44(1)	-6(1)	18(1)	0(1)
Si(2)	39(1)	44(1)	42(1)	0(1)	16(1)	-1(1)
C(1)	44(8)	34(8)	33(7)	1(6)	19(6)	1(6)
C(2)	62(11)	69(12)	63(11)	1(9)	33(9)	9(9)
C(3)	71(12)	89(15)	62(11)	-16(11)	36(10)	-8(11)
C(4)	74(13)	70(14)	80(14)	-1(11)	36(11)	-3(11)
C(5)	44(8)	36(8)	36(7)	-4(6)	21(6)	2(6)
C(6)	59(10)	47(9)	55(10)	-1(8)	29(8)	0(8)
C(7)	51(9)	55(10)	53(10)	1(8)	22(8)	5(8)
C(8)	75(13)	56(12)	80(14)	3(11)	25(11)	2(10)
C(1')	50(9)	63(11)	50(9)	6(8)	21(8)	-2(8)
C(2')	58(11)	70(13)	67(12)	-11(10)	28(9)	-5(10)
C(3')	57(10)	44(9)	60(10)	1(8)	25(8)	6(8)
C(4')	101(18)	79(17)	103(19)	5(14)	35(15)	-19(14)
C(5')	38(7)	29(7)	38(7)	0(6)	13(6)	6(6)
C(6')	48(9)	59(11)	71(11)	3(9)	33(9)	-4(8)
C(7')	63(11)	66(12)	56(11)	-11(9)	23(9)	-13(10)
C(8')	68(12)	79(14)	68(12)	0(11)	31(10)	5(11)

Table AI.10. Hydrogen coordinates (x 10^4) and isotropic displacement parameters (A^2 x 10^3) for sg412.

	x	y	z	U(eq)
H(1A)	-116	7070	2137	44
H(1B)	-970	7819	1802	44
H(2A)	727	6560	1117	93
H(2B)	764	8443	1045	93
H(2C)	384	7376	268	93
H(3A)	-1574	9745	166	108
H(3B)	-1089	9497	-335	108
H(3C)	-718	10519	458	108
H(4A)	-930	4931	546	111
H(4B)	-1166	5837	-269	111
H(4C)	-1707	6006	180	111
H(5A)	1378	9399	2776	45
H(5B)	962	10395	1991	45
H(6A)	1214	12499	4006	78
H(6B)	2061	13316	4297	78
H(6C)	1997	11442	4381	78
H(7A)	1219	13917	1957	81
H(7B)	1592	14878	2768	81
H(7C)	727	14134	2454	81
H(8A)	2675	11800	2615	111
H(8B)	2965	11035	3471	111
H(8C)	2983	12916	3376	111
H(1'A)	-332	10331	1122	65
H(1'B)	469	9373	1512	65
H(2'A)	526	5905	1221	97
H(2'B)	-278	4916	893	97
H(2'C)	76	5667	1757	97
H(3'A)	-1898	8290	633	81
H(3'B)	-1466	7196	1394	81
H(3'C)	-1828	6422	535	81
H(4'A)	-225	7924	-287	148
H(4'B)	-1104	8561	-555	148
H(4'C)	-939	6697	-519	148
H(5'A)	363	12665	2542	44
H(5'B)	682	12029	3415	44
H(6'A)	2339	10313	4128	85
H(6'B)	2893	10604	3703	85
H(6'C)	2163	9408	3326	85
H(7'A)	1423	12885	1716	95
H(7'B)	1568	11013	1800	95
H(7'C)	2302	12203	2149	95
H(8'A)	2110	13976	4085	107
H(8'B)	1877	14869	3268	107
H(8'C)	2711	13993	3700	107

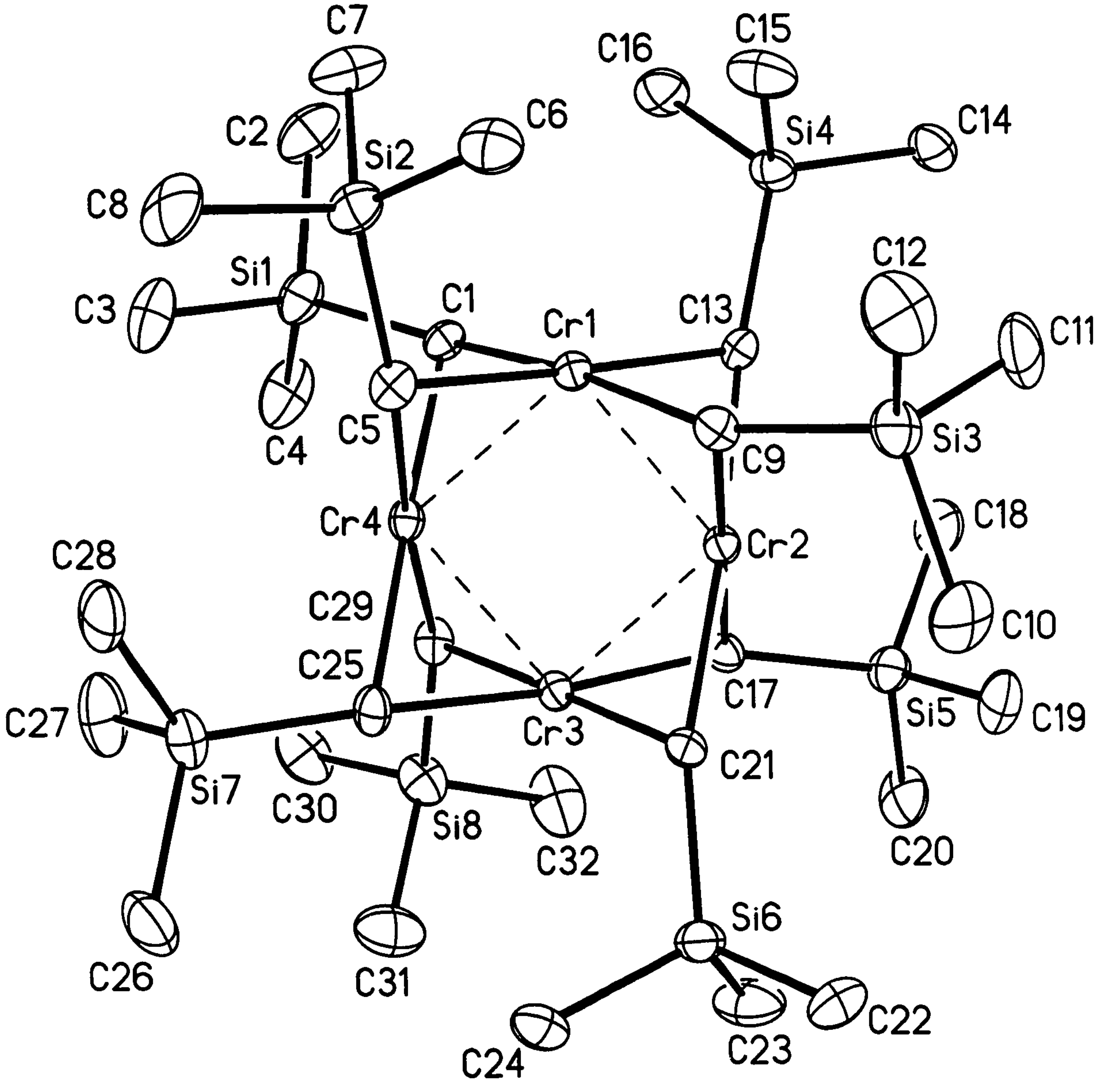
C7
C15
C16
C6
C2
Si2
Si4
C14
C8
C12
Si1
C3
C1
Cr1
C13
C11
C5
C9
Si3
C4
C18
Cr4
Cr2
C28
C29
C10
C25
C17
C27
Cr3
Si5
C19
C21
Si7
C30
Si8
C32
C20
Si6
C26
C31
C22
C23
C24

Table AI.11. Crystal data and structure refinement for sg415.

Identification code	sg415
Empirical formula	C32 H88 Cr4 Si8
Formula weight	905.74
Temperature	203(2) K
Wavelength	0.71073 A
Crystal system, space group	Monoclinic, P2(1)/n
Unit cell dimensions	a = 17.0805(16) A alpha = 90 deg. b = 13.4843(13) A beta = 99.603(2) deg. c = 22.873(2) A gamma = 90 deg.
Volume	5194.3(8) A^3
Z, Calculated density	4, 1.158 Mg/m^3
Absorption coefficient	1.018 mm^-1
F(000)	1952
Crystal size	0.10 x 0.10 x 0.02 mm
Theta range for data collection	1.38 to 26.37 deg.
Limiting indices	-21<=h<=21, 0<=k<=16, 0<=l<=28
Reflections collected / unique	46760 / 10605 [R(int) = 0.1157]
Completeness to theta = 26.37	99.9 %
Absorption correction	Semi-empirical from equivalents
Max. and min. transmission	0.928077 and 0.809644
Refinement method	Full-matrix least-squares on F^2
Data / restraints / parameters	10605 / 0 / 397
Goodness-of-fit on F^2	1.024
Final R indices [I>2sigma(I)]	R1 = 0.0541, wR2 = 0.1153
R indices (all data)	R1 = 0.1292, wR2 = 0.1429
Largest diff. peak and hole	0.677 and -0.452 e.A^-3

Table AI.12. Atomic coordinates (x 10^4) and equivalent isotropic displacement parameters (A^2 x 10^3) for sg415.
U(eq) is defined as one third of the trace of the orthogonalized Uij tensor.

	x	y	z	U(eq)
Cr(1)	5638(1)	6401(1)	2432(1)	25(1)
Cr(2)	5357(1)	7121(1)	3300(1)	25(1)
Cr(3)	4407(1)	8195(1)	2722(1)	26(1)
Cr(4)	4681(1)	7465(1)	1850(1)	27(1)
Si(1)	4066(1)	5568(1)	1001(1)	44(1)
C(1)	4605(3)	5837(3)	1758(2)	31(1)
C(2)	4229(4)	4242(5)	799(3)	69(2)
C(3)	4378(4)	6403(5)	427(2)	66(2)
C(4)	2967(3)	5702(6)	963(3)	70(2)
Si(2)	6755(1)	6612(1)	1396(1)	42(1)
C(5)	5970(3)	7295(3)	1715(2)	33(1)
C(6)	7707(3)	6485(4)	1940(2)	48(1)
C(7)	6449(4)	5335(4)	1141(3)	67(2)
C(8)	6970(4)	7309(5)	730(3)	66(2)
Si(3)	7267(1)	7044(1)	3872(1)	45(1)
C(9)	6582(3)	7077(3)	3143(2)	31(1)
C(10)	7171(3)	8168(4)	4331(3)	63(2)
C(11)	7102(4)	5940(5)	4330(2)	68(2)
C(12)	8320(3)	7001(6)	3730(3)	79(2)
Si(4)	5844(1)	4256(1)	3068(1)	36(1)
C(13)	5332(3)	5462(3)	3140(2)	30(1)
C(14)	5869(3)	3526(4)	3768(2)	46(1)
C(15)	6884(3)	4386(4)	2919(3)	59(2)
C(16)	5293(3)	3503(4)	2447(2)	52(2)
Si(5)	4140(1)	6826(1)	4239(1)	40(1)
C(17)	4115(3)	7185(3)	3448(2)	31(1)
C(18)	4129(4)	5444(4)	4316(2)	61(2)
C(19)	5034(4)	7305(5)	4739(2)	60(2)
C(20)	3244(4)	7301(5)	4506(3)	64(2)
Si(6)	5032(1)	10001(1)	3659(1)	39(1)
C(21)	5371(3)	8795(3)	3379(2)	30(1)
C(22)	5818(4)	10465(4)	4272(2)	61(2)
C(23)	4096(4)	9865(4)	3970(3)	67(2)
C(24)	4882(3)	10974(4)	3070(2)	51(2)
Si(7)	4594(1)	9708(1)	1227(1)	44(1)
C(25)	4775(3)	9083(3)	1967(2)	32(1)
C(26)	4491(4)	11074(4)	1324(3)	66(2)
C(27)	3655(4)	9286(5)	741(3)	80(2)
C(28)	5440(4)	9479(5)	822(3)	66(2)
Si(8)	2514(1)	8288(1)	2153(1)	46(1)
C(29)	3438(3)	7613(4)	2062(2)	35(1)
C(30)	1721(3)	8032(5)	1500(3)	65(2)
C(31)	2648(4)	9673(4)	2218(3)	75(2)
C(32)	2117(3)	7833(6)	2823(3)	79(2)

Table AI.13. Bond lengths [A] and angles [deg] for sg415.

Cr(1)-C(5)	2.184(4)
Cr(1)-C(13)	2.188(4)
Cr(1)-Cr(2)	2.3310(10)
Cr(1)-Cr(4)	2.4026(10)
Cr(2)-C(9)	2.183(4)
Cr(2)-C(17)	2.205(4)
Cr(2)-Cr(3)	2.4004(10)
Cr(3)-C(29)	2.192(5)
Cr(3)-C(21)	2.191(4)
Cr(3)-Cr(4)	2.3396(10)
Cr(4)-C(25)	2.200(5)
Cr(4)-C(1)	2.207(5)
Si(1)-C(1)	1.856(5)
Si(1)-C(4)	1.872(6)
Si(1)-C(3)	1.873(6)
Si(1)-C(2)	1.880(6)
Si(2)-C(7)	1.865(6)
Si(2)-C(8)	1.878(6)
Si(2)-C(5)	1.871(5)
Si(2)-C(6)	1.884(5)
Si(3)-C(10)	1.867(6)
Si(3)-C(11)	1.869(6)
Si(3)-C(12)	1.880(6)
Si(3)-C(9)	1.870(5)
Si(4)-C(14)	1.872(5)
Si(4)-C(15)	1.871(6)
Si(4)-C(16)	1.868(5)
Si(4)-C(13)	1.868(5)
Si(5)-C(20)	1.854(6)
Si(5)-C(19)	1.863(6)
Si(5)-C(18)	1.872(5)
Si(5)-C(17)	1.867(5)
Si(6)-C(23)	1.863(6)
Si(6)-C(24)	1.868(5)
Si(6)-C(22)	1.879(6)
Si(6)-C(21)	1.875(4)
Si(7)-C(28)	1.868(6)
Si(7)-C(26)	1.867(6)
Si(7)-C(27)	1.881(6)
Si(7)-C(25)	1.871(4)
Si(8)-C(30)	1.874(6)
Si(8)-C(32)	1.878(6)
Si(8)-C(29)	1.863(5)
Si(8)-C(31)	1.885(6)
C(5)-Cr(1)-C(13)	177.91(17)
C(5)-Cr(1)-Cr(2)	121.74(13)
C(13)-Cr(1)-Cr(2)	60.09(12)
C(5)-Cr(1)-Cr(4)	59.51(13)
C(13)-Cr(1)-Cr(4)	122.08(13)
Cr(2)-Cr(1)-Cr(4)	90.30(3)
C(9)-Cr(2)-C(17)	179.08(18)
C(9)-Cr(2)-Cr(1)	60.59(12)

C(17)-Cr(2)-Cr(1)	119.19(13)
C(9)-Cr(2)-Cr(3)	120.26(12)
C(17)-Cr(2)-Cr(3)	58.82(12)
Cr(1)-Cr(2)-Cr(3)	89.90(3)
C(29)-Cr(3)-C(21)	179.34(18)
C(29)-Cr(3)-Cr(4)	59.87(12)
C(21)-Cr(3)-Cr(4)	120.41(13)
C(29)-Cr(3)-Cr(2)	121.78(13)
C(21)-Cr(3)-Cr(2)	58.88(11)
Cr(4)-Cr(3)-Cr(2)	90.15(3)
C(25)-Cr(4)-C(1)	178.40(17)
C(25)-Cr(4)-Cr(3)	59.99(12)
C(1)-Cr(4)-Cr(3)	118.86(12)
C(25)-Cr(4)-Cr(1)	119.70(12)
C(1)-Cr(4)-Cr(1)	58.86(12)
Cr(3)-Cr(4)-Cr(1)	89.65(3)
C(1)-Si(1)-C(4)	111.2(2)
C(1)-Si(1)-C(3)	112.4(2)
C(4)-Si(1)-C(3)	108.1(3)
C(1)-Si(1)-C(2)	110.2(3)
C(4)-Si(1)-C(2)	105.6(3)
C(3)-Si(1)-C(2)	109.1(3)
Si(1)-C(1)-Cr(4)	107.2(2)
C(7)-Si(2)-C(8)	106.9(3)
C(7)-Si(2)-C(5)	113.3(2)
C(8)-Si(2)-C(5)	108.7(3)
C(7)-Si(2)-C(6)	106.7(3)
C(8)-Si(2)-C(6)	108.4(3)
C(5)-Si(2)-C(6)	112.6(2)
Si(2)-C(5)-Cr(1)	108.3(2)
C(10)-Si(3)-C(11)	107.2(3)
C(10)-Si(3)-C(12)	107.4(3)
C(11)-Si(3)-C(12)	108.0(3)
C(10)-Si(3)-C(9)	112.4(2)
C(11)-Si(3)-C(9)	112.9(2)
C(12)-Si(3)-C(9)	108.7(3)
Si(3)-C(9)-Cr(2)	109.1(2)
C(14)-Si(4)-C(15)	108.6(3)
C(14)-Si(4)-C(16)	107.5(2)
C(15)-Si(4)-C(16)	106.6(3)
C(14)-Si(4)-C(13)	109.1(2)
C(15)-Si(4)-C(13)	114.0(2)
C(16)-Si(4)-C(13)	110.8(2)
Si(4)-C(13)-Cr(1)	105.4(2)
C(20)-Si(5)-C(19)	108.4(3)
C(20)-Si(5)-C(18)	107.0(3)
C(19)-Si(5)-C(18)	107.9(3)
C(20)-Si(5)-C(17)	110.0(2)
C(19)-Si(5)-C(17)	112.8(2)
C(18)-Si(5)-C(17)	110.5(2)
Si(5)-C(17)-Cr(2)	105.8(2)
C(23)-Si(6)-C(24)	108.8(3)
C(23)-Si(6)-C(22)	107.5(3)
C(24)-Si(6)-C(22)	107.4(3)
C(23)-Si(6)-C(21)	112.2(2)
C(24)-Si(6)-C(21)	112.1(2)
C(22)-Si(6)-C(21)	108.7(2)

Si(6)-C(21)-Cr(3)	108.4(2)
C(28)-Si(7)-C(26)	108.6(3)
C(28)-Si(7)-C(27)	108.1(3)
C(26)-Si(7)-C(27)	106.3(3)
C(28)-Si(7)-C(25)	110.5(2)
C(26)-Si(7)-C(25)	110.0(2)
C(27)-Si(7)-C(25)	113.2(3)
Si(7)-C(25)-Cr(4)	109.8(2)
C(30)-Si(8)-C(32)	106.3(3)
C(30)-Si(8)-C(29)	109.5(3)
C(32)-Si(8)-C(29)	111.1(3)
C(30)-Si(8)-C(31)	107.9(3)
C(32)-Si(8)-C(31)	108.4(3)
C(29)-Si(8)-C(31)	113.5(3)
Si(8)-C(29)-Cr(3)	107.7(2)

Symmetry transformations used to generate equivalent atoms:

Table AI.14. Anisotropic displacement parameters (A^2 x 10^3) for sg415.
The anisotropic displacement factor exponent takes the form:
-2 pi^2 [h^2 a*^2 U11 + ... + 2 h k a* b* U12]

	U11	U22	U33	U23	U13	U12
Cr(1)	23(1)	27(1)	27(1)	-1(1)	6(1)	-1(1)
Cr(2)	25(1)	26(1)	24(1)	1(1)	4(1)	1(1)
Cr(3)	24(1)	28(1)	26(1)	3(1)	6(1)	1(1)
Cr(4)	24(1)	32(1)	24(1)	2(1)	4(1)	-3(1)
Si(1)	40(1)	58(1)	33(1)	-8(1)	4(1)	-12(1)
C(1)	27(3)	36(3)	32(3)	-4(2)	10(2)	-1(2)
C(2)	71(5)	75(5)	59(4)	-35(4)	10(3)	-19(4)
C(3)	60(4)	104(5)	31(3)	-2(3)	3(3)	-17(4)
C(4)	40(4)	119(6)	48(4)	-16(4)	-2(3)	-21(4)
Si(2)	37(1)	50(1)	45(1)	-3(1)	20(1)	-2(1)
C(5)	29(3)	35(3)	36(3)	-3(2)	10(2)	-10(2)
C(6)	35(3)	51(3)	63(4)	0(3)	21(3)	1(3)
C(7)	57(4)	65(4)	81(5)	-30(4)	21(4)	7(3)
C(8)	60(4)	92(5)	54(4)	6(4)	39(3)	-1(4)
Si(3)	33(1)	52(1)	45(1)	-4(1)	-7(1)	0(1)
C(9)	28(3)	27(3)	36(3)	-1(2)	2(2)	-2(2)
C(10)	49(4)	71(4)	62(4)	-21(3)	-14(3)	-17(3)
C(11)	74(5)	71(4)	47(4)	10(3)	-23(3)	-2(4)
C(12)	36(4)	105(6)	88(5)	-3(4)	-14(3)	2(4)
Si(4)	42(1)	26(1)	42(1)	4(1)	12(1)	1(1)
C(13)	33(3)	32(3)	25(3)	-4(2)	4(2)	-2(2)
C(14)	58(4)	33(3)	50(3)	10(2)	13(3)	6(3)
C(15)	59(4)	33(3)	89(5)	2(3)	25(3)	6(3)
C(16)	69(4)	29(3)	62(4)	-2(3)	18(3)	-5(3)
Si(5)	45(1)	43(1)	35(1)	4(1)	17(1)	0(1)
C(17)	30(3)	29(3)	34(3)	4(2)	8(2)	2(2)
C(18)	91(5)	50(4)	49(4)	9(3)	26(3)	-10(3)
C(19)	74(4)	72(4)	33(3)	2(3)	8(3)	-6(3)
C(20)	61(4)	88(5)	48(4)	12(3)	30(3)	8(4)
Si(6)	46(1)	30(1)	42(1)	-3(1)	13(1)	3(1)
C(21)	40(3)	21(2)	31(3)	2(2)	5(2)	0(2)
C(22)	88(5)	46(4)	47(4)	-20(3)	5(3)	1(3)
C(23)	68(4)	51(4)	91(5)	-5(3)	43(4)	14(3)
C(24)	67(4)	26(3)	62(4)	1(3)	12(3)	1(3)
Si(7)	49(1)	47(1)	36(1)	13(1)	4(1)	-4(1)
C(25)	35(3)	35(3)	27(3)	5(2)	6(2)	-9(2)
C(26)	81(5)	52(4)	67(4)	28(3)	18(4)	11(3)
C(27)	77(5)	101(6)	52(4)	20(4)	-21(4)	-17(4)
C(28)	81(5)	72(4)	49(4)	25(3)	27(3)	4(4)
Si(8)	27(1)	54(1)	59(1)	7(1)	7(1)	3(1)
C(29)	29(3)	43(3)	32(3)	3(2)	5(2)	-3(2)
C(30)	33(3)	71(4)	83(5)	17(4)	-7(3)	2(3)
C(31)	56(4)	65(4)	104(6)	-8(4)	12(4)	18(3)
C(32)	35(4)	124(6)	86(5)	34(5)	30(3)	21(4)

Table AI.15. Hydrogen coordinates (x 10^4) and isotropic displacement parameters (A^2 x 10^3) for sg415.

	x	y	z	U(eq)
H(1A)	5138	5547	1813	37
H(1B)	4318	5556	2057	37
H(2A)	4792	4128	808	103
H(2B)	3943	4109	403	103
H(2C)	4037	3805	1080	103
H(3A)	4290	7088	527	99
H(3B)	4070	6250	42	99
H(3C)	4938	6302	415	99
H(4A)	2844	6378	1060	105
H(4B)	2788	5251	1244	105
H(4C)	2700	5545	566	105
H(5A)	5505	7406	1407	40
H(5B)	6172	7941	1868	40
H(6A)	8093	6124	1755	72
H(6B)	7606	6127	2287	72
H(6C)	7914	7139	2057	72
H(7A)	5958	5366	859	100
H(7B)	6371	4934	1478	100
H(7C)	6861	5039	952	100
H(8A)	6484	7384	446	98
H(8B)	7357	6945	549	98
H(8C)	7181	7959	852	98
H(9A)	6664	6487	2910	37
H(9B)	6693	7665	2918	37
H(10A)	7251	8758	4105	95
H(10B)	7567	8145	4688	95
H(10C)	6645	8186	4438	95
H(11A)	6559	5942	4403	102
H(11B)	7463	5967	4705	102
H(11C)	7198	5339	4120	102
H(12A)	8419	7568	3492	119
H(12B)	8402	6395	3520	119
H(12C)	8681	7016	4105	119
H(13A)	5518	5761	3529	36
H(13B)	4756	5367	3092	36
H(14A)	6155	3898	4099	70
H(14B)	6135	2898	3733	70
H(14C)	5331	3404	3833	70
H(15A)	6879	4757	2555	89
H(15B)	7108	3733	2879	89
H(15C)	7203	4735	3246	89
H(16A)	5277	3859	2076	78
H(16B)	4755	3388	2516	78
H(16C)	5560	2872	2425	78
H(17A)	3901	7856	3376	37
H(17B)	3783	6723	3183	37
H(18A)	3668	5176	4059	92
H(18B)	4106	5270	4724	92

H(18C)	4608	5169	4204	92
H(19A)	5056	8021	4704	89
H(19B)	5508	7016	4627	89
H(19C)	5005	7127	5145	89
H(20A)	2772	7058	4251	95
H(20B)	3247	8021	4499	95
H(20C)	3244	7074	4909	95
H(21A)	5505	8327	3709	36
H(21B)	5845	8901	3198	36
H(22A)	5648	11088	4422	92
H(22B)	6309	10566	4120	92
H(22C)	5903	9981	4590	92
H(23A)	3676	9627	3663	100
H(23B)	3946	10503	4113	100
H(23C)	4178	9395	4295	100
H(24A)	4474	10760	2748	77
H(24B)	5375	11079	2921	77
H(24C)	4719	11589	3234	77
H(25A)	4384	9311	2206	38
H(25B)	5305	9255	2178	38
H(26A)	4402	11393	939	100
H(26B)	4972	11333	1559	100
H(26C)	4044	11204	1525	100
H(27A)	3596	9628	364	120
H(27B)	3204	9434	934	120
H(27C)	3681	8576	676	120
H(28A)	5337	9807	439	98
H(28B)	5497	8772	764	98
H(28C)	5925	9740	1051	98
H(29A)	3555	7716	1661	42
H(29B)	3372	6900	2122	42
H(30A)	1898	8254	1140	97
H(30B)	1240	8383	1547	97
H(30D)	1615	7325	1473	97
H(31A)	2858	9919	1877	113
H(31D)	3014	9828	2577	113
H(31B)	2139	9984	2232	113
H(32D)	2047	7120	2798	119
H(32A)	1611	8148	2839	119
H(32B)	2490	7998	3178	119

APPENDIX II

CRYSTALLOGRAPHIC DATA :

HOMOLEPTIC VANADIUM ALKYL

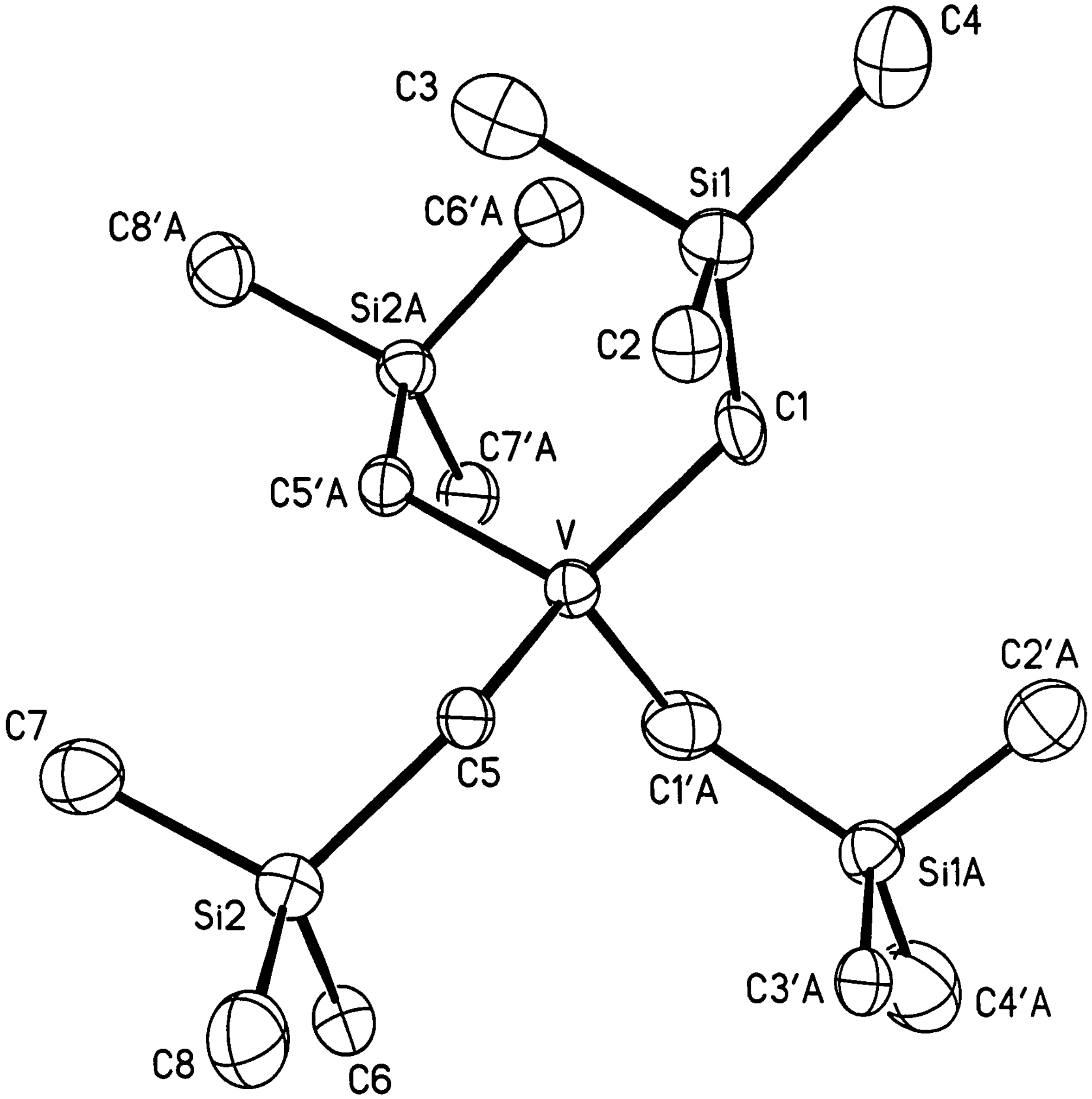
C4
C3
Si1
C8′A
C6′A
Si2A
C2
C1
C7′A
C5′A
V
C2′A
C7
C5
C1′A
Si1A
Si2
C3′A
C4′A
C8
C6

Table AII.1. Crystal data and structure refinement for sg426.

Identification code	sg426
Empirical formula	C16 H44 Si4 V
Formula weight	399.81
Temperature	203(2) K
Wavelength	0.71073 A
Crystal system, space group	Monoclinic, C2/c
Unit cell dimensions	a = 18.721(3) A alpha = 90 deg. b = 8.3574(16) A beta = 117.061(3) deg. c = 18.745(4) A gamma = 90 deg.
Volume	2611.8(8) A^3
Z, Calculated density	4, 1.017 Mg/m^3
Absorption coefficient	0.559 mm^-1
F(000)	876
Crystal size	0.2 x 0.2 x 0.2 mm
Theta range for data collection	2.44 to 28.61 deg.
Limiting indices	-24<=h<=21, 0<=k<=11, 0<=l<=24
Reflections collected / unique	20392 / 3113 [R(int) = 0.0452]
Completeness to theta = 28.61	92.8 %
Absorption correction	Semi-empirical from equivalents
Max. and min. transmission	0.928076 and 0.605516
Refinement method	Full-matrix least-squares on F^2
Data / restraints / parameters	3113 / 0 / 168
Goodness-of-fit on F^2	1.097
Final R indices [I>2sigma(I)]	R1 = 0.0921, wR2 = 0.2221
R indices (all data)	R1 = 0.1019, wR2 = 0.2287
Largest diff. peak and hole	1.011 and -0.555 e.A^-3

Table AII.2. Atomic coordinates (x 10^4) and equivalent isotropic displacement parameters (A^2 x 10^3) for sg426.
U(eq) is defined as one third of the trace of the orthogonalized Uij tensor.

	x	y	z	U(eq)
V	0	9889(2)	2500	35(1)
Si(1)	-551(1)	7650(2)	799(1)	49(1)
Si(2)	1703(1)	12149(2)	3039(1)	43(1)
C(1)	-420(8)	7982(13)	1837(8)	47(3)
C(2)	443(7)	7513(14)	792(7)	40(2)
C(3)	-1069(9)	9510(20)	166(9)	71(4)
C(4)	-1188(10)	5918(19)	199(10)	71(4)
C(5)	1049(6)	10417(12)	2519(6)	33(2)
C(6)	1742(8)	12411(15)	4051(7)	47(3)
C(7)	1275(9)	14026(19)	2499(8)	62(4)
C(8)	2695(10)	11970(20)	3137(10)	77(5)
C(1')	-54(9)	9407(19)	1477(8)	62(4)
C(2')	4(9)	5820(20)	1222(10)	73(4)
C(3')	-1583(7)	7417(14)	804(7)	40(2)
C(4')	-634(12)	7680(30)	-267(13)	100(6)
C(5')	685(7)	11903(13)	2874(7)	39(2)
C(6')	2341(8)	10494(16)	3630(8)	52(3)
C(7')	1735(8)	12194(17)	2068(8)	54(3)
C(8')	2204(9)	14084(19)	3602(9)	64(4)

Table AII.3. Bond lengths [A] and angles [deg] for sg426.

V-C(1')	1.916(14)
V-C(1')#1	1.916(14)
V-C(1)	1.953(11)
V-C(1)#1	1.953(11)
V-C(5)#1	1.998(10)
V-C(5)	1.998(10)
V-C(5')	2.037(11)
V-C(5')#1	2.037(11)
Si(1)-C(2')	1.814(18)
Si(1)-C(1)	1.869(13)
Si(1)-C(2)	1.869(11)
Si(1)-C(1')	1.887(15)
Si(1)-C(4)	1.887(16)
Si(1)-C(3)	1.931(17)
Si(1)-C(4')	1.93(2)
Si(1)-C(3')	1.946(11)
Si(2)-C(8)	1.787(18)

Si(2)-C(5')	1.800(11)
Si(2)-C(6')	1.834(14)
Si(2)-C(7)	1.841(15)
Si(2)-C(7')	1.847(13)
Si(2)-C(5)	1.860(10)
Si(2)-C(6)	1.879(12)
Si(2)-C(8')	1.925(16)
C(1')-V-C(1')#1	155.7(9)
C(1')-V-C(1)	50.9(6)
C(1')#1-V-C(1)	106.7(6)
C(1')-V-C(1)#1	106.7(6)
C(1')#1-V-C(1)#1	50.9(6)
C(1)-V-C(1)#1	70.6(7)
C(1')-V-C(5)#1	115.1(5)
C(1')#1-V-C(5)#1	70.6(5)
C(1)-V-C(5)#1	93.5(5)
C(1)#1-V-C(5)#1	107.4(5)
C(1')-V-C(5)	70.6(5)
C(1')#1-V-C(5)	115.1(5)
C(1)-V-C(5)	107.4(5)
C(1)#1-V-C(5)	93.5(5)
C(5)#1-V-C(5)	154.5(6)
C(1')-V-C(5')	104.9(6)
C(1')#1-V-C(5')	95.2(6)
C(1)-V-C(5')	154.4(5)
C(1)#1-V-C(5')	116.6(5)
C(5)#1-V-C(5')	106.5(4)
C(5)-V-C(5')	49.6(4)
C(1')-V-C(5')#1	95.2(6)
C(1')#1-V-C(5')#1	104.9(5)
C(1)-V-C(5')#1	116.6(5)
C(1)#1-V-C(5')#1	154.4(5)
C(5)#1-V-C(5')#1	49.6(4)
C(5)-V-C(5')#1	106.5(4)
C(5')-V-C(5')#1	68.6(6)
C(2')-Si(1)-C(1)	83.8(6)
C(2')-Si(1)-C(2)	65.0(6)
C(1)-Si(1)-C(2)	110.9(5)
C(2')-Si(1)-C(1')	110.6(7)
C(1)-Si(1)-C(1')	52.5(5)
C(2)-Si(1)-C(1')	82.3(6)
C(2')-Si(1)-C(4)	72.3(7)
C(1)-Si(1)-C(4)	118.8(6)
C(2)-Si(1)-C(4)	108.1(6)
C(1')-Si(1)-C(4)	169.2(7)
C(2')-Si(1)-C(3)	167.3(7)
C(1)-Si(1)-C(3)	108.1(6)
C(2)-Si(1)-C(3)	105.6(6)
C(1')-Si(1)-C(3)	75.0(6)
C(4)-Si(1)-C(3)	104.4(7)
C(2')-Si(1)-C(4')	102.9(8)
C(1)-Si(1)-C(4')	170.4(7)
C(2)-Si(1)-C(4')	66.8(7)
C(1')-Si(1)-C(4')	118.0(8)
C(4)-Si(1)-C(4')	70.2(8)
C(3)-Si(1)-C(4')	64.7(8)
C(2')-Si(1)-C(3')	106.7(6)

C(1)-Si(1)-C(3')	70.7(5)
C(2)-Si(1)-C(3')	170.8(5)
C(1')-Si(1)-C(3')	105.1(6)
C(4)-Si(1)-C(3')	64.3(6)
C(3)-Si(1)-C(3')	82.0(6)
C(4')-Si(1)-C(3')	113.2(7)
C(8)-Si(2)-C(5')	168.0(6)
C(8)-Si(2)-C(6')	60.9(6)
C(5')-Si(2)-C(6')	111.4(5)
C(8)-Si(2)-C(7)	107.5(7)
C(5')-Si(2)-C(7)	80.9(6)
C(6')-Si(2)-C(7)	167.4(6)
C(8)-Si(2)-C(7')	66.8(7)
C(5')-Si(2)-C(7')	109.9(6)
C(6')-Si(2)-C(7')	107.9(6)
C(7)-Si(2)-C(7')	69.0(6)
C(8)-Si(2)-C(5)	113.2(6)
C(5')-Si(2)-C(5)	55.1(5)
C(6')-Si(2)-C(5)	79.7(5)
C(7)-Si(2)-C(5)	110.9(6)
C(7')-Si(2)-C(5)	79.0(5)
C(8)-Si(2)-C(6)	110.2(7)
C(5')-Si(2)-C(6)	74.8(5)
C(6')-Si(2)-C(6)	76.2(6)
C(7)-Si(2)-C(6)	105.3(6)
C(7')-Si(2)-C(6)	171.4(6)
C(5)-Si(2)-C(6)	109.5(5)
C(8)-Si(2)-C(8')	77.9(7)
C(5')-Si(2)-C(8')	113.8(6)
C(6')-Si(2)-C(8')	106.3(6)
C(7)-Si(2)-C(8')	64.4(6)
C(7')-Si(2)-C(8')	107.3(6)
C(5)-Si(2)-C(8')	168.9(5)
C(6)-Si(2)-C(8')	64.0(6)
Si(1)-C(1)-V	127.4(7)
Si(2)-C(5)-V	126.1(5)
Si(1)-C(1')-V	128.6(8)
Si(2)-C(5')-V	127.2(6)

Symmetry transformations used to generate equivalent atoms:
#1 -x,y,-z+1/2

Table AII.4. Anisotropic displacement parameters (A^2 x 10^3) for sg426. The anisotropic displacement factor exponent takes the form: -2 pi^2 [h^2 a*^2 U11 + ... + 2 h k a* b* U12]

	U11	U22	U33	U23	U13	U12
V	35(1)	34(1)	36(1)	0	16(1)	0
Si(1)	48(1)	51(1)	47(1)	-2(1)	21(1)	0(1)
Si(2)	41(1)	44(1)	43(1)	0(1)	18(1)	-1(1)
C(1)	53(7)	23(5)	62(7)	-3(5)	23(6)	-2(5)
C(2)	38(6)	39(6)	47(6)	1(5)	22(5)	2(4)
C(3)	62(9)	83(12)	71(10)	-13(9)	33(8)	-6(8)
C(4)	72(10)	55(9)	90(11)	10(8)	42(9)	7(8)
C(5)	34(5)	29(5)	35(5)	-1(4)	15(4)	2(4)
C(6)	49(7)	43(7)	50(7)	-1(5)	24(6)	-4(5)
C(7)	57(8)	77(10)	53(8)	2(7)	24(7)	-1(7)
C(8)	93(12)	55(9)	74(10)	-1(8)	31(9)	-2(9)
C(1')	62(8)	68(10)	51(7)	12(7)	23(7)	-1(7)
C(2')	65(9)	82(12)	75(10)	-10(9)	35(8)	-11(9)
C(3')	43(6)	37(6)	42(6)	-3(5)	22(5)	0(5)
C(4')	81(13)	89(14)	128(18)	10(13)	47(13)	7(11)
C(5')	44(6)	33(5)	39(6)	-1(4)	19(5)	0(5)
C(6')	52(7)	54(8)	54(7)	2(6)	28(6)	-13(6)
C(7')	56(8)	52(7)	57(8)	0(6)	27(6)	-2(6)
C(8')	68(9)	63(9)	68(9)	1(7)	36(8)	7(7)

Table AII.5. Hydrogen coordinates (x 10^4) and isotropic displacement parameters (A^2 x 10^3) for sg426.

	x	y	z	U(eq)
H(1A)	-82	7097	2156	57
H(1B)	-951	7802	1806	57
H(2A)	731	6585	1098	60
H(2B)	752	8472	1030	60
H(2C)	360	7412	245	60
H(3A)	-1595	9642	141	106
H(3B)	-1125	9383	-371	106
H(3C)	-746	10455	411	106
H(4A)	-968	4926	483	106
H(4B)	-1192	5886	-320	106
H(4C)	-1732	6053	126	106
H(5A)	1385	9464	2731	39
H(5B)	939	10503	1957	39
H(6A)	1202	12539	3989	70
H(6B)	2056	13353	4309	70
H(6C)	1988	11476	4378	70
H(7A)	1237	13967	1966	93
H(7B)	1619	14914	2787	93
H(7C)	745	14185	2458	93
H(8A)	2668	11828	2611	115
H(8B)	2958	11051	3470	115
H(8C)	2998	12930	3383	115
H(1'A)	-294	10356	1148	74
H(1'B)	504	9381	1570	74
H(2'A)	525	5886	1229	109
H(2'B)	-290	4918	897	109
H(2'C)	75	5689	1764	109
H(3'A)	-1900	8376	585	60
H(3'B)	-1499	7258	1349	60
H(3'C)	-1864	6502	480	60
H(4'A)	-110	7890	-235	149
H(4'B)	-1005	8513	-581	149
H(4'C)	-828	6652	-522	149
H(5'A)	377	12738	2490	47
H(5'B)	688	12198	3382	47
H(6'A)	2321	10425	4138	78
H(6'B)	2889	10683	3728	78
H(6'C)	2150	9499	3338	78
H(7'A)	1396	13054	1741	81
H(7'B)	1542	11182	1794	81
H(7'C)	2282	12370	2159	81
H(8'A)	2167	14131	4102	97
H(8'B)	1933	15003	3275	97
H(8'C)	2763	14092	3715	97

APPENDIX III

CRYSTALLOGRAPHIC DATA :

{2,6-bis[2,6-(i-Pr)2PhN=C(Me)]$_2$(C_5H_3N)}Li_3

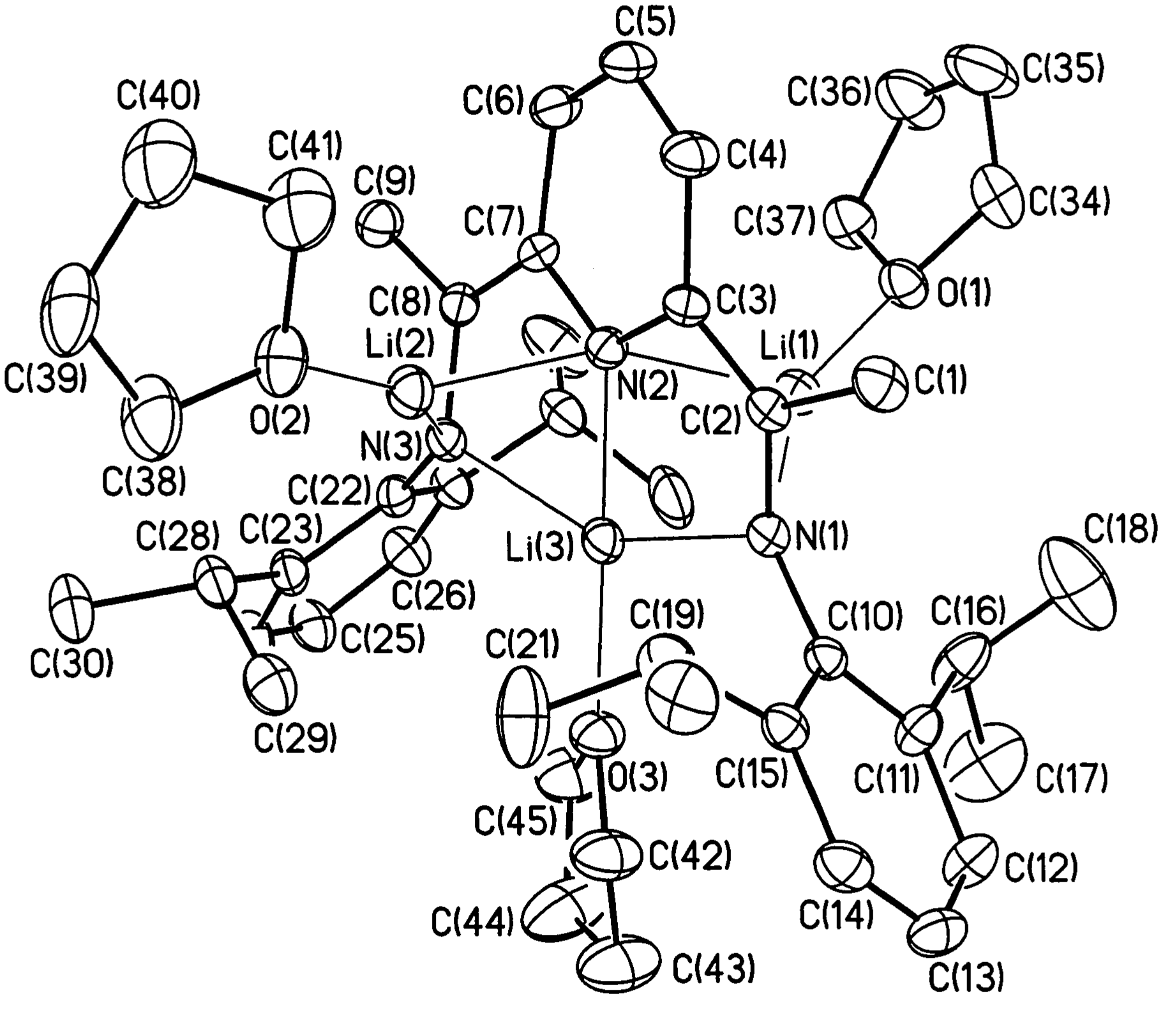
C(5)
C(36)
C(35)
C(40)
C(6)
C(41)
C(4)
C(9)
C(7)
C(37)
C(34)
C(8)
C(3)
O(1)
Li(2)
Li(1)
N(2)
C(1)
C(39)
C(2)
O(2)
N(3)
C(38)
C(22)
C(28)
C(23)
Li(3)
N(1)
C(18)
C(26)
C(16)
C(10)
C(19)
C(30)
C(25)
C(21)
C(29)
O(3)
C(15)
C(11)
C(17)
C(45)
C(42)
C(12)
C(44)
C(14)
C(43)
C(13)

Table AIII.1. Crystal data and structure refinement for sg2067.

Identification code	sg2067
Empirical formula	C45 H67 Li3 N3 O3
Formula weight	718.84
Temperature	233(2) K
Wavelength	0.71073 A
Crystal system, space group	Monoclinic, C2/c
Unit cell dimensions	a = 21.2094(11) A alpha = 90 deg. b = 11.5121(7) A beta = 103.279(2) deg. c = 37.855(2) A gamma = 90 deg.
Volume	8995.7(9) A^3
Z, Calculated density	8, 1.062 Mg/m^3
Absorption coefficient	0.064 mm^-1
F(000)	3128
Crystal size	0.20 x 0.20 x 0.20 mm
Theta range for data collection	1.11 to 26.37 deg.
Limiting indices	-22<=h<=21, 0<=k<=14, 0<=l<=47
Reflections collected / unique	13288 / 8169 [R(int) = 0.0215]
Completeness to theta = 26.37	88.7 %
Absorption correction	Semi-empirical from equivalents
Max. and min. transmission	1.000000 and 0.802047
Refinement method	Full-matrix least-squares on F^2
Data / restraints / parameters	8169 / 111 / 503
Goodness-of-fit on F^2	1.043
Final R indices [I>2sigma(I)]	R1 = 0.0789, wR2 = 0.2220
R indices (all data)	R1 = 0.1320, wR2 = 0.2595
Largest diff. peak and hole	0.699 and -0.292 e.A^-3

Table AIII.2. Atomic coordinates (x 10^4) and equivalent isotropic displacement parameters (A^2 x 10^3) for sg2067. U(eq) is defined as one third of the trace of the orthogonalized Uij tensor.

	x	y	z	U(eq)
Li(1)	2036(3)	9261(5)	1855(1)	51(1)
Li(2)	1246(3)	8927(5)	786(1)	60(2)
Li(3)	2247(3)	9659(5)	1235(1)	52(1)
N(1)	2641(1)	8314(2)	1640(1)	43(1)
N(2)	1463(1)	8917(2)	1342(1)	47(1)
N(3)	1392(1)	10614(2)	884(1)	47(1)
C(1)	2340(2)	6472(3)	1927(1)	59(1)
C(2)	2161(2)	7526(2)	1681(1)	43(1)
C(3)	1532(2)	7864(3)	1543(1)	44(1)
C(4)	955(2)	7270(3)	1616(1)	62(1)
C(5)	366(2)	7884(3)	1536(1)	62(1)
C(6)	285(2)	8963(3)	1354(1)	60(1)
C(7)	846(2)	9439(3)	1232(1)	44(1)
C(8)	821(2)	10377(3)	1002(1)	45(1)
C(9)	201(2)	11019(3)	839(1)	61(1)
C(10)	3289(2)	7985(3)	1702(1)	42(1)
C(11)	3766(2)	8673(3)	1934(1)	54(1)
C(12)	4414(2)	8433(3)	1973(1)	67(1)
C(13)	4624(2)	7517(3)	1795(1)	66(1)
C(14)	4172(2)	6837(3)	1570(1)	62(1)
C(15)	3508(2)	7042(3)	1513(1)	48(1)
C(16)	3551(2)	9653(4)	2146(1)	79(1)
C(17)	4036(3)	10709(5)	2210(2)	142(2)
C(18)	3464(4)	9241(5)	2496(2)	155(3)
C(19)	3040(2)	6342(3)	1225(1)	64(1)
C(20)	3243(2)	5078(3)	1202(1)	84(1)
C(21)	2955(3)	6900(4)	852(1)	115(2)
C(22)	1457(2)	11686(3)	721(1)	46(1)
C(23)	1577(2)	11704(3)	366(1)	53(1)
C(24)	1728(2)	12749(3)	221(1)	65(1)
C(25)	1745(2)	13781(3)	406(1)	71(1)
C(26)	1598(2)	13785(3)	744(1)	66(1)
C(27)	1458(2)	12753(3)	908(1)	53(1)
C(28)	1541(2)	10580(3)	151(1)	61(1)
C(29)	2164(2)	9889(4)	242(1)	79(1)
C(30)	1340(2)	10747(4)	-265(1)	90(1)
C(31)	1353(2)	12818(3)	1295(1)	65(1)
C(32)	925(3)	13832(4)	1352(2)	114(2)
C(33)	2017(3)	12852(5)	1568(1)	108(2)
O(1)	1737(1)	9846(2)	2254(1)	61(1)
C(34)	1603(2)	9073(4)	2522(1)	82(1)
C(35)	975(3)	9433(6)	2588(2)	125(2)
C(36)	840(3)	10572(6)	2443(2)	118(2)
C(37)	1265(2)	10757(3)	2197(1)	73(1)
O(2)	975(2)	7697(3)	453(1)	78(1)
C(38)	990(2)	7388(3)	92(1)	119(3)

C(39)	484(7)	6564(12)	-46(3)	121(5)
C(40)	76(7)	6404(14)	251(4)	140(4)
C(41)	458(6)	6981(10)	578(3)	122(3)
O(2')	860(4)	7854(6)	436(2)	78(1)
C(38')	477(7)	7910(10)	94(3)	119(3)
C(39')	147(8)	6814(13)	11(4)	121(5)
C(40')	355(9)	6093(14)	372(4)	140(4)
C(41')	968(7)	6675(9)	571(3)	122(3)
O(3)	3063(1)	10404(2)	1118(1)	73(1)
C(42)	3622(3)	9808(5)	1054(2)	102(2)
C(43)	4118(3)	10630(5)	1039(2)	132(2)
C(44)	3749(3)	11757(6)	946(2)	158(3)
C(45)	3150(3)	11623(4)	1046(2)	103(2)

Table AIII.3. Bond lengths [A] and angles [deg] for sg2067.

Li(1)-O(1)	1.891(5)
Li(1)-N(1)	1.994(6)
Li(1)-N(2)	2.077(6)
Li(1)-C(3)	2.132(6)
Li(1)-C(2)	2.138(6)
Li(1)-Li(3)	2.529(7)
Li(2)-O(2')	1.859(8)
Li(2)-O(2)	1.895(6)
Li(2)-N(3)	1.989(6)
Li(2)-N(2)	2.049(6)
Li(2)-C(7)	2.139(6)
Li(2)-C(8)	2.146(7)
Li(2)-Li(3)	2.540(8)
Li(2)-C(41')	2.740(12)
Li(3)-N(2)	1.993(6)
Li(3)-O(3)	2.068(6)
Li(3)-N(1)	2.203(6)
Li(3)-N(3)	2.272(6)
N(1)-C(10)	1.392(4)
N(1)-C(2)	1.400(4)
N(2)-C(7)	1.412(4)
N(2)-C(3)	1.421(4)
N(3)-C(22)	1.400(4)
N(3)-C(8)	1.409(4)
C(1)-C(2)	1.522(4)
C(2)-C(3)	1.373(4)
C(3)-C(4)	1.481(4)
C(4)-C(5)	1.407(5)
C(5)-C(6)	1.413(5)
C(6)-C(7)	1.477(5)
C(7)-C(8)	1.380(4)
C(8)-C(9)	1.512(4)
C(10)-C(11)	1.420(4)
C(10)-C(15)	1.435(4)
C(11)-C(12)	1.376(5)
C(11)-C(16)	1.514(5)

C(12)-C(13)	1.378(5)
C(13)-C(14)	1.374(5)
C(14)-C(15)	1.395(5)
C(15)-C(19)	1.524(5)
C(16)-C(18)	1.458(7)
C(16)-C(17)	1.576(7)
C(19)-C(21)	1.522(6)
C(19)-C(20)	1.526(5)
C(22)-C(27)	1.417(4)
C(22)-C(23)	1.424(4)
C(23)-C(24)	1.390(5)
C(23)-C(28)	1.522(5)
C(24)-C(25)	1.374(5)
C(25)-C(26)	1.386(5)
C(26)-C(27)	1.403(5)
C(27)-C(31)	1.535(4)
C(28)-C(29)	1.513(5)
C(28)-C(30)	1.545(5)
C(31)-C(32)	1.524(6)
C(31)-C(33)	1.544(6)
O(1)-C(34)	1.426(4)
O(1)-C(37)	1.431(4)
C(34)-C(35)	1.469(7)
C(35)-C(36)	1.424(7)
C(36)-C(37)	1.453(6)
O(2)-C(38)	1.4200
O(2)-C(41)	1.528(10)
C(38)-C(39)	1.437(10)
C(39)-C(40)	1.579(14)
C(40)-C(41)	1.473(13)
O(2')-C(38')	1.364(10)
O(2')-C(41')	1.450(11)
C(38')-C(39')	1.440(12)
C(39')-C(40')	1.573(14)
C(40')-C(41')	1.502(14)
O(3)-C(42)	1.439(6)
O(3)-C(45)	1.450(5)
C(42)-C(43)	1.424(6)
C(43)-C(44)	1.514(7)
C(44)-C(45)	1.416(7)
O(1)-Li(1)-N(1)	152.3(3)
O(1)-Li(1)-N(2)	125.6(3)
N(1)-Li(1)-N(2)	79.0(2)
O(1)-Li(1)-C(3)	119.6(3)
N(1)-Li(1)-C(3)	69.5(2)
N(2)-Li(1)-C(3)	39.43(14)
O(1)-Li(1)-C(2)	131.8(3)
N(1)-Li(1)-C(2)	39.40(14)
N(2)-Li(1)-C(2)	67.81(19)
C(3)-Li(1)-C(2)	37.52(15)
O(1)-Li(1)-Li(3)	147.1(3)
N(1)-Li(1)-Li(3)	56.83(19)
N(2)-Li(1)-Li(3)	50.11(18)
C(3)-Li(1)-Li(3)	78.2(2)
C(2)-Li(1)-Li(3)	79.8(2)
O(2')-Li(2)-O(2)	9.1(3)
O(2')-Li(2)-N(3)	143.8(4)

O(2)-Li(2)-N(3)	149.9(3)
O(2')-Li(2)-N(2)	133.4(4)
O(2)-Li(2)-N(2)	129.9(3)
N(3)-Li(2)-N(2)	79.9(2)
O(2')-Li(2)-C(7)	123.8(4)
O(2)-Li(2)-C(7)	128.0(3)
N(3)-Li(2)-C(7)	69.9(2)
N(2)-Li(2)-C(7)	39.33(14)
O(2')-Li(2)-C(8)	129.3(4)
O(2)-Li(2)-C(8)	138.1(4)
N(3)-Li(2)-C(8)	39.62(15)
N(2)-Li(2)-C(8)	68.09(19)
C(7)-Li(2)-C(8)	37.56(15)
O(2')-Li(2)-Li(3)	149.5(4)
O(2)-Li(2)-Li(3)	140.6(4)
N(3)-Li(2)-Li(3)	58.7(2)
N(2)-Li(2)-Li(3)	50.09(18)
C(7)-Li(2)-Li(3)	78.6(2)
C(8)-Li(2)-Li(3)	81.2(2)
O(2')-Li(2)-C(41')	29.6(3)
O(2)-Li(2)-C(41')	23.6(3)
N(3)-Li(2)-C(41')	173.3(4)
N(2)-Li(2)-C(41')	106.4(4)
C(7)-Li(2)-C(41')	113.4(4)
C(8)-Li(2)-C(41')	140.2(4)
Li(3)-Li(2)-C(41')	127.0(4)
N(2)-Li(3)-O(3)	179.0(3)
N(2)-Li(3)-N(1)	76.0(2)
O(3)-Li(3)-N(1)	103.8(3)
N(2)-Li(3)-N(3)	74.6(2)
O(3)-Li(3)-N(3)	105.6(2)
N(1)-Li(3)-N(3)	150.6(3)
N(2)-Li(3)-Li(1)	53.08(19)
O(3)-Li(3)-Li(1)	127.6(3)
N(1)-Li(3)-Li(1)	49.25(17)
N(3)-Li(3)-Li(1)	110.0(3)
N(2)-Li(3)-Li(2)	52.07(19)
O(3)-Li(3)-Li(2)	127.3(3)
N(1)-Li(3)-Li(2)	111.0(3)
N(3)-Li(3)-Li(2)	48.43(18)
Li(1)-Li(3)-Li(2)	105.2(3)
C(10)-N(1)-C(2)	121.3(2)
C(10)-N(1)-Li(1)	141.6(2)
C(2)-N(1)-Li(1)	75.9(2)
C(10)-N(1)-Li(3)	120.7(2)
C(2)-N(1)-Li(3)	111.3(2)
Li(1)-N(1)-Li(3)	73.9(2)
C(7)-N(2)-C(3)	119.7(2)
C(7)-N(2)-Li(3)	121.2(2)
C(3)-N(2)-Li(3)	119.1(3)
C(7)-N(2)-Li(2)	73.8(2)
C(3)-N(2)-Li(2)	121.6(3)
Li(3)-N(2)-Li(2)	77.8(2)
C(7)-N(2)-Li(1)	119.9(2)
C(3)-N(2)-Li(1)	72.4(2)
Li(3)-N(2)-Li(1)	76.8(2)
Li(2)-N(2)-Li(1)	154.6(3)

C(22)-N(3)-C(8)	119.3(3)
C(22)-N(3)-Li(2)	143.6(2)
C(8)-N(3)-Li(2)	76.2(2)
C(22)-N(3)-Li(3)	122.5(2)
C(8)-N(3)-Li(3)	110.4(2)
Li(2)-N(3)-Li(3)	72.8(2)
C(3)-C(2)-N(1)	116.3(2)
C(3)-C(2)-C(1)	122.9(3)
N(1)-C(2)-C(1)	119.9(3)
C(3)-C(2)-Li(1)	71.0(2)
N(1)-C(2)-Li(1)	64.7(2)
C(1)-C(2)-Li(1)	126.0(2)
C(2)-C(3)-N(2)	114.7(3)
C(2)-C(3)-C(4)	124.7(3)
N(2)-C(3)-C(4)	120.4(3)
C(2)-C(3)-Li(1)	71.5(2)
N(2)-C(3)-Li(1)	68.2(2)
C(4)-C(3)-Li(1)	125.1(3)
C(5)-C(4)-C(3)	117.3(3)
C(4)-C(5)-C(6)	123.3(3)
C(5)-C(6)-C(7)	117.5(3)
C(8)-C(7)-N(2)	114.7(3)
C(8)-C(7)-C(6)	124.8(3)
N(2)-C(7)-C(6)	120.5(3)
C(8)-C(7)-Li(2)	71.5(2)
N(2)-C(7)-Li(2)	66.9(2)
C(6)-C(7)-Li(2)	129.6(3)
C(7)-C(8)-N(3)	116.2(3)
C(7)-C(8)-C(9)	122.9(3)
N(3)-C(8)-C(9)	120.4(3)
C(7)-C(8)-Li(2)	71.0(2)
N(3)-C(8)-Li(2)	64.1(2)
C(9)-C(8)-Li(2)	128.8(3)
N(1)-C(10)-C(11)	119.2(3)
N(1)-C(10)-C(15)	122.8(3)
C(11)-C(10)-C(15)	117.7(3)
C(12)-C(11)-C(10)	120.4(3)
C(12)-C(11)-C(16)	120.5(3)
C(10)-C(11)-C(16)	119.1(3)
C(11)-C(12)-C(13)	121.9(4)
C(14)-C(13)-C(12)	118.8(4)
C(13)-C(14)-C(15)	122.4(3)
C(14)-C(15)-C(10)	118.8(3)
C(14)-C(15)-C(19)	119.3(3)
C(10)-C(15)-C(19)	121.6(3)
C(18)-C(16)-C(11)	110.8(4)
C(18)-C(16)-C(17)	109.1(5)
C(11)-C(16)-C(17)	113.0(4)
C(21)-C(19)-C(15)	111.0(3)
C(21)-C(19)-C(20)	109.0(3)
C(15)-C(19)-C(20)	113.5(3)
N(3)-C(22)-C(27)	122.3(3)
N(3)-C(22)-C(23)	119.1(3)
C(27)-C(22)-C(23)	118.5(3)
C(24)-C(23)-C(22)	119.5(3)
C(24)-C(23)-C(28)	120.8(3)
C(22)-C(23)-C(28)	119.7(3)

C(25)-C(24)-C(23)	121.9(3)
C(24)-C(25)-C(26)	119.2(3)
C(25)-C(26)-C(27)	121.3(3)
C(26)-C(27)-C(22)	119.4(3)
C(26)-C(27)-C(31)	118.2(3)
C(22)-C(27)-C(31)	122.3(3)
C(29)-C(28)-C(23)	112.9(3)
C(29)-C(28)-C(30)	108.6(3)
C(23)-C(28)-C(30)	114.1(3)
C(32)-C(31)-C(27)	113.2(3)
C(32)-C(31)-C(33)	111.5(4)
C(27)-C(31)-C(33)	109.3(3)
C(34)-O(1)-C(37)	108.4(3)
C(34)-O(1)-Li(1)	120.3(3)
C(37)-O(1)-Li(1)	119.5(3)
O(1)-C(34)-C(35)	106.3(4)
C(36)-C(35)-C(34)	107.8(4)
C(35)-C(36)-C(37)	106.3(4)
O(1)-C(37)-C(36)	108.2(3)
C(38)-O(2)-C(41)	109.8(4)
C(38)-O(2)-Li(2)	139.1(2)
C(41)-O(2)-Li(2)	109.2(5)
O(2)-C(38)-C(39)	109.6(5)
C(38)-C(39)-C(40)	107.6(7)
C(41)-C(40)-C(39)	105.0(9)
C(40)-C(41)-O(2)	106.2(8)
C(38')-O(2')-C(41')	113.0(7)
C(38')-O(2')-Li(2)	135.7(7)
C(41')-O(2')-Li(2)	111.2(6)
O(2')-C(38')-C(39')	108.5(9)
C(38')-C(39')-C(40')	104.4(9)
C(41')-C(40')-C(39')	103.8(9)
O(2')-C(41')-C(40')	101.0(10)
O(2')-C(41')-Li(2)	39.2(4)
C(40')-C(41')-Li(2)	132.3(11)
C(42)-O(3)-C(45)	106.5(3)
C(42)-O(3)-Li(3)	127.0(3)
C(45)-O(3)-Li(3)	126.2(3)
C(43)-C(42)-O(3)	109.6(5)
C(42)-C(43)-C(44)	103.4(5)
C(45)-C(44)-C(43)	107.0(4)
C(44)-C(45)-O(3)	108.4(4)

Symmetry transformations used to generate equivalent atoms:

Table AIII.4. Anisotropic displacement parameters (A^2 x 10^3) for sg2067. The anisotropic displacement factor exponent takes the form: -2 pi^2 [h^2 a*^2 U11 + ... + 2 h k a* b* U12]

	U11	U22	U33	U23	U13	U12
Li(1)	55(4)	52(3)	50(3)	-3(2)	18(2)	0(3)
Li(2)	66(4)	62(3)	51(3)	-8(2)	10(3)	-5(3)
Li(3)	56(4)	54(3)	46(3)	0(2)	13(2)	-9(3)
N(1)	45(2)	39(1)	45(1)	1(1)	14(1)	3(1)
N(2)	43(2)	47(2)	49(1)	9(1)	9(1)	-4(1)
N(3)	51(2)	49(2)	42(1)	4(1)	12(1)	-3(1)
C(1)	68(3)	48(2)	65(2)	13(2)	21(2)	6(2)
C(2)	49(2)	39(2)	44(1)	2(1)	17(1)	1(1)
C(3)	44(2)	41(2)	49(2)	2(1)	15(1)	-4(1)
C(4)	56(3)	53(2)	80(2)	15(2)	22(2)	-6(2)
C(5)	50(3)	64(2)	77(2)	5(2)	24(2)	-15(2)
C(6)	43(2)	63(2)	72(2)	10(2)	12(2)	-3(2)
C(7)	33(2)	53(2)	44(1)	0(1)	6(1)	-4(1)
C(8)	45(2)	47(2)	41(1)	0(1)	5(1)	-2(1)
C(9)	53(2)	65(2)	63(2)	11(2)	8(2)	5(2)
C(10)	44(2)	44(2)	41(1)	7(1)	13(1)	6(1)
C(11)	45(2)	55(2)	58(2)	-8(2)	1(2)	8(2)
C(12)	48(3)	70(2)	76(2)	-6(2)	-1(2)	4(2)
C(13)	45(2)	71(2)	83(2)	3(2)	16(2)	13(2)
C(14)	64(3)	59(2)	69(2)	-1(2)	29(2)	14(2)
C(15)	52(2)	48(2)	48(2)	1(1)	19(1)	6(2)
C(16)	55(3)	79(3)	89(3)	-37(2)	-11(2)	12(2)
C(17)	133(5)	98(4)	185(6)	-57(4)	17(4)	-10(4)
C(18)	267(9)	116(5)	114(4)	-7(4)	108(5)	58(5)
C(19)	66(3)	62(2)	65(2)	-20(2)	19(2)	4(2)
C(20)	102(4)	63(2)	90(3)	-22(2)	30(2)	1(2)
C(21)	178(6)	79(3)	66(3)	-13(2)	-15(3)	4(3)
C(22)	46(2)	49(2)	40(1)	6(1)	6(1)	-2(1)
C(23)	60(2)	59(2)	40(2)	3(1)	10(1)	-5(2)
C(24)	89(3)	62(2)	44(2)	8(2)	18(2)	-7(2)
C(25)	95(3)	58(2)	63(2)	16(2)	23(2)	-6(2)
C(26)	86(3)	51(2)	66(2)	0(2)	27(2)	-3(2)
C(27)	63(2)	50(2)	50(2)	2(1)	18(2)	-3(2)
C(28)	80(3)	61(2)	42(2)	-4(1)	17(2)	-16(2)
C(29)	99(4)	73(3)	68(2)	-6(2)	25(2)	-4(2)
C(30)	125(4)	91(3)	49(2)	-4(2)	12(2)	-11(3)
C(31)	86(3)	58(2)	57(2)	-7(2)	31(2)	-17(2)
C(32)	179(6)	74(3)	119(4)	-14(3)	94(4)	5(3)
C(33)	139(5)	141(4)	47(2)	-12(2)	24(2)	-47(4)
O(1)	67(2)	65(2)	57(1)	0(1)	27(1)	13(1)
C(34)	113(4)	74(3)	64(2)	7(2)	31(2)	4(2)
C(35)	102(5)	158(6)	140(5)	44(4)	78(4)	18(4)
C(36)	110(5)	143(5)	124(4)	31(4)	71(3)	48(4)
C(37)	79(3)	72(2)	74(2)	0(2)	29(2)	19(2)
O(2)	102(3)	56(2)	68(2)	-14(1)	2(2)	-6(2)
C(38)	160(9)	105(6)	83(4)	-27(4)	11(5)	-40(5)
C(39)	166(12)	93(6)	84(4)	-8(4)	-17(5)	-46(8)
C(40)	165(11)	118(7)	122(8)	-3(5)	5(6)	-53(8)

C(41)	151(9)	90(5)	118(4)	-11(4)	13(5)	-41(6)
O(2')	102(3)	56(2)	68(2)	-14(1)	2(2)	-6(2)
C(38')	160(9)	105(6)	83(4)	-27(4)	11(5)	-40(5)
C(39')	166(12)	93(6)	84(4)	-8(4)	-17(5)	-46(8)
C(40')	165(11)	118(7)	122(8)	-3(5)	5(6)	-53(8)
C(41')	151(9)	90(5)	118(4)	-11(4)	13(5)	-41(6)
O(3)	63(2)	73(2)	87(2)	20(1)	25(1)	-11(1)
C(42)	77(4)	99(4)	140(5)	49(3)	46(3)	5(3)
C(43)	90(4)	113(5)	202(7)	37(4)	52(4)	-19(4)
C(44)	88(5)	125(5)	252(8)	97(5)	21(5)	-24(4)
C(45)	90(4)	73(3)	149(5)	14(3)	35(3)	-21(3)

Table AIII.5. Hydrogen coordinates (x 10^4) and isotropic displacement parameters (A^2 x 10^3) for sg2067.

	x	y	z	U(eq)
H(1A)	1955	6015	1924	89
H(1B)	2527	6728	2172	89
H(1C)	2653	6002	1840	89
H(4A)	982	6514	1712	74
H(5A)	8	7560	1608	75
H(6A)	-112	9363	1311	72
H(9A)	-140	10752	952	92
H(9B)	78	10872	580	92
H(9C)	267	11846	882	92
H(12A)	4722	8907	2125	81
H(13A)	5069	7361	1828	80
H(14A)	4315	6211	1449	74
H(16A)	3127	9938	2005	94
H(17A)	3877	11307	2347	213
H(17B)	4073	11023	1977	213
H(17C)	4459	10448	2344	213
H(18A)	3166	8589	2458	233
H(18B)	3289	9863	2617	233
H(18C)	3879	8997	2644	233
H(19A)	2613	6346	1289	77
H(20A)	3296	4714	1438	126
H(20B)	3651	5048	1127	126
H(20C)	2913	4668	1026	126
H(21A)	2816	7700	863	172
H(21B)	2630	6475	678	172
H(21C)	3363	6881	779	172
H(24A)	1821	12750	-10	77
H(25A)	1854	14475	304	85
H(26A)	1593	14494	867	79
H(28A)	1202	10094	219	73
H(29A)	2291	9765	502	119
H(29B)	2502	10315	163	119
H(29C)	2099	9145	119	119

H(30A)	936	11175	-327	134
H(30B)	1284	9994	-383	134
H(30C)	1675	11178	-345	134
H(31A)	1132	12094	1340	78
H(32A)	512	13783	1178	171
H(32B)	1136	14558	1319	171
H(32C)	855	13801	1596	171
H(33A)	1952	12882	1814	163
H(33B)	2255	13535	1523	163
H(33C)	2262	12160	1540	163
H(34A)	1942	9126	2746	98
H(34B)	1581	8270	2434	98
H(35A)	635	8894	2469	150
H(35B)	993	9433	2849	150
H(36A)	925	11150	2638	142
H(36B)	385	10635	2312	142
H(37A)	1014	10748	1945	88
H(37B)	1481	11512	2245	88
H(38A)	1411	7047	88	143
H(38B)	930	8083	-61	143
H(39A)	671	5820	-95	146
H(39B)	206	6852	-273	146
H(40A)	-351	6766	173	167
H(40B)	18	5578	298	167
H(41A)	661	6404	759	147
H(41B)	181	7486	686	147
H(38C)	742	8067	-81	143
H(38D)	160	8538	78	143
H(39C)	282	6423	-189	146
H(39D)	-323	6925	-55	146
H(40C)	22	6127	513	167
H(40D)	435	5279	320	167
H(41C)	1016	6641	835	147
H(41D)	1351	6330	509	147
H(42A)	3690(30)	9140(50)	1152(15)	123
H(42B)	3490(20)	9450(40)	746(15)	123
H(43A)	4347	10421	851	158
H(43B)	4430	10686	1273	158
H(44A)	3994	12404	1080	190
H(44B)	3677	11917	686	190
H(45A)	2795	11895	850	123
H(45B)	3149	12084	1264	123

Table AIII.6. Torsion angles [deg] for sg2067.

O(1)-Li(1)-Li(3)-N(2)	-96.0(6)
N(1)-Li(1)-Li(3)-N(2)	104.4(2)
C(3)-Li(1)-Li(3)-N(2)	31.31(17)
C(2)-Li(1)-Li(3)-N(2)	69.5(2)
O(1)-Li(1)-Li(3)-O(3)	85.0(7)
N(1)-Li(1)-Li(3)-O(3)	-74.6(4)
N(2)-Li(1)-Li(3)-O(3)	-179.0(4)
C(3)-Li(1)-Li(3)-O(3)	-147.7(3)
C(2)-Li(1)-Li(3)-O(3)	-109.5(4)
O(1)-Li(1)-Li(3)-N(1)	159.6(6)
N(2)-Li(1)-Li(3)-N(1)	-104.4(2)
C(3)-Li(1)-Li(3)-N(1)	-73.1(2)
C(2)-Li(1)-Li(3)-N(1)	-34.86(15)
O(1)-Li(1)-Li(3)-N(3)	-44.9(7)
N(1)-Li(1)-Li(3)-N(3)	155.5(3)
N(2)-Li(1)-Li(3)-N(3)	51.1(2)
C(3)-Li(1)-Li(3)-N(3)	82.5(3)
C(2)-Li(1)-Li(3)-N(3)	120.7(3)
O(1)-Li(1)-Li(3)-Li(2)	-95.6(6)
N(1)-Li(1)-Li(3)-Li(2)	104.8(3)
N(2)-Li(1)-Li(3)-Li(2)	0.4(2)
C(3)-Li(1)-Li(3)-Li(2)	31.7(3)
C(2)-Li(1)-Li(3)-Li(2)	69.9(3)
O(2')-Li(2)-Li(3)-N(2)	-110.2(8)
O(2)-Li(2)-Li(3)-N(2)	-107.3(5)
N(3)-Li(2)-Li(3)-N(2)	103.9(3)
C(7)-Li(2)-Li(3)-N(2)	30.68(16)
C(8)-Li(2)-Li(3)-N(2)	68.8(2)
C(41')-Li(2)-Li(3)-N(2)	-80.2(5)
O(2')-Li(2)-Li(3)-O(3)	68.8(9)
O(2)-Li(2)-Li(3)-O(3)	71.7(6)
N(3)-Li(2)-Li(3)-O(3)	-77.1(4)
N(2)-Li(2)-Li(3)-O(3)	179.0(4)
C(7)-Li(2)-Li(3)-O(3)	-150.3(3)
C(8)-Li(2)-Li(3)-O(3)	-112.2(3)
C(41')-Li(2)-Li(3)-O(3)	98.8(6)
O(2')-Li(2)-Li(3)-N(1)	-58.9(8)
O(2)-Li(2)-Li(3)-N(1)	-56.1(6)
N(3)-Li(2)-Li(3)-N(1)	155.1(3)
N(2)-Li(2)-Li(3)-N(1)	51.2(2)
C(7)-Li(2)-Li(3)-N(1)	81.9(3)
C(8)-Li(2)-Li(3)-N(1)	120.0(3)
C(41')-Li(2)-Li(3)-N(1)	-29.0(6)
O(2')-Li(2)-Li(3)-N(3)	145.9(8)
O(2)-Li(2)-Li(3)-N(3)	148.7(6)
N(2)-Li(2)-Li(3)-N(3)	-103.9(3)
C(7)-Li(2)-Li(3)-N(3)	-73.2(2)
C(8)-Li(2)-Li(3)-N(3)	-35.15(15)
C(41')-Li(2)-Li(3)-N(3)	175.9(6)
O(2')-Li(2)-Li(3)-Li(1)	-110.6(8)
O(2)-Li(2)-Li(3)-Li(1)	-107.8(5)
N(3)-Li(2)-Li(3)-Li(1)	103.5(3)
N(2)-Li(2)-Li(3)-Li(1)	-0.4(2)
C(7)-Li(2)-Li(3)-Li(1)	30.3(3)

C(8)-Li(2)-Li(3)-Li(1)	68.3(3)
C(41')-Li(2)-Li(3)-Li(1)	-80.6(5)
O(1)-Li(1)-N(1)-C(10)	-36.5(9)
N(2)-Li(1)-N(1)-C(10)	168.6(3)
C(3)-Li(1)-N(1)-C(10)	-151.5(3)
C(2)-Li(1)-N(1)-C(10)	-123.0(4)
Li(3)-Li(1)-N(1)-C(10)	119.4(4)
O(1)-Li(1)-N(1)-C(2)	86.5(7)
N(2)-Li(1)-N(1)-C(2)	-68.36(19)
C(3)-Li(1)-N(1)-C(2)	-28.47(17)
Li(3)-Li(1)-N(1)-C(2)	-117.6(2)
O(1)-Li(1)-N(1)-Li(3)	-155.9(7)
N(2)-Li(1)-N(1)-Li(3)	49.22(19)
C(3)-Li(1)-N(1)-Li(3)	89.1(2)
C(2)-Li(1)-N(1)-Li(3)	117.6(2)
N(2)-Li(3)-N(1)-C(10)	166.1(2)
O(3)-Li(3)-N(1)-C(10)	-12.9(3)
N(3)-Li(3)-N(1)-C(10)	166.6(5)
Li(1)-Li(3)-N(1)-C(10)	-141.0(3)
Li(2)-Li(3)-N(1)-C(10)	126.7(3)
N(2)-Li(3)-N(1)-C(2)	14.4(2)
O(3)-Li(3)-N(1)-C(2)	-164.6(2)
N(3)-Li(3)-N(1)-C(2)	14.9(6)
Li(1)-Li(3)-N(1)-C(2)	67.3(2)
Li(2)-Li(3)-N(1)-C(2)	-24.9(3)
N(2)-Li(3)-N(1)-Li(1)	-52.9(2)
O(3)-Li(3)-N(1)-Li(1)	128.1(3)
N(3)-Li(3)-N(1)-Li(1)	-52.4(5)
Li(2)-Li(3)-N(1)-Li(1)	-92.3(3)
O(3)-Li(3)-N(2)-C(7)	-113(21)
N(1)-Li(3)-N(2)-C(7)	166.3(2)
N(3)-Li(3)-N(2)-C(7)	-13.5(3)
Li(1)-Li(3)-N(2)-C(7)	117.2(3)
Li(2)-Li(3)-N(2)-C(7)	-62.3(3)
O(3)-Li(3)-N(2)-C(3)	69(21)
N(1)-Li(3)-N(2)-C(3)	-11.8(3)
N(3)-Li(3)-N(2)-C(3)	168.5(2)
Li(1)-Li(3)-N(2)-C(3)	-60.9(3)
Li(2)-Li(3)-N(2)-C(3)	119.6(3)
O(3)-Li(3)-N(2)-Li(2)	-50(21)
N(1)-Li(3)-N(2)-Li(2)	-131.4(2)
N(3)-Li(3)-N(2)-Li(2)	48.9(2)
Li(1)-Li(3)-N(2)-Li(2)	179.5(3)
O(3)-Li(3)-N(2)-Li(1)	130(21)
N(1)-Li(3)-N(2)-Li(1)	49.13(19)
N(3)-Li(3)-N(2)-Li(1)	-130.6(2)
Li(2)-Li(3)-N(2)-Li(1)	-179.5(3)
O(2')-Li(2)-N(2)-C(7)	-93.1(6)
O(2)-Li(2)-N(2)-C(7)	-104.2(5)
N(3)-Li(2)-N(2)-C(7)	70.5(2)
C(8)-Li(2)-N(2)-C(7)	30.97(18)
Li(3)-Li(2)-N(2)-C(7)	127.9(3)
C(41')-Li(2)-N(2)-C(7)	-107.2(4)
O(2')-Li(2)-N(2)-C(3)	22.2(7)
O(2)-Li(2)-N(2)-C(3)	11.0(6)
N(3)-Li(2)-N(2)-C(3)	-174.3(3)
C(7)-Li(2)-N(2)-C(3)	115.3(3)

C(8)-Li(2)-N(2)-C(3)	146.2(3)
Li(3)-Li(2)-N(2)-C(3)	-116.8(3)
C(41')-Li(2)-N(2)-C(3)	8.1(5)
O(2')-Li(2)-N(2)-Li(3)	139.1(6)
O(2)-Li(2)-N(2)-Li(3)	127.9(5)
N(3)-Li(2)-N(2)-Li(3)	-57.4(2)
C(7)-Li(2)-N(2)-Li(3)	-127.9(3)
C(8)-Li(2)-N(2)-Li(3)	-96.9(2)
C(41')-Li(2)-N(2)-Li(3)	124.9(4)
O(2')-Li(2)-N(2)-Li(1)	140.2(6)
O(2)-Li(2)-N(2)-Li(1)	129.1(6)
N(3)-Li(2)-N(2)-Li(1)	-56.2(7)
C(7)-Li(2)-N(2)-Li(1)	-126.7(6)
C(8)-Li(2)-N(2)-Li(1)	-95.7(6)
Li(3)-Li(2)-N(2)-Li(1)	1.2(6)
C(41')-Li(2)-N(2)-Li(1)	126.1(6)
O(1)-Li(1)-N(2)-C(7)	19.8(5)
N(1)-Li(1)-N(2)-C(7)	-174.3(2)
C(3)-Li(1)-N(2)-C(7)	114.7(3)
C(2)-Li(1)-N(2)-C(7)	146.1(2)
Li(3)-Li(1)-N(2)-C(7)	-118.6(3)
O(1)-Li(1)-N(2)-C(3)	-94.9(4)
N(1)-Li(1)-N(2)-C(3)	71.1(2)
C(2)-Li(1)-N(2)-C(3)	31.49(18)
Li(3)-Li(1)-N(2)-C(3)	126.8(3)
O(1)-Li(1)-N(2)-Li(3)	138.4(4)
N(1)-Li(1)-N(2)-Li(3)	-55.7(2)
C(3)-Li(1)-N(2)-Li(3)	-126.8(3)
C(2)-Li(1)-N(2)-Li(3)	-95.3(2)
O(1)-Li(1)-N(2)-Li(2)	137.2(5)
N(1)-Li(1)-N(2)-Li(2)	-56.9(6)
C(3)-Li(1)-N(2)-Li(2)	-128.0(6)
C(2)-Li(1)-N(2)-Li(2)	-96.5(6)
Li(3)-Li(1)-N(2)-Li(2)	-1.2(6)
O(2')-Li(2)-N(3)-C(22)	-29.3(10)
O(2)-Li(2)-N(3)-C(22)	-17.1(11)
N(2)-Li(2)-N(3)-C(22)	171.1(4)
C(7)-Li(2)-N(3)-C(22)	-149.4(4)
C(8)-Li(2)-N(3)-C(22)	-121.2(5)
Li(3)-Li(2)-N(3)-C(22)	122.0(5)
C(41')-Li(2)-N(3)-C(22)	-29(4)
O(2')-Li(2)-N(3)-C(8)	91.9(7)
O(2)-Li(2)-N(3)-C(8)	104.1(8)
N(2)-Li(2)-N(3)-C(8)	-67.7(2)
C(7)-Li(2)-N(3)-C(8)	-28.22(17)
Li(3)-Li(2)-N(3)-C(8)	-116.9(2)
C(41')-Li(2)-N(3)-C(8)	92(4)
O(2')-Li(2)-N(3)-Li(3)	-151.3(8)
O(2)-Li(2)-N(3)-Li(3)	-139.0(8)
N(2)-Li(2)-N(3)-Li(3)	49.1(2)
C(7)-Li(2)-N(3)-Li(3)	88.6(2)
C(8)-Li(2)-N(3)-Li(3)	116.9(2)
C(41')-Li(2)-N(3)-Li(3)	-151(4)
N(2)-Li(3)-N(3)-C(22)	164.0(2)
O(3)-Li(3)-N(3)-C(22)	-17.0(4)
N(1)-Li(3)-N(3)-C(22)	163.5(5)
Li(1)-Li(3)-N(3)-C(22)	123.8(3)

Li(2)-Li(3)-N(3)-C(22)	-143.4(3)
N(2)-Li(3)-N(3)-C(8)	15.0(2)
O(3)-Li(3)-N(3)-C(8)	-166.0(2)
N(1)-Li(3)-N(3)-C(8)	14.5(6)
Li(1)-Li(3)-N(3)-C(8)	-25.2(3)
Li(2)-Li(3)-N(3)-C(8)	67.6(3)
N(2)-Li(3)-N(3)-Li(2)	-52.6(2)
O(3)-Li(3)-N(3)-Li(2)	126.4(3)
N(1)-Li(3)-N(3)-Li(2)	-53.1(5)
Li(1)-Li(3)-N(3)-Li(2)	-92.8(3)
C(10)-N(1)-C(2)-C(3)	-167.0(2)
Li(1)-N(1)-C(2)-C(3)	50.6(3)
Li(3)-N(1)-C(2)-C(3)	-15.5(3)
C(10)-N(1)-C(2)-C(1)	23.8(4)
Li(1)-N(1)-C(2)-C(1)	-118.6(3)
Li(3)-N(1)-C(2)-C(1)	175.3(3)
C(10)-N(1)-C(2)-Li(1)	142.4(3)
Li(3)-N(1)-C(2)-Li(1)	-66.1(2)
O(1)-Li(1)-C(2)-C(3)	85.6(4)
N(1)-Li(1)-C(2)-C(3)	-132.8(3)
N(2)-Li(1)-C(2)-C(3)	-33.01(17)
Li(3)-Li(1)-C(2)-C(3)	-83.9(2)
O(1)-Li(1)-C(2)-N(1)	-141.5(4)
N(2)-Li(1)-C(2)-N(1)	99.8(2)
C(3)-Li(1)-C(2)-N(1)	132.8(3)
Li(3)-Li(1)-C(2)-N(1)	48.9(2)
O(1)-Li(1)-C(2)-C(1)	-31.8(6)
N(1)-Li(1)-C(2)-C(1)	109.8(4)
N(2)-Li(1)-C(2)-C(1)	-150.4(3)
C(3)-Li(1)-C(2)-C(1)	-117.4(4)
Li(3)-Li(1)-C(2)-C(1)	158.7(3)
N(1)-C(2)-C(3)-N(2)	6.6(4)
C(1)-C(2)-C(3)-N(2)	175.4(3)
Li(1)-C(2)-C(3)-N(2)	54.2(3)
N(1)-C(2)-C(3)-C(4)	-168.0(3)
C(1)-C(2)-C(3)-C(4)	0.8(5)
Li(1)-C(2)-C(3)-C(4)	-120.4(3)
N(1)-C(2)-C(3)-Li(1)	-47.7(2)
C(1)-C(2)-C(3)-Li(1)	121.2(3)
C(7)-N(2)-C(3)-C(2)	-170.8(2)
Li(3)-N(2)-C(3)-C(2)	7.2(4)
Li(2)-N(2)-C(3)-C(2)	100.7(3)
Li(1)-N(2)-C(3)-C(2)	-56.0(3)
C(7)-N(2)-C(3)-C(4)	4.0(4)
Li(3)-N(2)-C(3)-C(4)	-177.9(3)
Li(2)-N(2)-C(3)-C(4)	-84.5(4)
Li(1)-N(2)-C(3)-C(4)	118.9(3)
C(7)-N(2)-C(3)-Li(1)	-114.9(3)
Li(3)-N(2)-C(3)-Li(1)	63.2(3)
Li(2)-N(2)-C(3)-Li(1)	156.6(3)
O(1)-Li(1)-C(3)-C(2)	-121.2(3)
N(1)-Li(1)-C(3)-C(2)	29.79(17)
N(2)-Li(1)-C(3)-C(2)	127.4(3)
Li(3)-Li(1)-C(3)-C(2)	88.5(2)
O(1)-Li(1)-C(3)-N(2)	111.3(3)
N(1)-Li(1)-C(3)-N(2)	-97.6(2)
C(2)-Li(1)-C(3)-N(2)	-127.4(3)

Li(3)-Li(1)-C(3)-N(2)	-38.9(2)
O(1)-Li(1)-C(3)-C(4)	-1.3(5)
N(1)-Li(1)-C(3)-C(4)	149.7(3)
N(2)-Li(1)-C(3)-C(4)	-112.7(3)
C(2)-Li(1)-C(3)-C(4)	119.9(3)
Li(3)-Li(1)-C(3)-C(4)	-151.5(3)
C(2)-C(3)-C(4)-C(5)	163.6(3)
N(2)-C(3)-C(4)-C(5)	-10.7(5)
Li(1)-C(3)-C(4)-C(5)	72.7(4)
C(3)-C(4)-C(5)-C(6)	7.6(5)
C(4)-C(5)-C(6)-C(7)	2.0(5)
C(3)-N(2)-C(7)-C(8)	-172.4(3)
Li(3)-N(2)-C(7)-C(8)	9.5(4)
Li(2)-N(2)-C(7)-C(8)	-54.8(3)
Li(1)-N(2)-C(7)-C(8)	101.8(3)
C(3)-N(2)-C(7)-C(6)	6.0(4)
Li(3)-N(2)-C(7)-C(6)	-172.0(3)
Li(2)-N(2)-C(7)-C(6)	123.6(3)
Li(1)-N(2)-C(7)-C(6)	-79.7(4)
C(3)-N(2)-C(7)-Li(2)	-117.6(3)
Li(3)-N(2)-C(7)-Li(2)	64.4(3)
Li(1)-N(2)-C(7)-Li(2)	156.7(3)
C(5)-C(6)-C(7)-C(8)	169.1(3)
C(5)-C(6)-C(7)-N(2)	-9.1(5)
C(5)-C(6)-C(7)-Li(2)	75.0(4)
O(2')-Li(2)-C(7)-C(8)	-112.4(5)
O(2)-Li(2)-C(7)-C(8)	-122.3(4)
N(3)-Li(2)-C(7)-C(8)	29.64(19)
N(2)-Li(2)-C(7)-C(8)	128.4(3)
Li(3)-Li(2)-C(7)-C(8)	90.3(2)
C(41')-Li(2)-C(7)-C(8)	-144.1(4)
O(2')-Li(2)-C(7)-N(2)	119.2(5)
O(2)-Li(2)-C(7)-N(2)	109.3(4)
N(3)-Li(2)-C(7)-N(2)	-98.8(2)
C(8)-Li(2)-C(7)-N(2)	-128.4(3)
Li(3)-Li(2)-C(7)-N(2)	-38.1(2)
C(41')-Li(2)-C(7)-N(2)	87.5(4)
O(2')-Li(2)-C(7)-C(6)	7.8(6)
O(2)-Li(2)-C(7)-C(6)	-2.1(6)
N(3)-Li(2)-C(7)-C(6)	149.9(3)
N(2)-Li(2)-C(7)-C(6)	-111.3(4)
C(8)-Li(2)-C(7)-C(6)	120.2(4)
Li(3)-Li(2)-C(7)-C(6)	-149.5(3)
C(41')-Li(2)-C(7)-C(6)	-23.9(5)
N(2)-C(7)-C(8)-N(3)	5.6(4)
C(6)-C(7)-C(8)-N(3)	-172.8(3)
Li(2)-C(7)-C(8)-N(3)	-46.9(3)
N(2)-C(7)-C(8)-C(9)	177.0(3)
C(6)-C(7)-C(8)-C(9)	-1.4(5)
Li(2)-C(7)-C(8)-C(9)	124.5(3)
N(2)-C(7)-C(8)-Li(2)	52.5(3)
C(6)-C(7)-C(8)-Li(2)	-125.9(4)
C(22)-N(3)-C(8)-C(7)	-165.5(3)
Li(2)-N(3)-C(8)-C(7)	50.1(3)
Li(3)-N(3)-C(8)-C(7)	-15.4(3)
C(22)-N(3)-C(8)-C(9)	22.8(4)
Li(2)-N(3)-C(8)-C(9)	-121.6(3)

Li(3)-N(3)-C(8)-C(9)	172.9(3)
C(22)-N(3)-C(8)-Li(2)	144.4(3)
Li(3)-N(3)-C(8)-Li(2)	-65.5(2)
O(2')-Li(2)-C(8)-C(7)	96.5(5)
O(2)-Li(2)-C(8)-C(7)	93.5(5)
N(3)-Li(2)-C(8)-C(7)	-133.3(3)
N(2)-Li(2)-C(8)-C(7)	-32.35(18)
Li(3)-Li(2)-C(8)-C(7)	-82.8(2)
C(41')-Li(2)-C(8)-C(7)	57.2(5)
O(2')-Li(2)-C(8)-N(3)	-130.2(5)
O(2)-Li(2)-C(8)-N(3)	-133.2(5)
N(2)-Li(2)-C(8)-N(3)	100.9(2)
C(7)-Li(2)-C(8)-N(3)	133.3(3)
Li(3)-Li(2)-C(8)-N(3)	50.5(2)
C(41')-Li(2)-C(8)-N(3)	-169.5(6)
O(2')-Li(2)-C(8)-C(9)	-20.9(6)
O(2)-Li(2)-C(8)-C(9)	-23.9(7)
N(3)-Li(2)-C(8)-C(9)	109.3(4)
N(2)-Li(2)-C(8)-C(9)	-149.7(3)
C(7)-Li(2)-C(8)-C(9)	-117.4(4)
Li(3)-Li(2)-C(8)-C(9)	159.8(3)
C(41')-Li(2)-C(8)-C(9)	-60.2(7)
C(2)-N(1)-C(10)-C(11)	-129.4(3)
Li(1)-N(1)-C(10)-C(11)	-21.5(5)
Li(3)-N(1)-C(10)-C(11)	81.8(3)
C(2)-N(1)-C(10)-C(15)	57.1(4)
Li(1)-N(1)-C(10)-C(15)	165.0(3)
Li(3)-N(1)-C(10)-C(15)	-91.7(3)
N(1)-C(10)-C(11)-C(12)	-173.8(3)
C(15)-C(10)-C(11)-C(12)	0.1(5)
N(1)-C(10)-C(11)-C(16)	7.9(5)
C(15)-C(10)-C(11)-C(16)	-178.3(3)
C(10)-C(11)-C(12)-C(13)	-1.1(6)
C(16)-C(11)-C(12)-C(13)	177.2(4)
C(11)-C(12)-C(13)-C(14)	0.9(6)
C(12)-C(13)-C(14)-C(15)	0.2(6)
C(13)-C(14)-C(15)-C(10)	-1.2(5)
C(13)-C(14)-C(15)-C(19)	172.8(3)
N(1)-C(10)-C(15)-C(14)	174.6(3)
C(11)-C(10)-C(15)-C(14)	1.0(4)
N(1)-C(10)-C(15)-C(19)	0.7(4)
C(11)-C(10)-C(15)-C(19)	-172.8(3)
C(12)-C(11)-C(16)-C(18)	-89.2(6)
C(10)-C(11)-C(16)-C(18)	89.1(5)
C(12)-C(11)-C(16)-C(17)	33.5(6)
C(10)-C(11)-C(16)-C(17)	-148.1(4)
C(14)-C(15)-C(19)-C(21)	-85.8(4)
C(10)-C(15)-C(19)-C(21)	88.0(4)
C(14)-C(15)-C(19)-C(20)	37.3(5)
C(10)-C(15)-C(19)-C(20)	-148.9(3)
C(8)-N(3)-C(22)-C(27)	61.9(4)
Li(2)-N(3)-C(22)-C(27)	169.5(4)
Li(3)-N(3)-C(22)-C(27)	-84.5(4)
C(8)-N(3)-C(22)-C(23)	-123.2(3)
Li(2)-N(3)-C(22)-C(23)	-15.6(6)
Li(3)-N(3)-C(22)-C(23)	90.4(3)
N(3)-C(22)-C(23)-C(24)	-171.5(3)

C(27)-C(22)-C(23)-C(24)	3.6(5)
N(3)-C(22)-C(23)-C(28)	8.4(5)
C(27)-C(22)-C(23)-C(28)	-176.5(3)
C(22)-C(23)-C(24)-C(25)	-2.1(6)
C(28)-C(23)-C(24)-C(25)	178.0(4)
C(23)-C(24)-C(25)-C(26)	-1.0(6)
C(24)-C(25)-C(26)-C(27)	2.5(6)
C(25)-C(26)-C(27)-C(22)	-0.9(6)
C(25)-C(26)-C(27)-C(31)	175.3(4)
N(3)-C(22)-C(27)-C(26)	172.8(3)
C(23)-C(22)-C(27)-C(26)	-2.2(5)
N(3)-C(22)-C(27)-C(31)	-3.2(5)
C(23)-C(22)-C(27)-C(31)	-178.2(3)
C(24)-C(23)-C(28)-C(29)	95.6(4)
C(22)-C(23)-C(28)-C(29)	-84.3(4)
C(24)-C(23)-C(28)-C(30)	-29.1(5)
C(22)-C(23)-C(28)-C(30)	151.0(3)
C(26)-C(27)-C(31)-C(32)	44.4(5)
C(22)-C(27)-C(31)-C(32)	-139.6(4)
C(26)-C(27)-C(31)-C(33)	-80.6(5)
C(22)-C(27)-C(31)-C(33)	95.4(4)
N(1)-Li(1)-O(1)-C(34)	-52.4(8)
N(2)-Li(1)-O(1)-C(34)	96.8(4)
C(3)-Li(1)-O(1)-C(34)	50.1(5)
C(2)-Li(1)-O(1)-C(34)	5.8(6)
Li(3)-Li(1)-O(1)-C(34)	166.6(5)
N(1)-Li(1)-O(1)-C(37)	168.9(6)
N(2)-Li(1)-O(1)-C(37)	-42.0(5)
C(3)-Li(1)-O(1)-C(37)	-88.7(4)
C(2)-Li(1)-O(1)-C(37)	-133.0(4)
Li(3)-Li(1)-O(1)-C(37)	27.8(7)
C(37)-O(1)-C(34)-C(35)	8.6(5)
Li(1)-O(1)-C(34)-C(35)	-134.1(4)
O(1)-C(34)-C(35)-C(36)	-16.2(7)
C(34)-C(35)-C(36)-C(37)	17.2(7)
C(34)-O(1)-C(37)-C(36)	1.8(5)
Li(1)-O(1)-C(37)-C(36)	144.9(4)
C(35)-C(36)-C(37)-O(1)	-11.9(6)
O(2')-Li(2)-O(2)-C(38)	88.8(19)
N(3)-Li(2)-O(2)-C(38)	35.9(9)
N(2)-Li(2)-O(2)-C(38)	-154.6(2)
C(7)-Li(2)-O(2)-C(38)	154.2(2)
C(8)-Li(2)-O(2)-C(38)	103.7(5)
Li(3)-Li(2)-O(2)-C(38)	-82.1(6)
C(41')-Li(2)-O(2)-C(38)	-147.5(10)
O(2')-Li(2)-O(2)-C(41)	-72.7(19)
N(3)-Li(2)-O(2)-C(41)	-125.6(9)
N(2)-Li(2)-O(2)-C(41)	43.9(8)
C(7)-Li(2)-O(2)-C(41)	-7.3(8)
C(8)-Li(2)-O(2)-C(41)	-57.8(8)
Li(3)-Li(2)-O(2)-C(41)	116.4(7)
C(41')-Li(2)-O(2)-C(41)	51.0(8)
C(41)-O(2)-C(38)-C(39)	4.1(9)
Li(2)-O(2)-C(38)-C(39)	-157.4(8)
O(2)-C(38)-C(39)-C(40)	4.3(14)
C(38)-C(39)-C(40)-C(41)	-11.1(17)
C(39)-C(40)-C(41)-O(2)	13.0(16)

C(38)-O(2)-C(41)-C(40)	-11.2(12)
Li(2)-O(2)-C(41)-C(40)	156.0(10)
O(2)-Li(2)-O(2')-C(38')	-141(3)
N(3)-Li(2)-O(2')-C(38')	-4.1(16)
N(2)-Li(2)-O(2')-C(38')	147.7(11)
C(7)-Li(2)-O(2')-C(38')	98.1(12)
C(8)-Li(2)-O(2')-C(38')	51.3(14)
Li(3)-Li(2)-O(2')-C(38')	-130.0(12)
C(41')-Li(2)-O(2')-C(38')	176.0(17)
O(2)-Li(2)-O(2')-C(41')	42.5(17)
N(3)-Li(2)-O(2')-C(41')	179.9(9)
N(2)-Li(2)-O(2')-C(41')	-28.3(11)
C(7)-Li(2)-O(2')-C(41')	-77.9(9)
C(8)-Li(2)-O(2')-C(41')	-124.7(9)
Li(3)-Li(2)-O(2')-C(41')	54.0(12)
C(41')-O(2')-C(38')-C(39')	16.4(17)
Li(2)-O(2')-C(38')-C(39')	-159.6(11)
O(2')-C(38')-C(39')-C(40')	3.7(19)
C(38')-C(39')-C(40')-C(41')	-21(2)
C(38')-O(2')-C(41')-C(40')	-29.2(17)
Li(2)-O(2')-C(41')-C(40')	147.8(11)
C(38')-O(2')-C(41')-Li(2)	-177.0(13)
C(39')-C(40')-C(41')-O(2')	28.7(18)
C(39')-C(40')-C(41')-Li(2)	56(2)
O(2)-Li(2)-C(41')-O(2')	-15.4(7)
N(3)-Li(2)-C(41')-O(2')	-1(4)
N(2)-Li(2)-C(41')-O(2')	158.9(8)
C(7)-Li(2)-C(41')-O(2')	117.6(9)
C(8)-Li(2)-C(41')-O(2')	83.7(10)
Li(3)-Li(2)-C(41')-O(2')	-149.1(8)
O(2')-Li(2)-C(41')-C(40')	-45.1(13)
O(2)-Li(2)-C(41')-C(40')	-60.5(12)
N(3)-Li(2)-C(41')-C(40')	-46(5)
N(2)-Li(2)-C(41')-C(40')	113.9(14)
C(7)-Li(2)-C(41')-C(40')	72.6(15)
C(8)-Li(2)-C(41')-C(40')	38.6(17)
Li(3)-Li(2)-C(41')-C(40')	165.9(13)
N(2)-Li(3)-O(3)-C(42)	-37(21)
N(1)-Li(3)-O(3)-C(42)	44.1(5)
N(3)-Li(3)-O(3)-C(42)	-135.6(4)
Li(1)-Li(3)-O(3)-C(42)	92.9(5)
Li(2)-Li(3)-O(3)-C(42)	-86.4(5)
N(2)-Li(3)-O(3)-C(45)	136(21)
N(1)-Li(3)-O(3)-C(45)	-142.9(4)
N(3)-Li(3)-O(3)-C(45)	37.4(4)
Li(1)-Li(3)-O(3)-C(45)	-94.1(5)
Li(2)-Li(3)-O(3)-C(45)	86.6(5)
C(45)-O(3)-C(42)-C(43)	14.9(6)
Li(3)-O(3)-C(42)-C(43)	-170.9(4)
O(3)-C(42)-C(43)-C(44)	-22.1(7)
C(42)-C(43)-C(44)-C(45)	21.3(8)
C(43)-C(44)-C(45)-O(3)	-12.9(8)
C(42)-O(3)-C(45)-C(44)	-0.6(6)
Li(3)-O(3)-C(45)-C(44)	-174.8(5)

Symmetry transformations used to generate equivalent atoms:

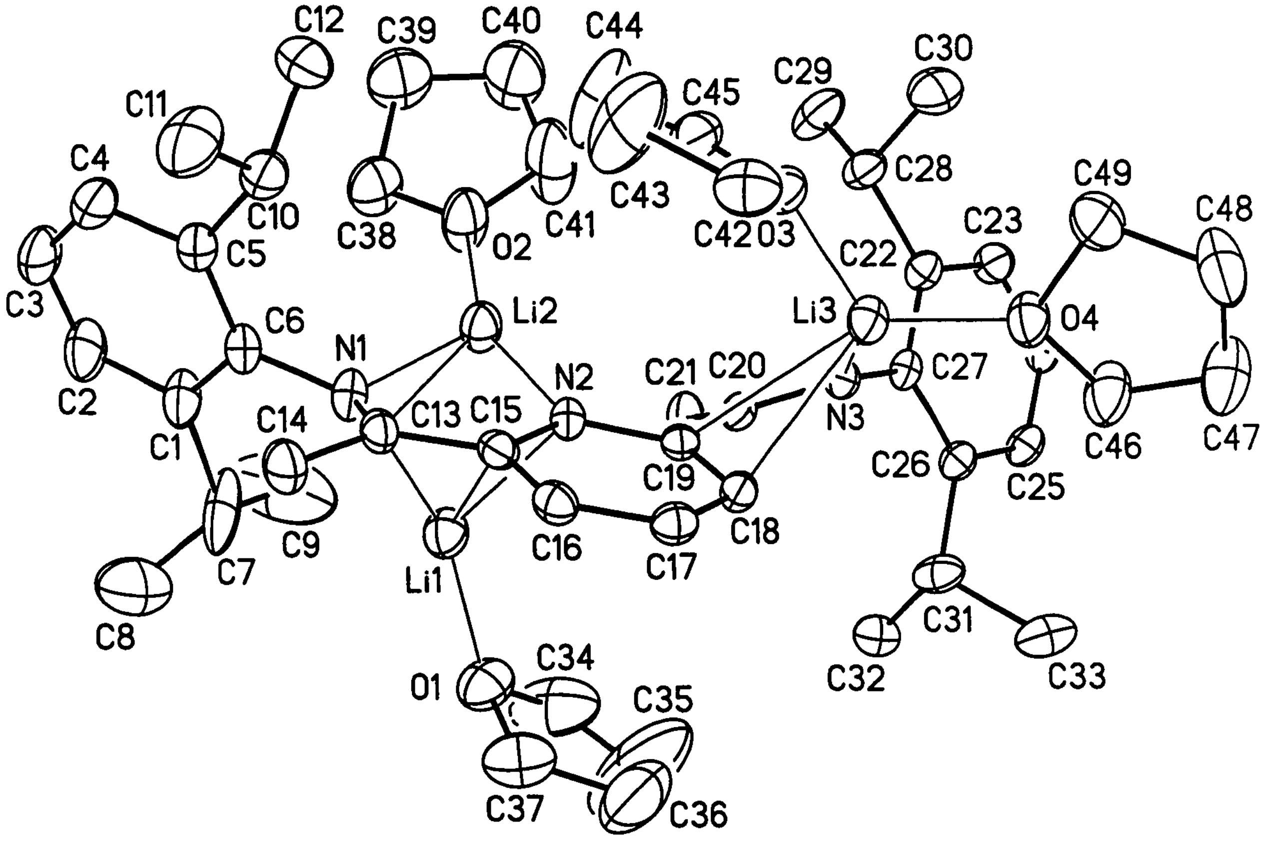
C12
C39
C40
C44
C11
C45
C29
C30
C4
C10
C28
C49
C48
C43
C38
O2
C41
C42
O3
C23
C5
C22
C3
C6
Li2
Li3
O4
N1
C21
C20
C27
C2
C14
C13
C15
N2
N3
C1
C19
C26
C25
C46
C47
C9
C18
C16
C17
C7
Li1
C8
C31
C32
C33
O1
C34
C35
C37
C36

Table AIII.7. Crystal data and structure refinement for sg2088.

Identification code	sg2088
Empirical formula	C49 H74 Li3 N3 O4
Formula weight	789.93
Temperature	203(2) K
Wavelength	0.71073 A
Crystal system, space group	Monoclinic, P2(1)/c
Unit cell dimensions	a = 15.0732(16) A alpha = 90 deg. b = 18.855(2) A beta = 105.170(2) deg. c = 17.9425(19) A gamma = 90 deg.
Volume	4921.6(9) A^3
Z, Calculated density	4, 1.066 Mg/m^3
Absorption coefficient	0.065 mm^-1
F(000)	1720
Crystal size	0.2 x 0.1 x 0.1 mm
Theta range for data collection	1.60 to 25.00 deg.
Limiting indices	-17<=h<=17, 0<=k<=22, 0<=l<=21
Reflections collected / unique	12127 / 8649 [R(int) = 0.0473]
Completeness to theta = 25.00	99.9 %
Absorption correction	Semi-empirical from equivalents
Max. and min. transmission	1.000000 and 0.921147
Refinement method	Full-matrix least-squares on F^2
Data / restraints / parameters	8649 / 16 / 532
Goodness-of-fit on F^2	1.067
Final R indices [I>2sigma(I)]	R1 = 0.0759, wR2 = 0.1971
R indices (all data)	R1 = 0.1190, wR2 = 0.2317
Largest diff. peak and hole	0.807 and -0.657 e.A^-3

Table AIII.8. Atomic coordinates (x 10^4) and equivalent isotropic displacement parameters (A^2 x 10^3) for sg2088.
U(eq) is defined as one third of the trace of the orthogonalized Uij tensor.

	x	y	z	U(eq)
Li(1)	971(4)	5828(3)	7131(3)	57(1)
Li(2)	1592(4)	6980(3)	7861(4)	54(1)
Li(3)	4888(3)	6127(3)	8600(3)	46(1)
N(1)	575(2)	6350(2)	7971(2)	46(1)
N(2)	2262(2)	6087(1)	7892(1)	37(1)
N(3)	4426(2)	6549(1)	7575(1)	34(1)
O(1)	912(2)	5214(2)	6268(1)	72(1)
O(2)	1498(2)	7987(1)	7874(2)	89(1)
O(3)	4564(2)	6403(1)	9541(1)	52(1)
O(4)	6149(2)	5797(1)	8863(1)	59(1)
C(1)	-994(2)	6803(2)	7538(2)	63(1)
C(2)	-1732(2)	7164(2)	7694(2)	73(1)
C(3)	-1731(3)	7365(2)	8433(3)	77(1)
C(4)	-972(3)	7211(2)	9032(2)	72(1)
C(5)	-202(2)	6868(2)	8914(2)	51(1)
C(6)	-200(2)	6655(2)	8152(2)	46(1)
C(7)	-1060(3)	6495(4)	6704(2)	109(2)
C(8)	-1983(5)	6220(4)	6296(4)	146(3)
C(9)	-766(8)	7037(5)	6260(4)	229(6)
C(10)	642(2)	6789(2)	9598(2)	62(1)
C(11)	441(3)	6397(3)	10288(2)	97(2)
C(12)	1052(3)	7527(3)	9853(3)	92(2)
C(13)	958(2)	5713(2)	8324(2)	41(1)
C(14)	392(2)	5194(2)	8650(2)	56(1)
C(15)	1837(2)	5548(2)	8262(2)	37(1)
C(16)	2334(2)	4894(2)	8493(2)	41(1)
C(17)	3162(2)	4784(2)	8354(2)	41(1)
C(18)	3568(2)	5317(2)	7971(2)	37(1)
C(19)	3095(2)	5939(2)	7757(2)	34(1)
C(20)	3489(2)	6524(2)	7351(2)	35(1)
C(21)	2903(2)	6949(2)	6830(2)	49(1)
C(22)	5223(2)	7653(2)	7406(2)	39(1)
C(23)	5791(2)	8028(2)	7036(2)	46(1)
C(24)	6004(2)	7752(2)	6387(2)	45(1)
C(25)	5648(2)	7101(2)	6107(2)	43(1)
C(26)	5094(2)	6702(2)	6466(2)	39(1)
C(27)	4888(2)	6977(2)	7142(2)	34(1)
C(28)	4973(2)	7994(2)	8099(2)	50(1)
C(29)	4618(3)	8757(2)	7923(3)	81(1)
C(30)	5773(3)	7960(3)	8821(2)	83(1)
C(31)	4724(3)	5988(2)	6131(2)	54(1)
C(32)	3975(3)	6071(2)	5367(2)	73(1)
C(33)	5491(3)	5499(2)	5999(2)	69(1)
C(34)	1240(6)	5457(3)	5632(3)	138(3)
C(35)	1879(11)	4985(6)	5519(9)	302(10)
C(36)	1989(5)	4402(5)	6044(5)	161(3)
C(37)	1213(4)	4492(3)	6414(3)	93(2)

C(38)	718(3)	8429(2)	7825(3)	87(1)
C(39)	1100(4)	9105(3)	8212(4)	113(2)
C(40)	2066(4)	9133(3)	8149(5)	129(2)
C(41)	2276(4)	8439(3)	7946(6)	169(4)
C(42)	4419(3)	5889(2)	10092(2)	73(1)
C(43)	3674(6)	6192(4)	10401(5)	153(3)
C(44)	3385(5)	6801(4)	10045(4)	144(3)
C(45)	3933(3)	6978(2)	9503(2)	63(1)
C(46)	6583(3)	5680(3)	8247(2)	81(1)
C(47)	7539(3)	5447(3)	8605(3)	93(2)
C(48)	7711(3)	5579(3)	9447(3)	95(2)
C(49)	6871(3)	5949(3)	9542(2)	73(1)

Table AIII.9. Bond lengths [A] and angles [deg] for sg2088.

Li(1)-O(1)	1.917(6)
Li(1)-N(1)	2.017(6)
Li(1)-N(2)	2.121(6)
Li(1)-C(13)	2.156(6)
Li(1)-C(15)	2.171(6)
Li(1)-Li(2)	2.582(9)
Li(2)-O(2)	1.905(6)
Li(2)-N(2)	1.956(6)
Li(2)-N(1)	1.989(6)
Li(2)-C(13)	2.779(6)
Li(3)-O(4)	1.937(5)
Li(3)-O(3)	1.946(5)
Li(3)-N(3)	1.958(5)
Li(3)-C(18)	2.528(6)
Li(3)-C(20)	2.750(6)
Li(3)-C(19)	2.754(6)
N(1)-C(13)	1.410(4)
N(1)-C(6)	1.414(4)
N(2)-C(19)	1.368(3)
N(2)-C(15)	1.451(4)
N(3)-C(20)	1.364(3)
N(3)-C(27)	1.422(3)
O(1)-C(34)	1.433(6)
O(1)-C(37)	1.437(5)
O(2)-C(38)	1.426(5)
O(2)-C(41)	1.428(6)
O(3)-C(45)	1.433(4)
O(3)-C(42)	1.442(4)
O(4)-C(49)	1.434(4)
O(4)-C(46)	1.442(4)
C(1)-C(2)	1.394(5)
C(1)-C(6)	1.426(4)
C(1)-C(7)	1.584(6)
C(2)-C(3)	1.379(6)
C(3)-C(4)	1.380(6)
C(4)-C(5)	1.393(5)
C(5)-C(6)	1.426(4)

C(5)-C(10)	1.526(5)
C(7)-C(9)	1.435(8)
C(7)-C(8)	1.486(7)
C(10)-C(11)	1.540(6)
C(10)-C(12)	1.543(6)
C(13)-C(15)	1.394(4)
C(13)-C(14)	1.514(4)
C(15)-C(16)	1.446(4)
C(16)-C(17)	1.352(4)
C(17)-C(18)	1.442(4)
C(18)-C(19)	1.374(4)
C(19)-C(20)	1.526(4)
C(20)-C(21)	1.366(4)
C(22)-C(23)	1.403(4)
C(22)-C(27)	1.407(4)
C(22)-C(28)	1.531(4)
C(23)-C(24)	1.388(4)
C(24)-C(25)	1.380(4)
C(25)-C(26)	1.401(4)
C(26)-C(27)	1.427(4)
C(26)-C(31)	1.519(4)
C(28)-C(30)	1.522(5)
C(28)-C(29)	1.539(5)
C(31)-C(32)	1.539(5)
C(31)-C(33)	1.545(5)
C(34)-C(35)	1.364(12)
C(35)-C(36)	1.429(12)
C(36)-C(37)	1.498(8)
C(38)-C(39)	1.493(7)
C(39)-C(40)	1.490(8)
C(40)-C(41)	1.416(7)
C(42)-C(43)	1.489(7)
C(43)-C(44)	1.331(8)
C(44)-C(45)	1.469(6)
C(46)-C(47)	1.483(6)
C(47)-C(48)	1.485(6)
C(48)-C(49)	1.494(6)
O(1)-Li(1)-N(1)	159.8(4)
O(1)-Li(1)-N(2)	120.0(3)
N(1)-Li(1)-N(2)	78.9(2)
O(1)-Li(1)-C(13)	137.0(4)
N(1)-Li(1)-C(13)	39.32(15)
N(2)-Li(1)-C(13)	68.24(19)
O(1)-Li(1)-C(15)	119.8(3)
N(1)-Li(1)-C(15)	69.1(2)
N(2)-Li(1)-C(15)	39.49(14)
C(13)-Li(1)-C(15)	37.58(14)
O(1)-Li(1)-Li(2)	148.3(3)
N(1)-Li(1)-Li(2)	49.4(2)
N(2)-Li(1)-Li(2)	47.92(19)
C(13)-Li(1)-Li(2)	71.2(2)
C(15)-Li(1)-Li(2)	71.4(2)
O(2)-Li(2)-N(2)	153.8(3)
O(2)-Li(2)-N(1)	122.1(3)
N(2)-Li(2)-N(1)	83.7(2)
O(2)-Li(2)-Li(1)	145.8(3)
N(2)-Li(2)-Li(1)	53.6(2)

N(1)-Li(2)-Li(1)	50.3(2)
O(2)-Li(2)-C(13)	145.1(3)
N(2)-Li(2)-C(13)	57.80(17)
N(1)-Li(2)-C(13)	28.76(12)
Li(1)-Li(2)-C(13)	47.24(17)
O(4)-Li(3)-O(3)	109.2(3)
O(4)-Li(3)-N(3)	116.4(3)
O(3)-Li(3)-N(3)	126.7(3)
O(4)-Li(3)-C(18)	121.5(3)
O(3)-Li(3)-C(18)	101.7(2)
N(3)-Li(3)-C(18)	77.32(19)
O(4)-Li(3)-C(20)	141.3(2)
O(3)-Li(3)-C(20)	108.7(2)
N(3)-Li(3)-C(20)	27.70(11)
C(18)-Li(3)-C(20)	56.91(14)
O(4)-Li(3)-C(19)	148.4(3)
O(3)-Li(3)-C(19)	94.4(2)
N(3)-Li(3)-C(19)	58.62(15)
C(18)-Li(3)-C(19)	29.77(10)
C(20)-Li(3)-C(19)	32.21(10)
C(13)-N(1)-C(6)	120.6(2)
C(13)-N(1)-Li(2)	108.5(2)
C(6)-N(1)-Li(2)	119.0(3)
C(13)-N(1)-Li(1)	75.6(2)
C(6)-N(1)-Li(1)	142.5(3)
Li(2)-N(1)-Li(1)	80.3(3)
C(19)-N(2)-C(15)	118.2(2)
C(19)-N(2)-Li(2)	131.4(3)
C(15)-N(2)-Li(2)	109.2(2)
C(19)-N(2)-Li(1)	124.7(2)
C(15)-N(2)-Li(1)	72.1(2)
Li(2)-N(2)-Li(1)	78.5(3)
C(20)-N(3)-C(27)	118.4(2)
C(20)-N(3)-Li(3)	110.4(2)
C(27)-N(3)-Li(3)	129.7(2)
C(34)-O(1)-C(37)	106.9(4)
C(34)-O(1)-Li(1)	119.9(4)
C(37)-O(1)-Li(1)	118.6(3)
C(38)-O(2)-C(41)	107.5(4)
C(38)-O(2)-Li(2)	130.2(3)
C(41)-O(2)-Li(2)	122.3(3)
C(45)-O(3)-C(42)	108.9(3)
C(45)-O(3)-Li(3)	118.4(2)
C(42)-O(3)-Li(3)	122.2(3)
C(49)-O(4)-C(46)	106.6(3)
C(49)-O(4)-Li(3)	128.4(3)
C(46)-O(4)-Li(3)	118.4(3)
C(2)-C(1)-C(6)	119.6(3)
C(2)-C(1)-C(7)	120.8(3)
C(6)-C(1)-C(7)	119.4(3)
C(3)-C(2)-C(1)	121.7(4)
C(2)-C(3)-C(4)	119.0(3)
C(3)-C(4)-C(5)	122.2(4)
C(4)-C(5)-C(6)	119.2(3)
C(4)-C(5)-C(10)	118.4(3)
C(6)-C(5)-C(10)	122.2(3)
N(1)-C(6)-C(5)	122.9(3)

N(1)-C(6)-C(1)	118.6(3)
C(5)-C(6)-C(1)	118.3(3)
C(9)-C(7)-C(8)	111.2(6)
C(9)-C(7)-C(1)	108.1(5)
C(8)-C(7)-C(1)	114.4(4)
C(5)-C(10)-C(11)	113.3(3)
C(5)-C(10)-C(12)	109.6(3)
C(11)-C(10)-C(12)	110.0(4)
C(15)-C(13)-N(1)	116.1(2)
C(15)-C(13)-C(14)	122.1(3)
N(1)-C(13)-C(14)	121.2(3)
C(15)-C(13)-Li(1)	71.8(2)
N(1)-C(13)-Li(1)	65.0(2)
C(14)-C(13)-Li(1)	127.0(3)
C(15)-C(13)-Li(2)	76.1(2)
N(1)-C(13)-Li(2)	42.76(17)
C(14)-C(13)-Li(2)	160.8(2)
Li(1)-C(13)-Li(2)	61.6(2)
C(13)-C(15)-C(16)	126.8(3)
C(13)-C(15)-N(2)	115.0(3)
C(16)-C(15)-N(2)	118.2(2)
C(13)-C(15)-Li(1)	70.6(2)
C(16)-C(15)-Li(1)	128.0(3)
N(2)-C(15)-Li(1)	68.4(2)
C(17)-C(16)-C(15)	120.8(3)
C(16)-C(17)-C(18)	120.6(3)
C(19)-C(18)-C(17)	118.3(3)
C(19)-C(18)-Li(3)	84.2(2)
C(17)-C(18)-Li(3)	126.2(2)
N(2)-C(19)-C(18)	124.0(3)
N(2)-C(19)-C(20)	115.3(2)
C(18)-C(19)-C(20)	120.7(2)
N(2)-C(19)-Li(3)	133.7(2)
C(18)-C(19)-Li(3)	65.99(19)
C(20)-C(19)-Li(3)	73.77(18)
N(3)-C(20)-C(21)	128.1(3)
N(3)-C(20)-C(19)	112.7(2)
C(21)-C(20)-C(19)	119.2(3)
N(3)-C(20)-Li(3)	41.85(16)
C(21)-C(20)-Li(3)	159.9(3)
C(19)-C(20)-Li(3)	74.02(18)
C(23)-C(22)-C(27)	120.4(3)
C(23)-C(22)-C(28)	118.9(3)
C(27)-C(22)-C(28)	120.7(2)
C(24)-C(23)-C(22)	120.8(3)
C(25)-C(24)-C(23)	119.1(3)
C(24)-C(25)-C(26)	122.1(3)
C(25)-C(26)-C(27)	118.9(3)
C(25)-C(26)-C(31)	119.7(3)
C(27)-C(26)-C(31)	121.3(3)
C(22)-C(27)-N(3)	121.0(2)
C(22)-C(27)-C(26)	118.5(2)
N(3)-C(27)-C(26)	120.2(3)
C(30)-C(28)-C(22)	111.4(3)
C(30)-C(28)-C(29)	111.7(3)
C(22)-C(28)-C(29)	111.8(3)
C(26)-C(31)-C(32)	111.7(3)

C(26)-C(31)-C(33)	112.2(3)
C(32)-C(31)-C(33)	109.1(3)
C(35)-C(34)-O(1)	108.2(7)
C(34)-C(35)-C(36)	111.7(7)
C(35)-C(36)-C(37)	103.6(6)
O(1)-C(37)-C(36)	105.8(5)
O(2)-C(38)-C(39)	105.0(4)
C(40)-C(39)-C(38)	105.1(4)
C(41)-C(40)-C(39)	105.9(5)
C(40)-C(41)-O(2)	110.0(5)
O(3)-C(42)-C(43)	105.2(4)
C(44)-C(43)-C(42)	109.7(4)
C(43)-C(44)-C(45)	110.1(5)
O(3)-C(45)-C(44)	106.1(4)
O(4)-C(46)-C(47)	107.3(3)
C(46)-C(47)-C(48)	106.4(4)
C(47)-C(48)-C(49)	105.4(3)
O(4)-C(49)-C(48)	106.7(3)

Symmetry transformations used to generate equivalent atoms:

Table AIII.10. Anisotropic displacement parameters (A^2 x 10^3) for sg2088. The anisotropic displacement factor exponent takes the form:
-2 pi^2 [h^2 a*^2 U11 + ... + 2 h k a* b* U12]

	U11	U22	U33	U23	U13	U12
Li(1)	51(3)	74(4)	47(3)	0(3)	13(3)	4(3)
Li(2)	45(3)	46(3)	76(4)	4(3)	22(3)	6(2)
Li(3)	42(3)	58(3)	39(3)	5(2)	10(2)	8(2)
N(1)	35(1)	59(2)	49(2)	10(1)	18(1)	6(1)
N(2)	31(1)	42(1)	38(1)	2(1)	11(1)	1(1)
N(3)	35(1)	37(1)	33(1)	3(1)	13(1)	0(1)
O(1)	82(2)	83(2)	51(2)	-6(1)	18(1)	9(2)
O(2)	68(2)	48(2)	163(3)	0(2)	51(2)	7(1)
O(3)	54(1)	65(2)	41(1)	-3(1)	18(1)	3(1)
O(4)	41(1)	91(2)	43(1)	0(1)	9(1)	9(1)
C(1)	36(2)	100(3)	54(2)	10(2)	16(2)	9(2)
C(2)	41(2)	107(3)	72(3)	13(2)	15(2)	17(2)
C(3)	46(2)	98(3)	92(3)	-9(3)	24(2)	21(2)
C(4)	54(2)	95(3)	70(2)	-21(2)	23(2)	6(2)
C(5)	39(2)	62(2)	55(2)	-4(2)	16(2)	0(2)
C(6)	34(2)	54(2)	53(2)	6(2)	18(1)	0(1)
C(7)	42(2)	232(7)	57(2)	42(3)	19(2)	45(3)
C(8)	160(6)	154(6)	121(5)	-50(5)	32(4)	-34(5)
C(9)	376(14)	229(10)	95(5)	-20(5)	82(7)	-174(10)
C(10)	49(2)	81(3)	55(2)	-13(2)	13(2)	4(2)
C(11)	92(3)	144(5)	55(2)	6(3)	20(2)	23(3)
C(12)	65(3)	110(4)	92(3)	-39(3)	4(2)	-6(3)
C(13)	35(2)	51(2)	38(2)	-1(1)	13(1)	-5(1)

C(14)	48(2)	63(2)	62(2)	1(2)	23(2)	-9(2)
C(15)	37(2)	41(2)	33(1)	-3(1)	9(1)	-7(1)
C(16)	44(2)	39(2)	41(2)	1(1)	11(1)	-7(1)
C(17)	46(2)	32(2)	44(2)	0(1)	11(1)	2(1)
C(18)	35(2)	38(2)	38(2)	-2(1)	12(1)	3(1)
C(19)	33(1)	39(2)	28(1)	-4(1)	7(1)	-1(1)
C(20)	37(2)	40(2)	32(1)	-1(1)	13(1)	4(1)
C(21)	39(2)	58(2)	51(2)	19(2)	16(1)	5(2)
C(22)	42(2)	38(2)	41(2)	1(1)	18(1)	2(1)
C(23)	51(2)	42(2)	51(2)	-1(1)	22(2)	-4(1)
C(24)	44(2)	49(2)	49(2)	13(2)	24(1)	4(1)
C(25)	50(2)	48(2)	36(2)	5(1)	22(1)	8(2)
C(26)	44(2)	42(2)	34(2)	2(1)	16(1)	3(1)
C(27)	32(1)	39(2)	33(1)	7(1)	12(1)	7(1)
C(28)	63(2)	43(2)	54(2)	-9(2)	32(2)	-7(2)
C(29)	108(3)	50(2)	107(3)	-14(2)	70(3)	0(2)
C(30)	82(3)	117(4)	55(2)	-27(2)	28(2)	-16(3)
C(31)	80(2)	50(2)	41(2)	-8(2)	32(2)	-10(2)
C(32)	64(2)	80(3)	75(3)	-31(2)	19(2)	-12(2)
C(33)	104(3)	49(2)	52(2)	-5(2)	17(2)	12(2)
C(34)	252(9)	111(5)	69(3)	-8(3)	71(4)	-34(5)
C(35)	490(20)	129(8)	460(20)	-17(10)	420(20)	-17(10)
C(36)	129(5)	200(9)	149(6)	-66(6)	25(5)	62(6)
C(37)	127(4)	77(3)	71(3)	-6(2)	19(3)	0(3)
C(38)	84(3)	62(3)	117(4)	3(3)	29(3)	21(2)
C(39)	123(5)	67(3)	153(5)	-13(3)	43(4)	9(3)
C(40)	122(5)	84(4)	197(7)	-16(4)	68(5)	-20(3)
C(41)	104(4)	67(4)	365(12)	-30(5)	114(6)	-20(3)
C(42)	99(3)	68(3)	51(2)	5(2)	18(2)	-6(2)
C(43)	197(7)	139(6)	184(7)	27(5)	158(6)	-3(5)
C(44)	139(5)	164(7)	173(7)	29(5)	119(5)	49(5)
C(45)	64(2)	72(3)	52(2)	-10(2)	12(2)	13(2)
C(46)	60(2)	135(4)	54(2)	-2(2)	24(2)	18(3)
C(47)	67(3)	125(4)	97(3)	21(3)	43(3)	23(3)
C(48)	46(2)	146(5)	88(3)	15(3)	8(2)	0(3)
C(49)	62(2)	95(3)	51(2)	0(2)	-3(2)	12(2)

Table AIII.11. Hydrogen coordinates (x 10^4) and isotropic displacement parameters (A^2 x 10^3) for sg2088.

	x	y	z	U(eq)
H(2A)	-2244	7275	7283	88
H(3A)	-2239	7602	8527	93
H(4A)	-975	7342	9537	86
H(7)	-620	6097	6762	131
H(8A)	-2183	5878	6621	219
H(8B)	-1951	5993	5818	219
H(8C)	-2418	6610	6180	219
H(9A)	-160	7203	6536	344
H(9B)	-1196	7430	6181	356
H(9C)	-742	6845	5765	344
H(10A)	1108	6512	9423	74
H(11A)	186	5933	10124	145
H(11B)	3	6668	10483	145
H(11C)	1006	6343	10693	145
H(12A)	1183	7768	9416	138
H(12B)	1616	7473	10260	138
H(12C)	615	7804	10044	138
H(14A)	424	4728	8429	84
H(14B)	-243	5351	8524	84
H(14C)	631	5169	9207	84
H(16A)	2077	4542	8743	50
H(17A)	3476	4356	8509	49
H(18A)	4142	5241	7869	44
H(21A)	3137	7313	6577	58
H(21B)	2265	6879	6724	58
H(23A)	6030	8471	7231	55
H(24A)	6384	8005	6141	54
H(25A)	5783	6920	5661	51
H(28A)	4465	7712	8204	60
H(29A)	4461	8953	8372	121
H(29B)	4077	8754	7488	121
H(29C)	5092	9045	7798	121
H(30A)	5974	7472	8918	124
H(30B)	5577	8140	9259	124
H(30C)	6277	8246	8746	124
H(31A)	4443	5752	6506	65
H(32A)	3488	6373	5448	110
H(32B)	3726	5609	5188	110
H(32C)	4241	6284	4982	110
H(33A)	5965	5445	6479	103
H(33B)	5756	5707	5612	103
H(33C)	5234	5038	5823	103
H(34A)	729	5491	5165	166
H(34B)	1517	5929	5745	166
H(35A)	2470	5228	5589	362
H(35B)	1689	4807	4988	362
H(36A)	2584	4425	6430	194
H(36B)	1942	3949	5769	194
H(37A)	711	4163	6187	111

H(37B)	1422	4402	6970	111
H(38A)	295	8211	8090	104
H(38B)	388	8515	7285	104
H(39A)	748	9513	7953	136
H(39B)	1085	9104	8755	136
H(40A)	2122	9474	7751	155
H(40B)	2484	9276	8642	155
H(41A)	2799	8252	8344	202
H(41B)	2447	8452	7456	202
H(42A)	4981	5821	10508	87
H(42B)	4231	5431	9841	87
H(43A)	3161	5856	10318	183
H(43B)	3905	6273	10957	183
H(44A)	3441	7180	10427	173
H(44B)	2736	6760	9763	173
H(45A)	3536	7030	8978	76
H(45B)	4267	7424	9653	76
H(46A)	6582	6118	7953	98
H(46B)	6251	5314	7894	98
H(47A)	7973	5718	8394	111
H(47B)	7611	4942	8506	111
H(48A)	8257	5876	9635	114
H(48B)	7804	5130	9734	114
H(49A)	6708	5776	10004	87
H(49B)	6979	6462	9594	87

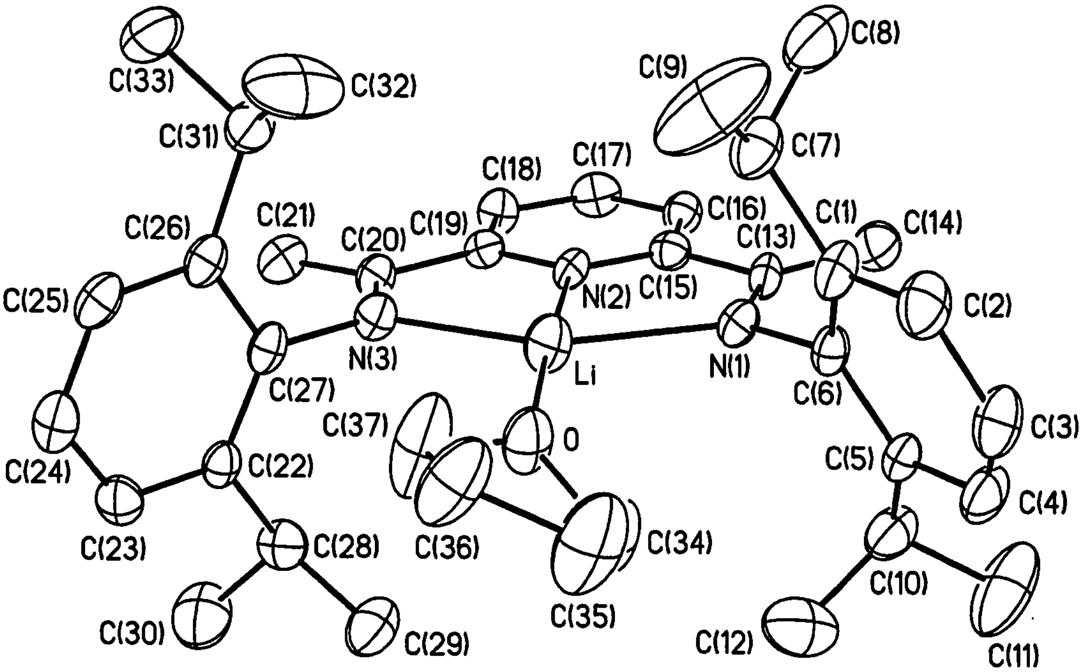
C(33)
C(32)
C(31)
C(9)
C(8)
C(7)
C(18)
C(17)
C(16)
C(26)
C(21)
C(20)
C(19)
C(1)
C(14)
C(13)
C(25)
N(2)
C(15)
C(2)
N(3)
Li
N(1)
C(6)
C(27)
C(37)
O
C(3)
C(24)
C(22)
C(5)
C(4)
C(36)
C(34)
C(23)
C(28)
C(10)
C(35)
C(30)
C(29)
C(12)
C(11)

Table AIII.12. Crystal data and structure refinement for sg2103.

Identification code	sg2103
Empirical formula	C37 H51 Li N3 O
Formula weight	560.75
Temperature	203(2) K
Wavelength	0.71073 A
Crystal system, space group	Triclinic, P-1
Unit cell dimensions	a = 8.311(2) A alpha = 105.705(5) deg. b = 12.739(3) A beta = 95.552(6) deg. c = 17.885(4) A gamma = 107.712(5) deg.
Volume	1702.9(7) A^3
Z, Calculated density	2, 1.094 Mg/m^3
Absorption coefficient	0.065 mm^-1
F(000)	610
Crystal size	0.20 x 0.10 x 0.10 mm
Theta range for data collection	1.21 to 20.81 deg.
Limiting indices	-8<=h<=8, -12<=k<=12, -17<=l<=17
Reflections collected / unique	8331 / 3561 [R(int) = 0.0859]
Completeness to theta = 20.81	99.7 %
Absorption correction	Semi-empirical from equivalents
Max. and min. transmission	1.000000 and 0.697422
Refinement method	Full-matrix least-squares on F^2
Data / restraints / parameters	3561 / ? / 379
Goodness-of-fit on F^2	1.031
Final R indices [I>2sigma(I)]	R1 = 0.0639, wR2 = 0.1222
R indices (all data)	R1 = 0.1485, wR2 = 0.1432
Largest diff. peak and hole	0.216 and -0.174 e.A^-3

Table AIII.13. Atomic coordinates (x 10^4) and equivalent isotropic displacement parameters (A^2 x 10^3) for sg2103. U(eq) is defined as one third of the trace of the orthogonalized Uij tensor.

	x	y	z	U(eq)
N(1)	9720(5)	6369(3)	8223(2)	42(1)
N(2)	10408(5)	4770(4)	8701(2)	37(1)
N(3)	8499(5)	2716(3)	7749(2)	44(1)
O	6638(5)	4149(3)	6850(2)	66(1)
Li	8595(12)	4436(8)	7757(5)	58(3)
C(1)	9810(7)	7145(4)	7128(3)	50(2)
C(2)	9237(8)	7788(5)	6717(3)	64(2)
C(3)	8170(8)	8382(5)	7003(3)	66(2)
C(4)	7706(7)	8386(5)	7717(3)	61(2)
C(5)	8272(7)	7780(4)	8165(3)	45(1)
C(6)	9313(6)	7157(4)	7859(3)	39(1)
C(7)	10968(8)	6475(5)	6817(3)	61(2)
C(8)	12798(9)	7155(6)	7093(4)	117(3)
C(9)	10600(10)	5993(7)	5922(4)	165(4)
C(10)	7724(8)	7776(5)	8955(3)	66(2)
C(11)	7541(10)	8920(6)	9408(4)	140(3)
C(12)	6079(9)	6784(6)	8838(3)	100(2)
C(13)	10950(7)	6775(4)	8862(3)	40(1)
C(14)	11997(7)	7983(5)	9270(3)	58(2)
C(15)	11304(7)	5858(5)	9156(3)	38(1)
C(16)	12468(6)	6101(4)	9846(3)	43(1)
C(17)	12695(7)	5180(5)	10055(3)	52(2)
C(18)	11771(7)	4057(5)	9584(3)	45(1)
C(19)	10626(6)	3870(5)	8906(3)	35(1)
C(20)	9512(7)	2703(4)	8363(3)	40(1)
C(21)	9629(7)	1685(5)	8536(3)	60(2)
C(22)	5735(7)	1094(4)	7324(3)	39(1)
C(23)	4620(7)	155(4)	6722(3)	49(2)
C(24)	5082(8)	-281(5)	6013(3)	51(2)
C(25)	6702(8)	222(5)	5905(3)	48(2)
C(26)	7905(8)	1178(5)	6486(3)	41(1)
C(27)	7388(8)	1642(4)	7198(3)	39(1)
C(28)	5222(7)	1569(5)	8108(3)	55(2)
C(29)	4342(7)	2460(5)	8059(3)	81(2)
C(30)	4079(8)	629(5)	8384(3)	95(2)
C(31)	9716(7)	1696(5)	6353(3)	55(2)
C(32)	9764(9)	2217(7)	5679(4)	129(3)
C(33)	10614(7)	797(5)	6194(3)	76(2)
C(34)	5585(8)	4861(5)	6796(4)	94(2)
C(35)	4970(10)	4609(6)	5940(4)	118(3)
C(36)	5128(9)	3457(6)	5530(3)	98(2)
C(37)	5871(10)	3161(6)	6175(4)	114(3)

Table AIII.14. Bond lengths [A] and angles [deg] for sg2103.

N(1)-C(13)	1.322(5)
N(1)-C(6)	1.436(5)
N(1)-Li	2.230(10)
N(2)-C(15)	1.336(6)
N(2)-C(19)	1.350(5)
N(2)-Li	2.007(10)
N(3)-C(20)	1.325(5)
N(3)-C(27)	1.422(6)
N(3)-Li	2.164(10)
O-C(37)	1.410(6)
O-C(34)	1.453(6)
O-Li	2.053(10)
C(1)-C(2)	1.391(6)
C(1)-C(6)	1.406(6)
C(1)-C(7)	1.520(7)
C(2)-C(3)	1.380(7)
C(3)-C(4)	1.368(6)
C(4)-C(5)	1.394(6)
C(5)-C(6)	1.397(6)
C(5)-C(10)	1.526(6)
C(7)-C(8)	1.459(8)
C(7)-C(9)	1.514(7)
C(10)-C(12)	1.504(7)
C(10)-C(11)	1.524(7)
C(13)-C(14)	1.454(6)
C(13)-C(15)	1.496(6)
C(15)-C(16)	1.391(6)
C(16)-C(17)	1.383(6)
C(17)-C(18)	1.378(6)
C(18)-C(19)	1.384(6)
C(19)-C(20)	1.489(6)
C(20)-C(21)	1.441(6)
C(22)-C(23)	1.372(6)
C(22)-C(27)	1.409(6)
C(22)-C(28)	1.527(6)
C(23)-C(24)	1.382(6)
C(24)-C(25)	1.361(6)
C(25)-C(26)	1.392(6)
C(26)-C(27)	1.417(6)
C(26)-C(31)	1.519(7)
C(28)-C(30)	1.515(7)
C(28)-C(29)	1.541(6)
C(31)-C(32)	1.523(7)
C(31)-C(33)	1.528(6)
C(34)-C(35)	1.482(7)
C(35)-C(36)	1.503(7)
C(36)-C(37)	1.446(7)
C(13)-N(1)-C(6)	119.9(4)
C(13)-N(1)-Li	114.1(4)
C(6)-N(1)-Li	125.8(4)
C(15)-N(2)-C(19)	119.9(4)
C(15)-N(2)-Li	121.1(4)
C(19)-N(2)-Li	118.8(4)
C(20)-N(3)-C(27)	118.9(4)

C(20)-N(3)-Li	114.2(4)
C(27)-N(3)-Li	126.7(4)
C(37)-O-C(34)	103.3(4)
C(37)-O-Li	128.5(4)
C(34)-O-Li	127.9(4)
N(2)-Li-O	175.7(5)
N(2)-Li-N(3)	77.3(3)
O-Li-N(3)	104.5(4)
N(2)-Li-N(1)	75.5(3)
O-Li-N(1)	102.8(4)
N(3)-Li-N(1)	152.7(5)
C(2)-C(1)-C(6)	117.5(5)
C(2)-C(1)-C(7)	121.8(5)
C(6)-C(1)-C(7)	120.7(5)
C(3)-C(2)-C(1)	121.2(5)
C(2)-C(3)-C(4)	120.4(5)
C(3)-C(4)-C(5)	121.1(5)
C(4)-C(5)-C(6)	118.0(5)
C(4)-C(5)-C(10)	120.6(5)
C(6)-C(5)-C(10)	121.4(5)
C(5)-C(6)-C(1)	121.8(5)
C(5)-C(6)-N(1)	121.0(4)
C(1)-C(6)-N(1)	116.6(4)
C(8)-C(7)-C(9)	108.9(6)
C(8)-C(7)-C(1)	113.1(5)
C(9)-C(7)-C(1)	112.8(5)
C(12)-C(10)-C(11)	110.2(5)
C(12)-C(10)-C(5)	110.8(5)
C(11)-C(10)-C(5)	113.1(5)
N(1)-C(13)-C(14)	127.0(5)
N(1)-C(13)-C(15)	114.4(5)
C(14)-C(13)-C(15)	118.5(5)
N(2)-C(15)-C(16)	121.8(5)
N(2)-C(15)-C(13)	114.6(5)
C(16)-C(15)-C(13)	123.6(5)
C(17)-C(16)-C(15)	118.3(5)
C(18)-C(17)-C(16)	119.8(5)
C(17)-C(18)-C(19)	119.3(5)
N(2)-C(19)-C(18)	120.9(5)
N(2)-C(19)-C(20)	114.6(5)
C(18)-C(19)-C(20)	124.5(5)
N(3)-C(20)-C(21)	126.2(5)
N(3)-C(20)-C(19)	114.9(5)
C(21)-C(20)-C(19)	118.9(5)
C(23)-C(22)-C(27)	118.3(5)
C(23)-C(22)-C(28)	122.0(5)
C(27)-C(22)-C(28)	119.7(5)
C(22)-C(23)-C(24)	122.2(5)
C(25)-C(24)-C(23)	119.4(5)
C(24)-C(25)-C(26)	121.8(5)
C(25)-C(26)-C(27)	118.1(5)
C(25)-C(26)-C(31)	120.3(5)
C(27)-C(26)-C(31)	121.6(5)
C(22)-C(27)-C(26)	120.2(5)
C(22)-C(27)-N(3)	120.6(4)
C(26)-C(27)-N(3)	119.0(5)
C(30)-C(28)-C(22)	113.3(5)

C(30)-C(28)-C(29)	110.0(5)
C(22)-C(28)-C(29)	110.8(4)
C(26)-C(31)-C(32)	113.1(5)
C(26)-C(31)-C(33)	111.3(4)
C(32)-C(31)-C(33)	109.0(5)
O-C(34)-C(35)	106.0(5)
C(34)-C(35)-C(36)	106.2(5)
C(37)-C(36)-C(35)	103.1(5)
O-C(37)-C(36)	111.2(5)

Symmetry transformations used to generate equivalent atoms:

Table AIII.15. Anisotropic displacement parameters (A^2 x 10^3) for sg2103.
The anisotropic displacement factor exponent takes the form:
-2 pi^2 [h^2 a*^2 U11 + ... + 2 h k a* b* U12]

	U11	U22	U33	U23	U13	U12
N(1)	49(3)	43(3)	42(3)	14(2)	7(2)	25(3)
N(2)	43(3)	35(3)	39(3)	12(2)	10(2)	22(3)
N(3)	47(3)	43(3)	40(3)	9(2)	2(2)	20(3)
O	69(3)	52(3)	73(3)	16(2)	-15(2)	29(2)
Li	70(7)	55(6)	51(6)	17(5)	5(5)	27(5)
C(1)	71(5)	41(4)	49(4)	16(3)	14(3)	31(3)
C(2)	84(5)	58(4)	61(4)	28(3)	20(4)	31(4)
C(3)	91(5)	56(4)	69(5)	33(3)	9(4)	39(4)
C(4)	71(5)	55(4)	75(5)	28(4)	16(4)	40(4)
C(5)	50(4)	37(4)	56(4)	17(3)	12(3)	24(3)
C(6)	47(4)	32(3)	42(4)	14(3)	3(3)	18(3)
C(7)	86(6)	58(4)	48(4)	15(3)	22(4)	35(4)
C(8)	93(7)	88(6)	174(8)	15(5)	30(6)	57(5)
C(9)	202(10)	249(11)	62(5)	-17(6)	13(5)	163(9)
C(10)	81(6)	73(5)	74(5)	37(4)	33(4)	48(4)
C(11)	253(10)	131(7)	97(6)	38(5)	89(6)	134(7)
C(12)	79(6)	140(7)	118(6)	88(5)	32(5)	43(5)
C(13)	50(4)	27(4)	44(4)	10(3)	10(3)	17(3)
C(14)	61(4)	57(4)	58(4)	17(3)	18(3)	24(3)
C(15)	38(4)	41(4)	32(3)	7(3)	8(3)	13(3)
C(16)	50(4)	42(4)	40(4)	12(3)	11(3)	19(3)
C(17)	48(4)	71(5)	38(4)	18(4)	-1(3)	24(4)
C(18)	50(4)	46(4)	39(3)	15(3)	-1(3)	20(3)
C(19)	34(4)	42(4)	27(3)	6(3)	3(3)	15(3)
C(20)	46(4)	39(4)	39(4)	16(3)	7(3)	20(3)
C(21)	63(5)	65(4)	61(4)	21(3)	16(3)	34(4)
C(22)	43(4)	34(4)	39(4)	9(3)	-1(3)	19(3)
C(23)	42(4)	48(4)	51(4)	14(3)	-2(3)	15(3)
C(24)	64(5)	46(4)	40(4)	8(3)	-7(3)	24(4)
C(25)	64(5)	49(4)	41(4)	15(3)	10(4)	37(4)
C(26)	57(4)	39(4)	35(4)	14(3)	8(3)	26(3)
C(27)	55(4)	35(4)	35(4)	13(3)	1(3)	26(3)
C(28)	54(4)	63(4)	41(4)	11(3)	5(3)	18(4)
C(29)	87(5)	71(5)	85(5)	7(4)	23(4)	41(4)
C(30)	122(7)	88(5)	85(5)	31(4)	57(5)	38(5)
C(31)	59(5)	52(4)	57(4)	14(3)	14(3)	24(4)
C(32)	111(7)	185(8)	184(8)	150(7)	83(6)	80(6)
C(33)	69(5)	87(5)	81(5)	17(3)	16(4)	46(4)
C(34)	101(6)	68(5)	111(6)	12(4)	-22(5)	52(4)
C(35)	155(8)	110(7)	95(6)	19(5)	-37(5)	84(6)
C(36)	134(7)	111(6)	66(5)	15(4)	-7(4)	85(5)
C(37)	173(8)	82(6)	75(5)	-10(4)	-47(5)	76(6)

Table AIII.16. Hydrogen coordinates (x 10^4) and isotropic displacement parameters (A^2 x 10^3) for sg2103.

	x	y	z	U(eq)
H(2A)	9581	7818	6236	77
H(3A)	7761	8785	6705	80
H(4A)	6995	8805	7908	73
H(7A)	10731	5805	7020	73
H(8A)	13037	7491	7665	176
H(8B)	13104	7771	6856	176
H(8C)	13468	6655	6943	176
H(9A)	11379	5582	5755	248
H(9B)	10765	6626	5700	248
H(9C)	9420	5461	5737	248
H(10A)	8633	7654	9285	80
H(11A)	8595	9556	9465	209
H(11B)	7322	8901	9928	209
H(11C)	6588	9031	9120	209
H(12A)	5755	6798	9346	150
H(12B)	6248	6055	8598	150
H(12C)	5172	6858	8494	150
H(14A)	11618	8477	9019	87
H(14B)	13195	8094	9243	87
H(14C)	11876	8186	9819	87
H(16A)	13084	6872	10162	52
H(17A)	13478	5319	10517	62
H(18A)	11917	3425	9722	53
H(21A)	8841	994	8130	90
H(21B)	9327	1693	9047	90
H(21C)	10796	1682	8547	90
H(23A)	3504	-203	6795	58
H(24A)	4285	-919	5608	61
H(25A)	7017	-85	5424	57
H(28A)	6292	1983	8515	66
H(29A)	4023	2748	8562	122
H(29B)	3318	2089	7645	122
H(29C)	5132	3102	7940	122
H(30A)	4678	105	8451	142
H(30B)	3025	198	7992	142
H(30C)	3804	982	8885	142
H(31A)	10385	2328	6844	66
H(32A)	10951	2564	5636	194
H(32B)	9230	2807	5785	194
H(32C)	9142	1611	5186	194
H(33A)	10684	515	6644	114
H(33B)	11765	1152	6113	114
H(33C)	9961	153	5725	114
H(34A)	6267	5686	7045	113
H(34B)	4610	4661	7061	113
H(35A)	5676	5217	5751	142
H(35B)	3769	4568	5837	142
H(36A)	3998	2875	5259	118
H(36B)	5884	3527	5145	118

H(37A)	4970	2578	6308	137
H(37B)	6741	2822	6008	137

ESR Spectrum of
{α,α’-[2,6-(i-Pr)2PhN=C(Me)]2 (C5H3N)}[Li(THF)]3} (11)

Frequency: 9.76260 GHz
Corrected Field: 3482.416 G
g Parameter: 2.00256(9)